

JOINT TRANSPORTATION RESEARCH PROGRAM

INDIANA DEPARTMENT OF TRANSPORTATION
AND PURDUE UNIVERSITY



Investigation of Design Alternatives for the Subbase of Concrete Pavements



**Amy Getchell, Luis Garzon Sabogal,
Philippe L. Bourdeau, Marika Santagata**

RECOMMENDED CITATION

Getchell, A., Garzon Sabogal, L., Bourdeau, P. L., Santagata, M. (2020). *Investigation of design alternatives for the sub-base of concrete pavements* (Joint Transportation Research Program Publication No. FHWA/IN/JTRP-2020/03). West Lafayette, IN: Purdue University. <https://doi.org/10.5703/1288284317114>

AUTHORS

Amy Getchell

Luis Garzon Sabogal

Graduate Research Assistants

Lyles School of Civil Engineering

Purdue University

Philippe L. Bourdeau, PhD

Emeritus Professor of Civil Engineering

Lyles School of Civil Engineering

Purdue University

Marika Santagata, PhD

Associate Professor of Civil Engineering

Lyles School of Civil Engineering

Purdue University

(765) 494-0697

mks@purdue.edu

Corresponding Author

ACKNOWLEDGMENTS

This project was made possible by the sponsorship of the Joint Transportation Research Program (JTRP) and the Indiana Department of Transportation (INDOT). The authors would like to thank the study advisory committee for their valuable assistance and technical guidance in the course of performing this study.

JOINT TRANSPORTATION RESEARCH PROGRAM

The Joint Transportation Research Program serves as a vehicle for INDOT collaboration with higher education institutions and industry in Indiana to facilitate innovation that results in continuous improvement in the planning, design, construction, operation, management and economic efficiency of the Indiana transportation infrastructure. https://engineering.purdue.edu/JTRP/index_html

Published reports of the Joint Transportation Research Program are available at <http://docs.lib.purdue.edu/jtrp/>.

NOTICE

The contents of this report reflect the views of the authors, who are responsible for the facts and the accuracy of the data presented herein. The contents do not necessarily reflect the official views and policies of the Indiana Department of Transportation or the Federal Highway Administration. The report does not constitute a standard, specification or regulation.

TECHNICAL REPORT DOCUMENTATION PAGE

1. Report No. FHWA/IN/JTRP-2020/03	2. Government Accession No.	3. Recipient's Catalog No.	
4. Title and Subtitle Investigation of Design Alternatives for the Subbase of Concrete Pavements		5. Report Date June 2019	
		6. Performing Organization Code	
7. Author(s) Amy Getchell, Luis Garzon Sabogal, Philippe L. Bourdeau, and Marika Santagata		8. Performing Organization Report No. FHWA/IN/JTRP-2020/03	
9. Performing Organization Name and Address Joint Transportation Research Program Hall for Discovery and Learning Research (DLR), Suite 204 207 S. Martin Jischke Drive West Lafayette, IN 47907		10. Work Unit No.	
		11. Contract or Grant No. SPR-4116	
12. Sponsoring Agency Name and Address Indiana Department of Transportation (SPR) State Office Building 100 North Senate Avenue Indianapolis, IN 46204		13. Type of Report and Period Covered Final Report	
		14. Sponsoring Agency Code	
15. Supplementary Notes Conducted in cooperation with the U.S. Department of Transportation, Federal Highway Administration.			
16. Abstract <p>In all pavement structures, one or more support layers separate the pavement from the subgrade. In addition to offering structural support, these layers have several important functions, which include: providing a stable and uniform construction platform, facilitating drainage, mitigating pumping of the subgrade fines, and protecting the pavement from the effects of frost heave. Their performance is critical in achieving the desired pavement smoothness, and in extending the service life of the structure. A range of designs, making use of unbound or stabilized aggregates and in some cases geosynthetics, are employed by different agencies to fulfill these functions.</p> <p>This project was motivated by constructability and long term performance concerns with the existing base/subbase design employed by INDOT for concrete pavements, as well as the desire to identify state of the art design solutions that could be applicable to both concrete and asphalt pavements. The primary objectives of the study were to: critically reexamine INDOT's existing design; perform a preliminary evaluation (based on aggregate compaction, hydraulic conductivity, strength and compatibility properties) of select unbound design options identified in collaboration with the Study Advisory Committee (SAC); explore the potential use of geotextiles as separator; and develop recommendations for base/subbase aggregate laboratory testing and evaluation.</p>			
17. Key Words separator layer, pavement layer compatibility, unbound aggregate, hydraulic conductivity, shear strength, compaction, geotextiles, pavement subbase, drainage layer, strength		18. Distribution Statement No restrictions. This document is available through the National Technical Information Service, Springfield, VA 22161.	
19. Security Classif. (of this report) Unclassified	20. Security Classif. (of this page) Unclassified	21. No. of Pages 108 including appendices	22. Price

EXECUTIVE SUMMARY

Introduction

In all pavement structures, one or more support layers separate the pavement from the subgrade. In addition to structural support, these layers have many important functions, which include providing a stable and uniform construction platform, facilitating drainage, mitigating pumping of the subgrade fines, and protecting the pavement from the effects of frost heave. A range of designs making use of unstabilized or stabilized aggregates, and in some cases geosynthetics, are employed by different agencies to fulfill these functions. Their performance is critical in achieving the desired pavement smoothness and in extending the service life of the pavement.

This project was motivated by constructability and long-term performance concerns with the existing base/subbase design employed by INDOT for concrete pavements, as well as the desire to identify state-of-the-art design solutions that could be applicable to both concrete and asphalt pavements. The primary objectives of the study were as follows:

- Critically reexamine INDOT's existing design.
- Perform a preliminary evaluation (based on aggregate compaction, hydraulic conductivity, strength, and compatibility properties) of select unbound design options identified in collaboration with the Study Advisory Committee (SAC).
- Explore the potential use of geotextiles as separators.
- Develop recommendations for base/subbase aggregate laboratory testing and evaluation.

Findings

The work performed included the following:

- Review of existing practices for base and subbase design in Indiana and in other states.
- Laboratory evaluation of the compaction and hydraulic conductivity (k) properties of select aggregates available in Indiana.
- Collection of data for similar materials from the literature.
- Analysis of the stability of the aggregates under the action of construction equipment.
- Review of the guidelines for establishing compatibility between aggregate layers and subgrades.
- Analysis of the compatibility between select aggregates using the software DRIP.
- Assessment of the applicability of select geotextiles as separators in place of an aggregate layer.

In general, the use of a drainage layer in combination with a separator layer seems to be the preferred design. Experiences from other states also indicates that it is possible to identify design solution(s) that can be employed for both asphalt and concrete pavements. With regard to the drainage layer, use of a material such as #8, which is currently in use in Indiana, is found to be problematic due to the unnecessarily high hydraulic conductivity (expected $k > 10^4$ ft/day) and the inadequate stability for several of the loading cases examined in this study.

Consistent with practices in other states, aggregates with particle size distribution falling within the band for Indiana #43 (or even #53) are better candidate materials for the drainage

layer. Data from preliminary tests as well as results from the literature indicate that with appropriate aggregate particle size selection and compaction, values of k between 150 and 1,000 ft/day (depending on gradation, aggregate source, and level of compaction) can be achieved. Given the dependence of the hydraulic conductivity on the particle size distribution (with changes in k as large as 2 orders of magnitude observed as a result of relatively small variations in particle size distribution), reference gradation bands may need to be further constrained to more reliably achieve target values of hydraulic conductivity. Furthermore, due to the challenges of measuring k in the field and laboratory, it is problematic to verify or enforce the current specifications that prescribe the hydraulic conductivity of the compacted aggregate in the field should fall within a narrow interval.

Selection of aggregates for the separator layer requires site-specific consideration of the subgrade conditions, as the analyses performed show that lack of compatibility with the subgrade at the lower interface is the primary reason for considering a material inadequate as a separator. Aggregates used for the separator layer in the states that were interviewed as part of this project have particle size distributions comparable to or finer than #53.

Geotextile separators can be an economic alternative to aggregate separator layers, with non-woven geotextiles being better candidates than woven fabrics in a number of situations. Their design requires consideration of the site-specific subgrade characteristics and assessment of the construction condition severity for the survivability of the fabric. For the geotextiles examined in this project, survivability criteria were found to be the most stringent factor and to control the design.

Compatibility analyses also suggest that a separator may not always be necessary for pavements on cement-treated subgrades, but this conclusion requires additional validation.

The analyses performed demonstrate that the stability of materials, such as INDOT #43 and #53, require density and frictional resistance that are achievable with thorough compaction. Static compaction alone is unlikely to be sufficient for this purpose. In the laboratory, the vibratory hammer method was confirmed as the most effective method for the compaction of all the aggregates examined, and it should be used as a laboratory reference. Similarly, in the field, vibratory compaction is highly desirable. An adequate procedure could include first passes of static compaction for gaining strength so that the material can sustain further passes in vibratory mode. Equally critical to the performance of materials such as #43 and #53, is controlling the placement of water content and avoiding segregation (e.g., through the use of a spreader box).

This study also highlighted some of the limitations in relying exclusively on the DRIP software for the design of drainage and separator layers, as DRIP provides no assessment of the soundness/abrasion characteristics of aggregates, and it does not include survivability criteria in the evaluation of geotextiles. Moreover, predictions of the hydraulic conductivity of aggregate layers generated through DRIP should be considered with care, since all aggregates examined in this research yielded generally unreliable estimates of k.

Finally, only a few empirical relationships between strength parameters and aggregate characteristics emerged from this study, quantified by medium to high values of correlation coefficients, which can be trusted after hypothesis testing. These are generally not strong enough to allow the development of empirical formulas applicable in engineering practice.

Implementation

Based on the work performed, the following primary recommendations for implementation are provided:

- Indiana #8 should no longer be used for the base drainage layer.
- The use of geotextiles, including non-woven, should be encouraged for the separator layer. The design should rely on both survivability and filtration criteria, with consideration of the site-specific subgrade conditions.
- Construction methods to limit segregation of the aggregates in the field should be enforced.
- Compaction of aggregates in the field should be performed using vibratory rollers, while potentially early passes should be performed using static compaction to address stability problems.
- When placing materials such as #43 and #53, verification of the water content should be required.
- When available, asphalt paving machines *on tracks* should be considered preferable to pavers on wheels.

The study also highlighted areas where additional research is warranted to aid in predicting the performance of the support layers and to support INDOT's move towards performance-based specifications. In particular, it is suggested that future efforts be directed to the following:

- Obtaining both shear strength and hydraulic conductivity data for aggregates of interest (e.g., #43 and #53) under a range of field-relevant testing conditions.
- Identifying/developing techniques for measuring the in-situ hydraulic conductivity of compacted aggregates.
- Investigating the migration of fines through and from treated subgrades.
- Incorporating survivability and filtration criteria in a software that would be used for geotextile separator selection in place of DRIP.
- Extending the statistical analysis of shear strength data to a broader database.

CONTENTS

1. INTRODUCTION	1
1.1 Background and Problem Statement	1
1.2 Research Objectives	1
1.3 Activities and Organization of Report	2
2. RESULTS OF SURVEY ON DESIGN OF SUBBASE LAYERS	2
3. LABORATORY RESULTS AND COMPARISON TO LITERATURE DATA	5
3.1 Materials Investigated	5
3.2 Compaction Behavior	6
3.3 Hydraulic Conductivity	10
3.4 Design and Construction of Horizontal Permeameter	17
4. REVIEW OF LITERATURE SHEAR STRENGTH DATA	21
4.1 Peak Friction Angle Database	21
4.2 Statistical Analysis of Peak Friction Angle Data	24
5. MECHANICAL STABILITY OF AGGREGATE LAYERS	25
5.1 Principle	25
5.2 Geometry and Load Configurations for Sensitivity Analysis	26
5.3 Material Data for Sensitivity Analysis	26
5.4 Results of Analysis and Discussion	27
6. COMPATIBILITY BETWEEN MATERIALS AND USE OF GEOTEXTILES	33
6.1 Need for Separator Between Drainage Layer and Subgrade	34
6.2 Granular Separators	35
6.3 Geotextile Separators	37
7. CONCLUSIONS AND RECOMMENDATIONS	42
7.1 Introduction	42
7.2 Conclusions	42
7.3 Recommendations	44
REFERENCES	44
APPENDICES	
APPENDIX A. Purdue University Survey on Pavement Subbase Design	48
APPENDIX B. State Survey Summaries	48
APPENDIX C. Particle Size Data	48
APPENDIX D. Details on Empirical Correlations Used to Estimate K	48
APPENDIX E. Technical Drawings of Permeameter	48
APPENDIX F. Shear Strength Database	48
APPENDIX G. Details of Statistical Analyses	48
APPENDIX H. Overview of Bearing Capacity Analysis	48
APPENDIX I. Supporting Data for Compatibility Analyses	48
APPENDIX J. List of Geotextiles Approved by INDOT	48

LIST OF TABLES

Table	Page
Table 2.1 Interviews conducted between July 2017 and March 2018	3
Table 2.2 State interview pavement structure summary	3
Table 2.3 Material summary for subbase below concrete pavement	4
Table 2.4 Material summary for subbase below asphalt pavement	5
Table 2.5 State interview construction method summary	5
Table 3.1 INDOT proposed alternatives for pavement subbase	6
Table 3.2 Compaction testing methods	7
Table 3.3 Data sources used for comparison of compaction data	7
Table 3.4 Compaction data for INDOT #8	7
Table 3.5 Compaction data for INDOT #53	8
Table 3.6 Compaction data for INDOT #43	9
Table 3.7 Summary of falling head test results	13
Table 4.1 Testing conditions and parameters investigated in the three studies	21
Table 5.1 Example loads used for comparison	27
Table 5.2 Geometry constants used for different equipment in sensitivity analysis	28
Table 5.3 Dry unit weight and friction angle ranges used in analysis	29
Table 5.4 Average values of material parameters for sensitivity analysis	29
Table 6.1 Summary of proposed options by INDOT (2/17/17)	36
Table 6.2 Summary of INDOT design options without separator layer, according to criteria from FHWA-TS-80-224 (Moulton, 1980/90) and DRIP, with subgrade examples from Jung and Bobet (2008)	36
Table 6.3 Summary of separator analysis for Design Option 1	37
Table 6.4 Summary of separator analysis for Design Option 2	38
Table 6.5 Summary of separator analysis for Design Option 6	38
Table 6.6 Construction survivability ratings	39
Table 6.7 Geotextile survivability requirements	39
Table 6.8 Compiled data for list of INDOT approved geotextiles and assessment of separator and filter functions for Design Option 3 with untreated A-7-6 subgrade from Jung and Bobet (2008), assuming Class 1 geotextiles are needed	40
Table 6.9 Compiled data for list of INDOT approved geotextiles and assessment of separator and filter functions for Design Option 3 with untreated A-7-6 subgrade from Jung and Bobet (2008), assuming Class 2 geotextiles are needed	41

LIST OF FIGURES

Figure	Page
Figure 2.1 Ohio pavement structure	4
Figure 2.2 Western/Central Kentucky pavement structure (Option 1)	4
Figure 2.3 Western/Central Kentucky pavement structure (Option 2)	4
Figure 3.1 Particle size distribution ranges for #8, #43, #53	6
Figure 3.2 Compaction behavior of INDOT #8	8
Figure 3.3 Dry unit weight behavior for INDOT #53	9
Figure 3.4 Compaction behavior of INDOT #53 and INDOT #43	10
Figure 3.5 Values of k estimated from four prediction models for #8, #43, and #53	11
Figure 3.6 Hydraulic conductivity values for different gradations	11
Figure 3.7 (a) Falling head permeameter and view of sample, (b) immediately after setup, and (c) after a test in which significant migration of the fines was observed	12
Figure 3.8 (a) Hydraulic conductivity results (average +/- standard deviation) from falling head tests on #43 and #53; (b) dependence of k data on hydraulic gradient for test #53_4	14
Figure 3.9 Comparison of particle size distribution bands of ODOT 57 and ODOT 67 aggregates to the gradation bands for INDOT #8, #43, and #53	14
Figure 3.10 Comparison of particle size distribution band of ODOT 304 aggregate to the gradation bands for INDOT #8, #43, and #53	15
Figure 3.11 Comparison of particle size distribution band of aggregates investigated by Roy and Sayer (1989) to the gradation bands for INDOT #8, #43, and #53	15
Figure 3.12 Comparison of particle size distributions of coarse, medium, and fine aggregates investigated by Jones and Jones (1989) to the gradation bands for INDOT #8, #43, and #53	16
Figure 3.13 Comparison of hydraulic conductivity results from this study to literature data for similar aggregates	16
Figure 3.14 Comparison of hydraulic conductivity data for #43 and #53 and similar materials to predictions using the model by Moulton	17
Figure 3.15 Comparison of hydraulic conductivity data to predictions using empirical models	18
Figure 3.16 Purdue horizontal flow permeameter	19
Figure 3.17 (a) Vibrating hammer and tamper used to compact each layer; (b) aggregate surface after compaction	20
Figure 3.18 Foam sheet used to avoid preferential flow: (a) top view of specimen covered with the foam; (b) top view of the contact between foam and specimen after a test	20
Figure 4.1 (a) Particle size distributions of aggregates; (b) peak friction angles measured on specimens with $Dr \sim 30\%$	22
Figure 4.2 (a) Particle size distribution of aggregates; (b) peak friction angles measured on specimens with $Dr \sim 148\%$	23
Figure 4.3 (a) Particle size distribution of aggregates; (b) peak friction angles measured on specimens with $Dr \sim 148\%$	24
Figure 5.1 Conceptual model of wheel-granular layer interaction: (a) stability, and (b) instability caused by bearing capacity failure	26
Figure 5.2 Caterpillar CS56 vibratory soil compactor	27
Figure 5.3 Caterpillar CAT AP1480F asphalt paver with wheels	28
Figure 5.4 Weiler P385B asphalt paver with tracks	28
Figure 5.5 Effect of aggregate friction angle on ultimate bearing load, under a wheel of compactor	29
Figure 5.6 Effect of aggregate unit weight on the ultimate bearing load, under a wheel of compactor	30
Figure 5.7 Effect of aggregate friction angle on ultimate bearing load, under compactor drum (horizontal dotted lines represent the static and total applied force with force ratio FR)	30
Figure 5.8 Effects of aggregate unit weight on ultimate bearing load, under roller of compactor (horizontal dotted lines represent the static and total applied force with force ratio FR)	31

Figure 5.9 Load transfer through asphaltic concrete pavement layer during compaction	31
Figure 5.10 Effect of aggregate friction angle on ultimate bearing load, under track of asphalt paver	32
Figure 5.11 Effects of aggregate unit weight on ultimate bearing load, under track of asphalt paver	32
Figure 5.12 Effect of aggregate friction angle on ultimate bearing load, under a wheel of asphalt paver	33
Figure 5.13 Effects of aggregate unit weight on the ultimate bearing load, under a wheel of asphalt paver, for different friction angles	33
Figure 6.1 Incompatibility by intrusion—requires a separator	34
Figure 6.2 Incompatibility by contamination—requires a filter	34
Figure 6.3 Concept of geotextile separation in roadways	42

1. INTRODUCTION

1.1 Background and Problem Statement

In all pavement structures, one or more support layers typically separate the pavement from the subgrade. These layers as well as the subgrade play a critical role in achieving the desired pavement smoothness, and in extending the service life of the pavement. It is widely established that many pavement failures are a result of inadequate performance of the underlying layers. The focus of this project is on the support layers, herein referred to with the term subbase. (In some states, the term subbase is reserved solely for the separator layer, while the drainage layer is denoted as base. Additionally, according to the ACPA (2007) the term subbase should be reserved for the support layer(s) of concrete pavements, while the term base is more commonly used for an asphalt pavement structure.) In addition to structural support, the functions of these layers are to: improve the constructability of the upper pavement layers providing a stable and uniform construction platform; to mitigate pumping of the subgrade fines; to protect the pavement from the effects of frost heave, and to facilitate drainage (ACPA, 2007; FHWA, 2016). Subbase types generally fall in two main categories: granular (unstabilized) subbases and subbases stabilized using either cement (or other pozzolanic materials such as fly ash) or asphalt. The type of subbase may or may not differ depending on the type of pavement.

Up until 2017, according to INDOT's Concrete Pavement Manual, two types of subbase were used for concrete pavements in Indiana. The first was a dense graded subbase consisting of 6" of coarse aggregate size No. 53. The second, which continues to be most commonly used in practice, was a composite subbase comprised of 3" of an aggregate drainage layer (typically Indiana No. 8) placed over a 6" aggregate separation layer (typically Indiana No. 53). Section 904.03 of the INDOT Standard Specifications INDOT contains the requirements for these aggregates. INDOT's use of a series of unstabilized layers for the subbase is generally in line with the practice of most agencies operating in the U.S. Based on a study by the ACPA (2010), a significant fraction of agencies specify non-stabilized subbases. When appropriately designed (e.g., limiting the percentage of fines, using aggregates with adequate abrasion resistance, and selecting a gradation that guarantees the desired permeability and facilitates compaction) and constructed, this type of subbase does, indeed, provide a cost-effective solution for pavement support and drainage.

The research study summarized in this report was motivated by the following three main factors.

First, field observations conducted by INDOT engineers both during and after construction suggested that the existing subbase design had shortcomings that affected constructability and long-term performance. In particular, the following was reported:

- The #8 aggregate used for the drainage layer was not easily compactable, and its maximum particle size of 1" could hinder placement of the 3" layer.
- Use of the #8 aggregate often produced a working platform that was unstable under the weight of the construction equipment.
- Uneven deformations of the pavement, which in some cases led to cracking, could be ascribed to non-uniform post construction settlement of the #8 layer under the pavement.
- Particularly for A-6 and A-7-6 soils, the #53 separation layer was in some cases not effective in avoiding pumping of the fines.

Second, was the realization that the current design options did not reflect some of the developments that had instead found acceptance in other agencies. These included the use of geosynthetics. While these materials have for years found wide and successful application in pavement structures fulfilling the functions of reinforcement (e.g., to mitigate problems with poor quality subgrades), stabilization (e.g., in embankments), and, most relevant to the proposed study, separation, filtration and drainage (e.g., geotextiles as separation layers to mitigate pumping of fines or as components of underdrains), and their use could potentially address some of the above mentioned concerns with the #53 separation layer, existing subbase specifications did not call for their use.

Along the same lines, nationally the subbase specifications have for over a decade shown a major shift from "permeable" (permeability > 548 ft/day) to "free draining" (permeability < 350 ft/day) drainage layers (ACPA, 2010). This came as a result of documented performance issues (aggregate breakdown, early age cracking from penetration of concrete mortar, instability of the construction platform (ACPA, 2007) associated with permeable (open graded) subbases. This trend was not reflected in the existing INDOT specifications, which continued to prescribe a high permeability (>3,480 ft/day) layer (#8).

Finally, was the desire to develop a design solution for the support layers that could be common for both rigid and flexible pavements. While the project title reflects an initial focus on concrete pavements, after the start the project was redirected to examining solutions that would be applicable also for asphalt pavements (T. Nantung, personal communication, February 2017).

1.2 Research Objectives

The four primary objectives of the work conducted as part of this research project were the following:

1. Critically reexamine INDOT's existing subbase design, based on feedback from INDOT's technical staff and a review of current practices in the United States.
2. Perform a preliminary evaluation (based on aggregate compaction, hydraulic conductivity, strength and compatibility properties) of select unbound design options identified in collaboration with the Study Advisory Committee (SAC).

3. Explore the potential use of geotextiles in the subbase, based on a review of the literature and of the state of practice, and develop recommendations for geotextile selection.
4. Develop recommendations for subbase aggregate laboratory testing and evaluation.

1.3 Activities and Organization of Report

The research plan was developed to address the objectives outlined above. Over the duration of the project, the research team was tasked by the project PA and the SAC with examining a number of different design alternatives. In general, these included two categories of solutions: one in which both the drainage and the separator functions were fulfilled by aggregate layers; the second in which a geotextile was used as separator. Various aggregates were suggested. Of these, only Indiana #8, #43, and #53, which are commonly available in the state, could be tested in the laboratory. While INDOT also demonstrated interest in investigating subbase design options which incorporated an open-graded hot mix asphalt layer for drainage, study of these options was considered outside of the scope of the study, which remained instead focused solely on unbound materials.

The research plan comprised the following seven activities which are described in the subsequent sections, with additional information included in Appendices A–J:

- A. Surveys among experts in neighboring states of current practices for the design and construction of subbases (Section 2 and Appendices A and B).
- B. Experimental program to characterize index properties, compaction behavior (using modified Proctor and vibratory hammer), and hydraulic conductivity (using falling head setup) of the aggregates (Indiana #8, #43, and #53) readily available in the state (Sections 3.1, 3.2, and 3.3.2, and Appendices C and D).
- C. Design and construction of a new horizontal permeameter for measuring the hydraulic conductivity of aggregates under field relevant conditions (Section 3.4 and Appendix E).
- D. Collection and analysis of literature data on the hydraulic and strength properties of aggregates similar to those of interest to the study (Sections 3.3.3 and 3.3.4, and Appendices F and G).
- E. Analysis of the stability of aggregates under the weight and the action of construction equipment (Section 5 and Appendix H).
- F. Review of the guidelines for establishing the compatibility between two aggregate layers, and analysis of the compatibility between select aggregates (including some not at this time available in Indiana (e.g., New Jersey dense grade aggregate gradation) using the software DRIP (Drainage Requirements in Pavement) (Sections 6.1–6.2 and Appendix I).
- G. Review of the list of INDOT's approved geotextiles, and assessment of their suitability as separator (Section 6.3 and Appendices I and J).

2. RESULTS OF SURVEY ON DESIGN OF SUBBASE LAYERS

A series of interviews were performed with DOT personnel in neighboring states and other countries using the questionnaire found in Appendix A to address the following topics:

- Pavement structure.
- Materials used for the drainage and separator layers.
- Construction of pavement layers.

A modified questionnaire was used to interview a representative of the Concrete Paving Association of Minnesota. A list of all interviews is presented in Table 2.1. Interviewees were selected based on recommendations from colleagues at INDOT, Purdue University and other academic institutions. Summaries of the individual interviews are presented in Appendix B.








The design of the pavement structure can vary from state to state and be dependent on the pavement (asphalt or concrete) type, geology, climate, and traffic conditions. The first set of questions focused on the actual design of the pavement structure below both concrete and asphalt. Table 2.2 summarizes the main findings from this set of questions.

As seen in Table 2.2, Kentucky and Ohio are the only states interviewed that implement the same pavement structure for both concrete and asphalt pavements. Ohio is the only state to consider a single design option for both concrete and asphalt pavements. This structure is shown in Figure 2.1 and includes only a drainage layer between pavement and subgrade. Ohio is also the only state to not have any subbase design option with a separator layer. Kentucky, Minnesota, and Pennsylvania have options both with and without a separator layer, depending on the nature of the subgrade (e.g., rock versus soil) and/or traffic loading conditions. Conversely, Michigan and Ontario always implement a two-layer structure (drainage and separator layer). Finally, Kentucky was the only state interviewed to have an option utilizing a geotextile as seen in Figure 2.2 (single sheet) and Figure 2.3 (wrapped around an unbound aggregate layer).

Table 2.3 and Table 2.4 summarize the main findings regarding the materials used for the subbases of concrete and asphalt pavements, respectively. The cells shaded in blue reflect particle size distributions similar to INDOT #43 and INDOT #53. As seen in both tables, a majority of the agencies are using an aggregate similar to #43 and #53 as a drainage layer below the pavement. None of the agencies interviewed use an aggregate similar in gradation to #8 for the drainage layer. Similarly, for the separator or bottom layer, the interviewed agencies use aggregates similar to #43, #53, or smaller, or a stabilized layer or a geotextile.

As for the permeability of the aggregates being used by other agencies, there was mixed response. It was reported that in the past Ohio tried using a free draining base, but experienced stability issues. Currently, Ohio does not have any permeability specifications for

TABLE 2.1
Interviews conducted between July 2017 and March 2018

State	Affiliation	Name(s)	Date	
Indiana	INDOT	KS	7/6/17	
Kentucky	KY Transportation Cabinet	AR	11/17/17	
Minnesota	MnDOT	JS	11/28/17	
	Concrete Paving Association of MN	MZ	12/11/17	
Ohio	ODOT	AM & SS	11/30/17 12/5/17	
Pennsylvania ^a	PennDOT	RP	1/24/18	
Michigan ^a	Michigan Department of Transportation	AI	2/23/18	
Ontario ^a	Ontario Ministry of Transportation	SL	3/20/18	

^aInterview conducted via email.

TABLE 2.2
State interview pavement structure summary

State	Is Pavement Structure Same for Concrete and Asphalt?	Is More Than 1 Option Considered?	Is There a Subbase Layer?	Are There Options with Geotextiles?	What Type of Pavement is Most Common?
KY	Yes	Yes	Not always	Yes	Asphalt
MN	No	Yes	Not always	No	Asphalt
OH	Yes	No	No	No	Asphalt
PA	No	Yes	Not always	No	Both
MI	No	Yes	Yes	No	Both
Ontario	No	Yes	Yes	No	Both

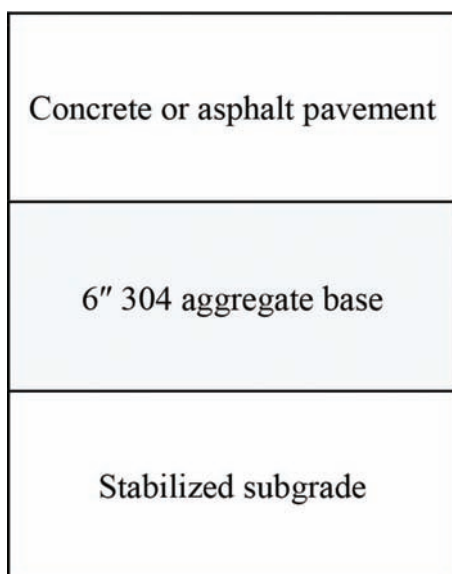


Figure 2.1 Ohio pavement structure.

OH 304 (Figure B.12). Pennsylvania rarely tests for permeability, however, it does require free draining conditions. Ontario performs lab and field testing for permeability, but no testing methods or required values for permeability were provided. Finally, Minnesota performs field testing with a commercial pavement permeameter to check for draining conditions. No information was collected from Michigan or Kentucky on this topic.

The last focus of the survey was on the method of construction. A brief summary of these findings can be found in Table 2.5. In all instances, the aggregate is delivered to the site wet. None of those interviewed reported problems with segregation of the aggregate. Note that Indiana does not require the aggregate to be delivered wet and does observe segregation issues. As far as the method of compaction, each state seems to use a type of vibratory roller. In all cases compaction is controlled by use of a test section. Minnesota and Ontario do not identify a prescribed method in their

8–13" concrete layer <i>OR</i> min. 5.5" to 18" asphalt layer
4–6" aggregate (Dense Graded Aggregate (DGA) or Crushed Stone Base (CSB))
2-ft shot rock bed
Subgrade

Figure 2.2 Western/Central Kentucky pavement structure (Option 1).

8–13" concrete layer <i>OR</i> min. 5.5" to 18" asphalt layer
DGA
Geotextile
18" quarry processed limestone (1–4")
Geotextile
Subgrade

Figure 2.3 Western/Central Kentucky pavement structure (Option 2).

TABLE 2.3
Material summary for subbase below concrete pavement

State	Concrete Pavement	
	Top Layer (primary function = drainage)	Bottom Layer (primary function = separation)
KY	Single layer–aggregate with particle size distribution similar to #43 and #53	
MN	Aggregate with particle size distribution similar to #43 and #53	Aggregate with particle size distribution similar to #43 and #53
OH	Single layer–aggregate with particle size distribution similar to #43 and #53	
PA	Cement–aggregate mix (may be eliminated in low volume roads)	Aggregate with particle size distribution similar to #43
MI	Aggregate with particle size distribution between #43 and #53	Sand subbase (if not present, thickness of drainage layer is increased)
Ontario	Asphalt or cement treated aggregate	Aggregate with particle size distribution similar to #43 and #53

TABLE 2.4
Material summary for subbase below asphalt pavement

State	Asphalt Pavement	
	Top Layer (primary function = drainage)	Bottom Layer (primary function = separation)
KY	Single layer–aggregate with particle size distribution similar to #43 and #53.	
MN	Aggregate with particle size distribution similar to #43 and #53.	Aggregate with variable size distribution that overlaps with #53 and finer.
OH	Single layer–aggregate with particle size distribution similar to #43 and #53.	
PA	Cement or asphalt stabilized layer (functions as a working platform).	Aggregate with particle size distribution similar to #43 (functions as drainage layer).
MI	Aggregate with particle size distribution between #43 and #53.	Sand subbase (if not present, thickness of drainage layer is increased).
Ontario	Aggregate with particle size distribution similar to #53.	Aggregate with variable size distribution that overlaps with #53, #43 and finer.

TABLE 2.5
State interview construction method summary

State	Is Aggregate Delivered to Site Wet?	Is Segregation an Issue?	How are Layers Compacted?	How is Compaction Controlled?
KY	Yes	No	Single or double drum flat roller (vibrating)	Control strips and test sections
MN	Yes	No	Dependent on project, contractor must prove	method is sufficient
OH	Yes	No	Vibratory smooth drum roller	Test section
PA	Yes	No	Roller or vibratory compaction equipment	Control strip and nuclear density reading
MI	Yes	No	Various types of rollers	Test strip and nuclear density gauges
Ontario	Yes	No	Dependent on project, contractor must prove	method is sufficient

specifications; instead, it is dependent on the project and the contractors must prove the method is sufficient.

In summary, the unbound material used for the top (drainage) layer by other states is comparable to #43 and #53. None of the other states seem to use anything comparable to #8 as a top layer.

The bottom (separator) layer is also comparable to #43 and #53, or smaller in size (Ontario, Pennsylvania OGS, Minnesota class 3 and class 4). Kentucky also considers geotextiles for the separator function. The agencies interviewed do not report problems with segregation of unbound materials. Test strips are commonly used to determine the number of passes of a vibratory roller for best compaction results instead of a prescribed method.

3. LABORATORY RESULTS AND COMPARISON TO LITERATURE DATA

3.1 Materials Investigated

Data on the compaction behavior were experimentally obtained for three aggregates: Indiana #8, #43, and #53. Hydraulic conductivity data were collected only for #43 and #53. Aggregates #8 and #53 are used in the existing subbase design, while both #43 and

#53 appear in one or more of the subbase design options (Table 3.1) recommended by the project PA for analysis (T. Nantung, personal communication, February, 2017). The aggregates were purchased from the Delphi plant of U.S. Aggregates (#8 and #53), and the Richmond plant of Barrett Paving (#43). The gradation bands for these materials based on INDOT's Standard Specifications are shown in Figure 3.1. Values of coefficient of uniformity and coefficient of curvature determined for the average gradation are: 2.6 and 1.1 (#8), 46.6 and 2.9 (#43), 69.4 and 1.6 (#53).

Appendix C presents particle size distributions determined in the laboratory for samples of these aggregates obtained at various stages of the experimental program. In general, all curves fall inside or close to the required gradation bands. It is observed that the particle size distribution of the #53 aggregate employed in this study falls at the low (coarser) end of the band, with the percentage of material finer than <0.5 mm consistently falling below the required limit. In the case of #8, data are presented for both virgin samples as well as for samples previously used for vibratory compaction tests. All curves fall in a relatively tight band indicating that no significant fracturing of the aggregates occurs as a result of compaction.

TABLE 3.1
INDOT proposed alternatives for pavement subbase

	Option 1	Option 2	Option 3	Option 4	Option 5	Option 6
Drainage	#8	#43	#43	HMA Open-graded	HMA Open-graded	#8
Separator	#53	NJDOT	Geotextile Woven	NJDOT	Geotextile Woven	NJDOT

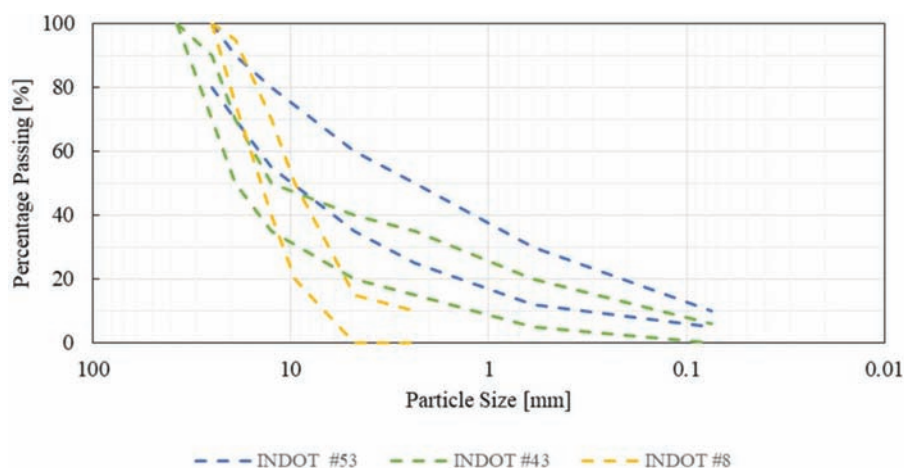


Figure 3.1 Particle size distribution ranges for #8, #43, #53 (INDOT, 2020).

For all three aggregates the percentage of fines (<0.075 mm) falls below 15%, in accordance with a general requirement for subbase aggregates (e.g., ACPA, 2007; AASHTO M-147, 2017).

Coarse fractions of each material were tested to measure the specific gravity (Gs) following ASTM C127-15 (2015). Two tests were performed on each material, yielding generally repeatable results. The average values were 2.76, 2.76, 2.77 for #8, #43, and #53, respectively.

3.2 Compaction Behavior

As summarized in Table 3.2, four different methods were used to determine the maximum dry unit weight of each aggregate.

In the scalping procedure, the particles retained on the 0.75" sieve were removed from the specimen to allow compaction in a 6" mold. The dry unit weight values reported in the following reflect the correction to the measured data recommended in ASTM D4718/D4718M-15 (2015). As free-draining granular soils typically present the maximum dry unit weight under either dry condition or close to saturation (Bergeron et al., 1998; Drnevich et al., 2007; Forssblad, 1981; Hilf, 1991; Parsons, 1992; Pike, 1972), each test type was performed at both water content conditions. Two replicate tests were conducted for each condition.

The results collected in this study were compared to data obtained in previous research projects (Drnevich et al., 2007; Evans, 2006; Prochaska, 2004) on similar pavement materials (Table 3.3).

A summary of the compaction results for INDOT #8 is presented in Table 3.4. It can be observed that the experiments performed with the 11" mold on the oven-dried aggregate ($w = 0\%$) provide the maximum dry unit weight.

Figure 3.2 presents both the results summarized in Table 3.4 and those obtained by Evans (2006). The data are presented both as absolute values (right ordinate) and normalized by the maximum unit weight obtained across both data sets (left ordinate). For the #8 aggregate, the result at 0% water content from the 11" vibratory hammer test was used to normalize all the data, and the values on the y axis represent the relative compaction with this value as the reference. The 148% saturation line is shown as a gray band, to reflect the potential variation in specific gravity ($G = 2.77\text{--}2.85$). The following observations can be drawn based on Table 3.4 and Figure 3.2:

- Replicate tests yield generally repeatable results.
- The results from the two studies are generally consistent, with the tests in dry conditions yielding the highest values of maximum dry unit weight.
- In both studies the Proctor results fall at the low end of the data, with relative compaction as low as $\sim 91.5\%$ (standard Proctor from Evans, 2006).
- As expected, scalping significantly impacts the results, as shown by the fact that the results obtained from the vibratory hammer tests using the 6" mold without scalping fall significantly below all other results including those obtained by Evans (2006) using the same method but with scalping.

TABLE 3.2
Compaction testing methods

Method	Source of Compaction Energy	Mold Size [in]	Scalp [Y/N]	Standard
1	Modified Proctor Hammer	6	N	ASTM D1557-12e1 (2012)
2	Vibratory Hammer	6	N	ASTM D7382-08 (2008)
3		6	Y	ASTM D7382-08 (2008); ASTM D4718/ D4718M-15 (2015)
4		11	N	ASTM D7382-08 (2008)

TABLE 3.3
Data sources used for comparison of compaction data

Source	Gradation	Standard Proctor	Vibratory H. 6"	Vibratory H. 11"
Evans (2006)	INDOT #8	Y	Y (scalped)	Y
	INDOT #53	Y	Y (scalped)	Y
Prochaska (2004)	INDOT #53	Y	Y	Y

TABLE 3.4
Compaction data for INDOT #8

Mold Diameter [in]	Method	Scalped [Y/N]	Specimen ID	Water Cont. [%]	Dry Unit Weight [kN/m ³] (pcf)
6	Modified Proctor	N	1	0.0	16.5 (105)
			2	0.0	17.0 (108)
6	Vibratory Hammer	N	1	0.0	16.0 (102)
			2	0.0	16.1 (102)
			1	27.6	15.9 (101)
			2	27.6	15.9 (101)
		Y	1	0.0	16.6 (105)
			2	0.0	17.1 (109)
			1	25.1	16.6 (106)
			2	24.6	16.7 (106)
11	Vibratory Hammer	N	1	0.0	17.2 (109)
			2	0.0	17.6 (112)
			1	23.4	16.8 (107)
			2	22.9	16.9 (108)

- Differences between the two sets of data may be related to variability in gradation of the materials tested.

The results for INDOT #53 are presented in Table 3.5. Also, in this case the replicate tests yield generally repeatable results. Note that, as a result of the better graded particle size distribution, the dry unit weight values are consistently larger (by 20%–25%) than those measured on #8. For #53, Table 3.5 shows that the highest values of maximum dry unit weight are obtained from the scalped specimens compacted by vibration in the 6" mold, after applying the correction that accounts for the removal of

the oversize particles (ASTM D4718/D4718M-15, 2015). The fact that these data exceed the results from the vibratory hammer in the 11" mold suggests that, at least in dry conditions, the correction leads to overestimate the unit weight. As a result, these data are not considered reliable.

Figure 3.3 presents the results included in Table 3.5, alongside additional data from two research projects (Prochaska, 2004; Evans, 2006) that employed similar materials (crushed limestone) with gradation falling within the band prescribed for INDOT #53. In both these studies the highest dry unit weight was reached before saturation using the vibratory 11" mold test, with

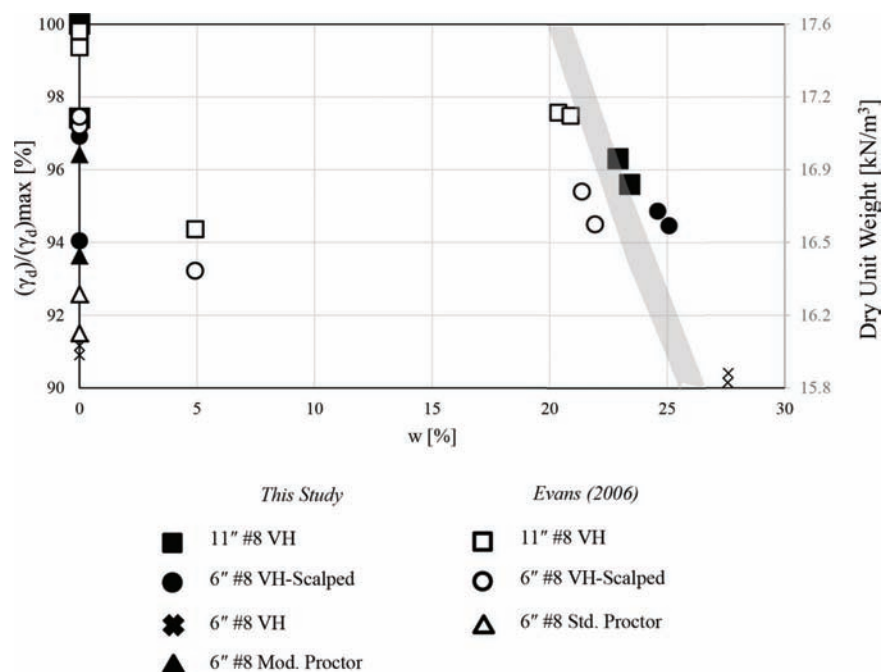


Figure 3.2 Compaction behavior of INDOT #8.

TABLE 3.5
Compaction data for INDOT #53

Mold Diameter [in]	Method	Scalped [Y/N]	Specimen ID	Water Cont. [%]	Dry Unit Weight [kN/m³ (pcf)]
6	Modified Proctor	N	1	0.0	21.4 (136)
			2	0.0	20.5 (130)
	Vibratory Hammer	N	1	0.0	21.9 (139)
			2	0.0	21.7 (138)
			1	13.9	20.7 (132)
			2	15.6	20.0 (128)
		Y	1	0.0	22.4 (143)
			2	0.0	22.1 (141)
			1	12.6	21.2 (135)
			2	9.3	22.7 (144)
11	Vibratory Hammer	N	1	0.0	21.8 (139)
			2	0.0	21.7 (138)
			1	11.8	21.3 (136)
			2	13.2	20.6 (131)
			3	3.3	19.4 (123)
			4	5.4	20.1 (128)
			5	7.2	21.4 (136)

lower values measured at both higher and lower water contents. While the two studies show qualitatively similar results, the optimum water content does appear to vary, likely a reflection of differences in the gradation. The value at 6% water content from the work by Evans (2006) is used to normalize the rest of the data. The following can be observed:

- As stated above, for #53 the maximum dry unit weight occurs at a water content below saturation.
- Proctor tests yield lower values of the dry unit weight relative to the vibratory tests, with values of the relative compaction equal to 95% or lower.
- Overall the data collected in this study are consistent with previous experience.

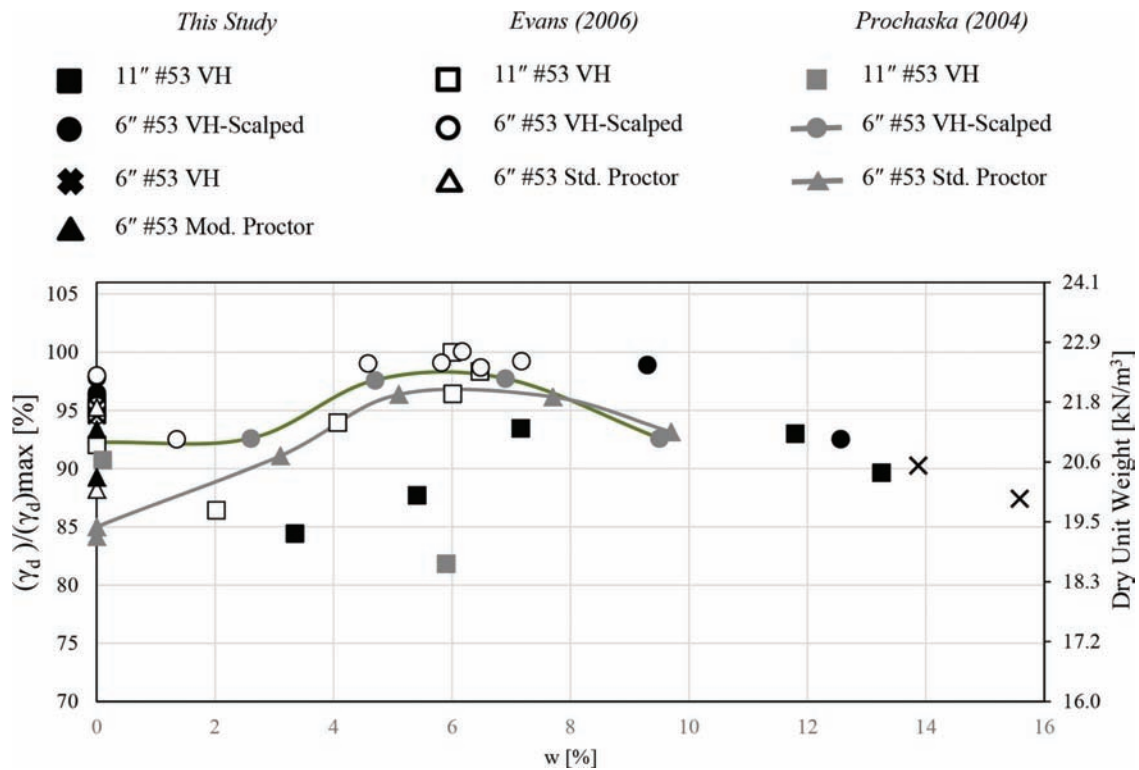


Figure 3.3 Dry unit weight behavior for INDOT #53.

TABLE 3.6
Compaction data for INDOT #43

Mold Diameter [in]	Method	Scalped [Y/N]	Specimen ID	Water Cont. [%]	Dry Unit Weight [kN/m ³ (pcf)]
6	Modified Proctor	N	1	0.0	21.2 (135)
			2	0.0	17.0 (108)
	Vibratory Hammer	N	1	0.0	20.7 (132)
			2	0.0	21.6 (137)
			1	11.4	21.8 (139)
			2	10.0	22.7 (144)
		Y	1	0.0	22.6 (143)
			2	0.0	22.8 (145)
			1	6.6	23.9 (152)
			2	6.4	23.9 (152)
11	Vibratory Hammer	N	1	0.0	22.2 (141)
			2	0.0	22.1 (140)
			1	8.6	21.5 (137)
			2	10.5	21.6 (137)
			3	5.6	18.3 (116)
			4	6.7	20.6 (131)

The results for aggregate #43 are presented in Table 3.6. They are on the same order of those collected for #53. No previous data were available for #43. Given the similarity in particle size distribution between #43 and #53, the data presented in Figure 3.3

are included in Figure 3.4, with the maximum value from the #53 data utilized to calculate the relative compaction. Also, for #43, the correction for scalping appears to lead to overestimate the dry unit weight.

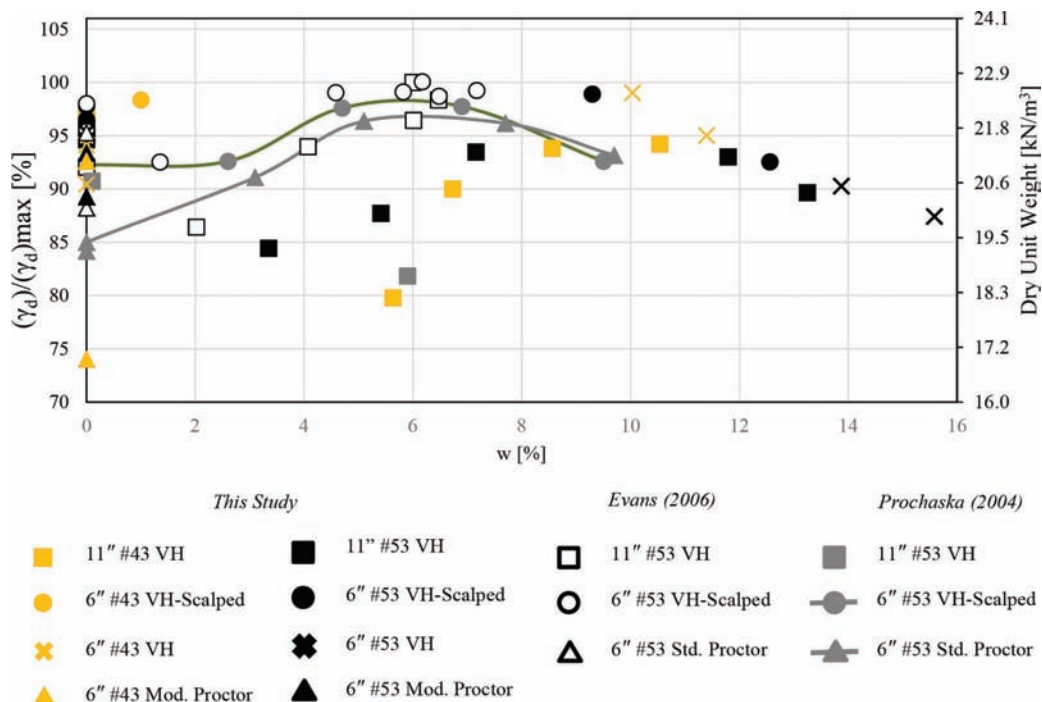


Figure 3.4 Compaction behavior of INDOT #53 and INDOT #43.

3.3 Hydraulic Conductivity

This section discusses the hydraulic conductivity of the aggregates (INDOT #8, #43, and #53) of interest to this study. First, estimates of the hydraulic conductivity obtained from empirical prediction models are discussed. Laboratory results of the vertical hydraulic conductivity obtained testing non compacted samples of #43 and #53 in a falling head setup are then presented. These data are then compared to existing literature results for materials with similar gradation and to predictions from empirical models. Finally, the design of a newly constructed apparatus built for measuring hydraulic conductivity is presented.

3.3.1 Empirical Prediction Models Used for Estimating Hydraulic Conductivity

Four prediction models were considered in this study: Moulton (1980/1990), Hazen (1892), Kenney et al. (1984) and Kozeny (1927)-Carman (1938, 1956). Predictions using these four models are presented in Figure 3.5 for the aggregates examined in this research. Details on these models and a summary of the input parameters used for each of the aggregates are summarized in Appendix D.

The values predicted by the models above are markedly dependent on the input parameters. All correlations consider, in one way or the other, the impact of particle size distribution, while only the ones by Moulton (1980/1990), Kozeny and Ofoegbu (1927), and Carman (1938, 1956) consider the effect of the state of compaction (as measured by porosity and void ratio, respectively).

For the correlations by Hazen (1982) and Kenney et al. (1984), the figures identify a single interval of values of k . This interval is defined by the values determined from the upper and lower bands of the particle size distribution curves shown in Figure 3.1 for each aggregate.

For the other two correlations two intervals are shown for each aggregate. Each was obtained using limit values for porosity (Moulton, 1980/1990) or void ratio (Kozeny, 1927; Carman, 1938, 1956) corresponding to a “dense” and “loose” condition. Specifically, e_{min} (and n_{min}) were derived directly from the vibratory hammer tests performed for this project. Estimates of e and n for the “loose” condition were obtained from measurements on the samples used for the hydraulic conductivity tests, in which the aggregates were pluviated vertically and not compacted. Again, for each compaction state, the interval shown reflects the variation in the particle size distribution parameters from the upper bound and lower bound curves presented in Figure 3.1. Overall, the broad ranges in k depicted in Figure 3.5 reflect the great uncertainty associated with the prediction of hydraulic conductivity using empirical correlations, especially when the input parameters are not well defined.

Finally, Figure 3.6 presents a plot adapted from Cedergren (1974), which shows reference values of hydraulic conductivity (in m/s) for different particle size distributions. The gradation bands for INDOT #8, #43, and #53 are also included. According to these data, the hydraulic conductivity of the #8 aggregate is expected to fall between 10^{-2} and 10^{-1} m/s. Always based on these data, the hydraulic conductivity of #43 and #53 is expected to be in the 10^{-3} to 10^{-4} m/s range.

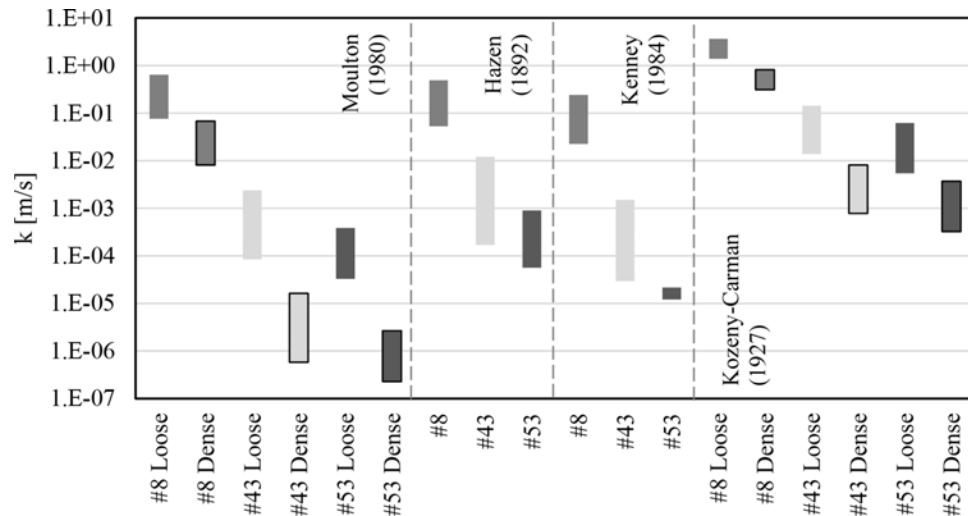


Figure 3.5 Values of k estimated from four prediction models for #8, #43, and #53.

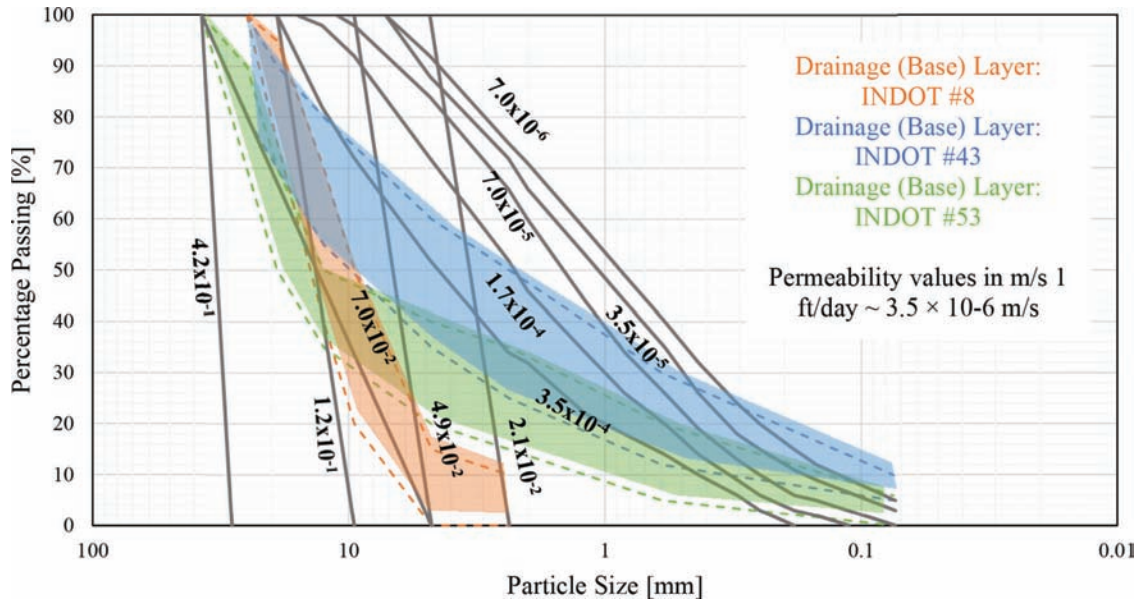


Figure 3.6 Hydraulic conductivity values for different gradations (based on Cedergren, 1974).

3.3.2 Falling Head Laboratory Results

Hydraulic conductivity tests were performed in Purdue's Geotechnical Laboratory using a vertical falling head permeameter on loan from INDOT's Research Laboratory. Testing focused only on INDOT #43 and #53. The setup used for testing is shown in Figure 3.7(a). It is comprised of an acrylic prismatic chamber with rectangular cross section (8 in \times 6 in), which rests on a stand that allows control of its inclination. Samples are prepared with the chamber in the vertical position, pluviating the dry aggregate from the top (Figure 3.7(b)). The chamber is built with a trap door at its bottom, which is kept closed during pluviating. A removable perforated screen is positioned at the bottom of the chamber prior

to pluviating to avoid loss of the material during the subsequent flow stages.

The height of the samples tested in this research varied between 0.70 and 1 m. For each sample a value of the preparation dry density can be calculated from the mass of the pluviated material and the sample dimensions. As summarized in Table 3.7, the preparation procedure generates medium-loose samples with relative compaction between 73% and 78%. These values of relative compaction use as a reference γ_{dmax} values of 21.8 kN/m³ and 22.1 kN/m³ determined for #53 and #43, respectively, from vibratory hammer tests performed in the 11" mold on unscalped dry material (see Section 3.2).

Following pluviating, a second perforated screen is placed at the top of the sample to maintain the surface

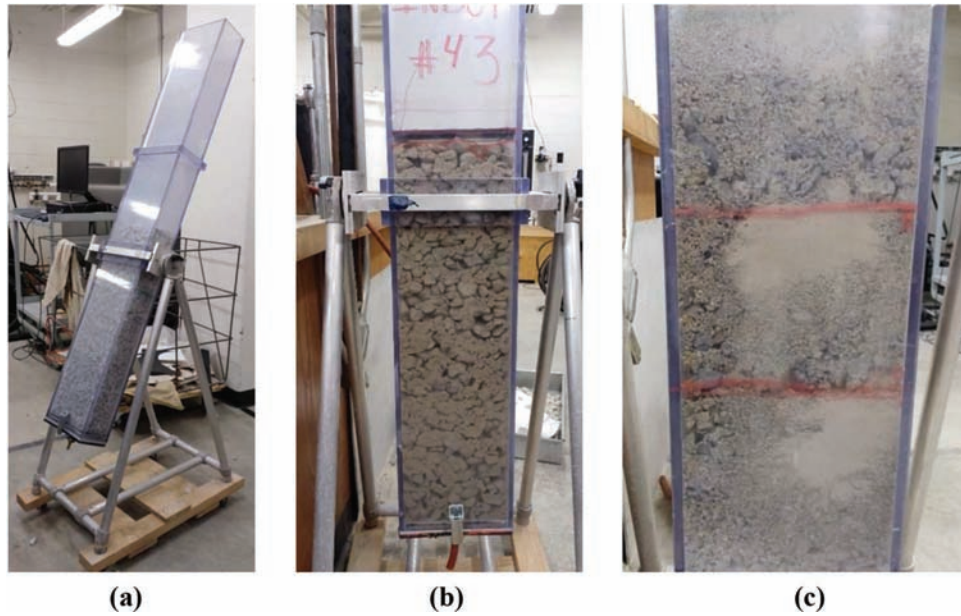


Figure 3.7 (a) Falling head permeameter and view of sample, (b) immediately after setup, and (c) after a test in which significant migration of the fines was observed.

of the aggregate sample perpendicular to the walls when the chamber is inclined. Both screens are designed to contribute negligible head loss during the experiment. The sample is then saturated by flushing de-aired, de-ionized water upwards through a valve installed in the bottom trap door of the chamber. Once the specimen is saturated, water is added at the top of the sample to reach a desired height (which corresponds to a target initial gradient). The chamber is then tilted to its flattest inclination and the bottom trap is released to start the downward flow. The variation of the hydraulic head is registered with time using a video camera and a stop watch mounted on the chamber. Once the water level reaches 1–2" above the soil surface, the measurement is stopped to avoid desaturation of the samples. Values of hydraulic conductivity are calculated as outlined in ASTM D5856-15 (2015), using the expression below:

$$k = \frac{aL_f}{A\Delta t} \ln\left(\frac{h_1}{h_2}\right) \quad (\text{Equation 3.1})$$

where a is the cross section of the reservoir containing water at the top of the sample, A is the cross section area of the chamber, L is the height of sample, and h_1 and h_2 are the values of the head differential across the sample at the start and end of the time interval Δt . Given that in the setup shown in Figure 3.7, a is equal to A , their ratio is 1, and does not come into play. Several values of k are derived during a single falling head test as the gradient decreases, and more than one set of measurements can be performed at a given inclination after refilling the water above the sample. After completing measurements under the first inclination, the inclination is changed and a new set of measurements are made. This procedure is repeated

until the chamber is positioned vertically. In select tests, the chamber is rotated back to the previous inclinations to conduct additional measurements and ensure that the testing order does not affect the results.

Table 3.7 summarizes the results of the 8 tests performed on #43 and on #53. For each test, the table includes the starting values of dry density and relative compaction, the gradient range and the number of repetitions performed at each inclination, the range in k values measured at each inclination, and, finally, the average and standard deviation values obtained from all measurements performed on a given sample. These same values are plotted in Figure 3.8(a). In general, with the exception of the first test on #53 the data are found to be repeatable, and no significant difference is observed between the results for #43 and #53. As shown in Figure 3.8(b), which shows data from a single test (#53_4), the results are found to be gradient dependent. This indicates that the flow conditions are not laminar. For both aggregates almost all measured values of k exceed the 50–150 ft/day range ($\sim 15\text{--}46$ m/day $\sim 1.7 \times 10^{-4} - 5.7 \times 10^{-4}$ m/s) for free-draining sub-bases proposed by the ACPA (2007). In many cases the upper limit of 350 ft/day ($\sim 1.2 \times 10^{-3}$ m/s) recommended by this agency is also exceeded. These limits on the hydraulic conductivity have superseded older recommendations (e.g., FHWA, 1992) which allowed materials with target k of 548–3,480 ft/day in laboratory tests. These values which are typical of open-graded aggregates were found to be associated with a number of issues, from stability problems under heavy equipment, to early age cracking of the pavement as a result of penetration of the concrete into the subbase voids, to loss of support due to aggregate breakdown.

While the data obtained from these tests can be generally considered representative of medium-loose

TABLE 3.7
Summary of falling head test results

Material Test	γ_d (kN/m ³)RC ^a	Gradient Range (at each inclination)	Repetitions (at same inclination)	Hydraulic Conductivity [$\times 10^{-3}$ m/s]	Average [$\times 10^{-3}$ m/s]	Standard Deviation [10^{-3} m/s]
#43 1	17.26 78%	0.35–0.39	1	3.5–7.1	5.29	0.91
		0.64–0.76	2	3.9–7.0		
		0.99–1.21	2	3.9–6.9		
		1.18–1.32	2	5.1–8.0		
		1.31–1.60	1	3.9–6.2		
#43 2	17.26 78%	0.33–0.34	1	5.1–7.0	8.16	1.66
		0.52–0.64	1	4.2–13.4		
		0.81–0.96	1	6.1–10.8		
		1.01–1.11	1	6.7–9.4		
		1.17–1.31	1	5.4–9.3		
#43 3	16.48 75%	0.31–0.37	3	2.7–6.6	5.30	0.86
		0.58–0.67	3	3.9–5.7		
		0.79–0.94	2	4.3–5.9		
		1.05–1.19	2	4.9–6.4		
		1.22–1.38	2	3.6–7.6		
#43 4	16.77 76%	0.30–0.32	1	1.6–1.8	1.48	0.94
		0.59–0.62	1	2.9–3.5		
		1.11–1.20	1	1.0–1.1		
		1.80–1.87	1	0.3–0.4		
		0.25–0.28	1	3.4–4.5		
#53 1	15.79 73%	1.10–1.13	1	0.5	1.67	1.57
		1.48–1.54	1	0.6–0.7		
		0.63–0.77	1	8.8–17.6		
		1.12–1.34	1	3.3–4.4		
		1.35–1.59	1	4.6–7.3		
#53 2	16.38 75%	0.64–0.80	1	9.6–30.8	9.09	5.81
		0.23–0.27	1	6.3–16.9		
		0.37–0.41	2	1.1–2.6		
		0.71–0.84	2	1.6–3.8		
		1.01–1.26	2	2.1–3.6		
#53 3	16.67 77%	1.26–1.60	2	2.8–4.1	2.75	0.66
		1.39–1.60	1	2.2–4.9		
		0.37–0.40	2	1.6–2.5		
		0.64–0.81	2	1.9–3.2		
		1.02–1.23	2	2.4–4.0		
#53 4	16.57 76%	1.22–1.54	2	2.9–4.8	2.94	0.58
		1.46–1.74	1	2.5–4.3		

^aRelative compaction (RC) calculated based on γ_{dmax} from vibratory hammer tests in 11" mold on dry unscalped material.

samples, the apparatus does not allow compaction of the soil. Moreover, migration of the fines is often observed during the test (see Figure 3.7(c)). This suggested that alternative testing approaches should be pursued and was the motivation for designing and building a new apparatus (see Section 3.4).

Finally, hydraulic conductivity tests were also conducted using a 6-in diameter rigid wall permeameter. These tests, however, indicated that, due to the high conductivity of the samples, the measurements were controlled by head losses within the apparatus. As a result, these tests were discontinued.

3.3.3 Comparison to Data from Literature

Hydraulic conductivity data for aggregates having particle size distribution similar to that of the aggregates considered in this research were collected from

studies by Randolph et al. (1996), Roy and Sayer (1989) and Jones and Jones (1989). Before presenting a comparison to the data collected in this project, the materials and testing methods employed in these three studies are briefly reviewed.

3.3.1.1 Randolph et al. (1996). The study from the Ohio Department of Transportation provides horizontal hydraulic conductivity data measured in the laboratory on dense samples compacted vertically using a vibratory hammer (flow perpendicular to compaction direction). Data sets for three aggregates, ODOT #57, ODOT #67 and ODOT #304, are directly relevant to this study.

The first two—ODOT #57 and ODOT #67—both have gradation similar to that of #8 (see Figure 3.9). In the case of ODOT #57, Randolph et al. (1996) tested

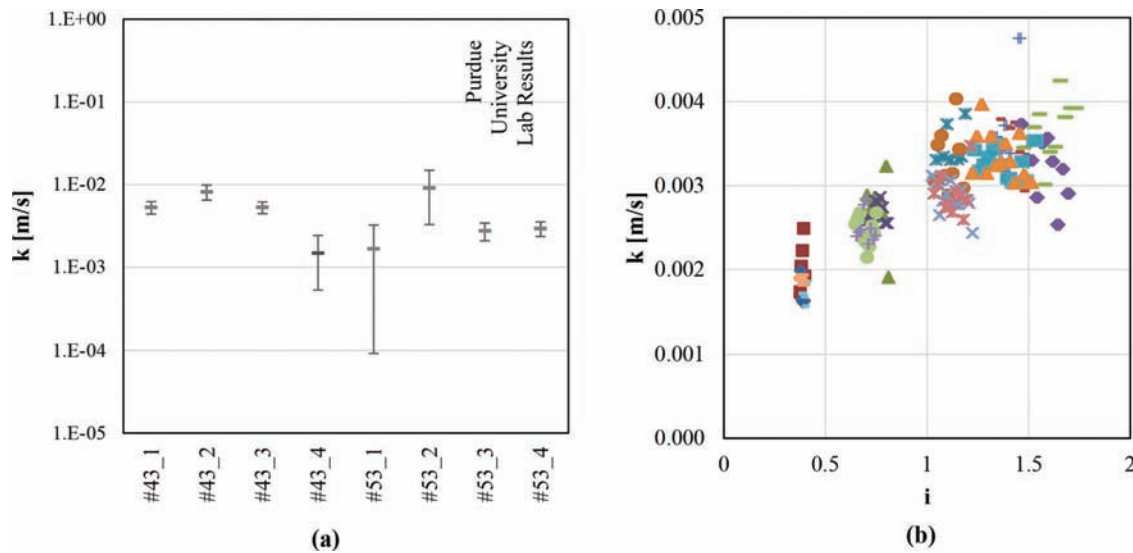


Figure 3.8 (a) Hydraulic conductivity results (average +/- standard deviation) from falling head tests on #43 and #53; (b) dependence of k data on hydraulic gradient for test #53_4.

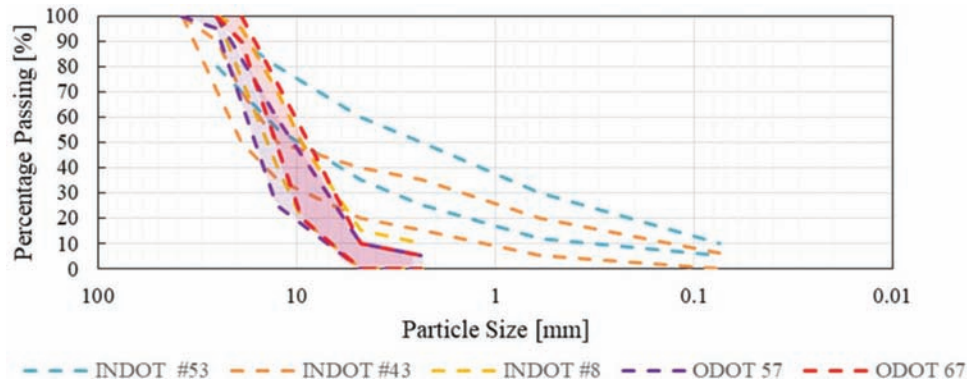


Figure 3.9 Comparison of particle size distribution bands of ODOT 57 and ODOT 67 aggregates to the gradation bands for INDOT #8, #43, and #53.

three materials of different origin (a slag, a gravel, and a crushed limestone), all falling within the #57 band. For one of these materials—the slag—three different gradations (fine, medium, and coarse) were tested. For the other two materials data are available only for the medium gradation. Also, in the case of ODOT #67, Randolph et al. (1996) tested three materials of different origin (a slag, a gravel, and a crushed limestone), all with medium gradation within the #67 band, and all characterized by identical values of D_{10} , D_{60} , and C_u . The k data obtained by Randolph et al. (1996) for ODOT #57 and #67 all fall above 0.1 m/s (over 20,480 ft/day), exceeding the thresholds recommended for a drainage layer. Given the similarity in gradation, this is expected to be the case also for #8. Indeed, the high hydraulic conductivity of #8 precluded using the falling head permeameter described above.

The third aggregate tested by Randolph et al. (1996), ODOT #304, has a particle size band that encompasses that of #53 and the top half of #43 (see Figure 3.10). The experiments performed by Randolph et al. (1996) were done blending an aggregate to three specific

particle size distributions corresponding to the end limits and the average of the ODOT 304 gradation. These three gradations are referred to as #304 fine, medium and coarse. This was done for three different aggregate sources: limestone, gravel and slag. The results from tests on these gradations (each symbol corresponds to an individual test) are shown in Figure 3.13 alongside the data obtained in this research.

3.3.1.2 Roy and Sayer (1989). The data contained in Roy and Sayer (1989) are from laboratory and field tests conducted on aggregates falling within the range identified by the black dashed lines in Figure 3.11. Constant head tests with vertical flow were performed in the lab on samples vertically compacted to conditions similar to those encountered in the field. The field data are from pumping tests between two vertical holes and thus reflect the horizontal hydraulic conductivity. The results from tests on these gradations are shown in Figure 3.13 (each symbol corresponds to an individual test) alongside the data obtained in this research.

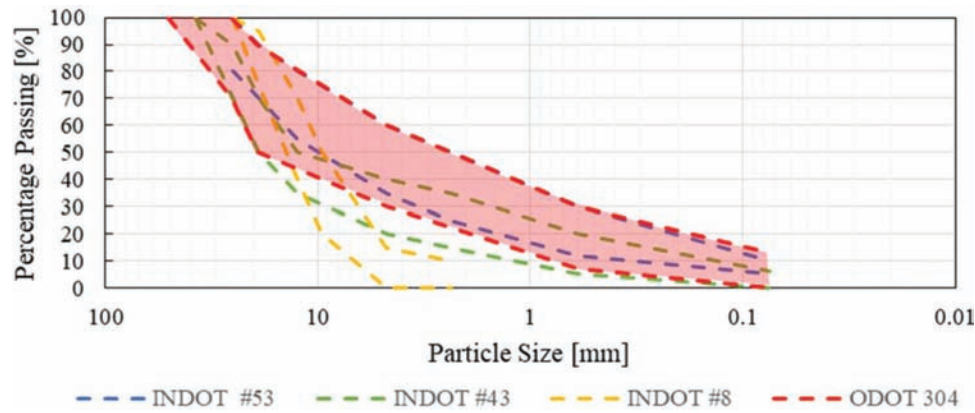


Figure 3.10 Comparison of particle size distribution band of ODOT 304 aggregate to the gradation bands for INDOT #8, #43, and #53.

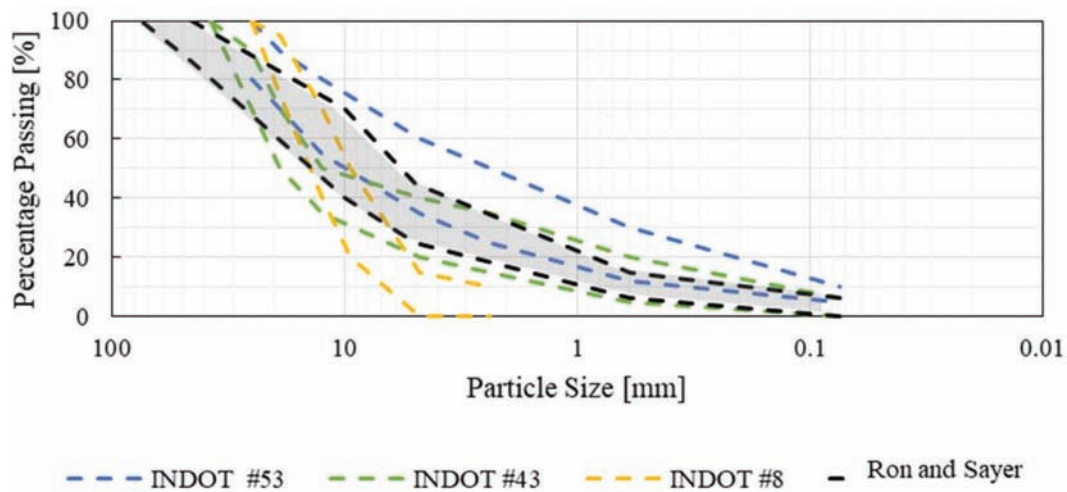


Figure 3.11 Comparison of particle size distribution band of aggregates investigated by Roy and Sayer (1989) to the gradation bands for INDOT #8, #43, and #53.

3.3.3.3 Jones and Jones (1989). Jones and Jones provide data for three sources of aggregates: crushed limestone, sandy gravel and granite. For each of these materials three different gradations (coarse, middle and fine) identified by the curves shown in Figure 3.12 were examined. The fine and medium curves fall within the #53 band, while the coarse one is inside the #43 band. Hydraulic conductivity was measured performing constant head tests with horizontal flow through samples of dimensions 1 m (length) \times 0.3 m (height) \times 0.3 m (width). The aggregate sample was vertically compacted in dry conditions in 4–5 layers using a vibratory hammer, and then saturated with de-aired water. Gradients applied were low enough to ensure the applicability of Darcy’s Law. Measurements were performed on three independent samples for each aggregate source and each gradation. The values reported in Figure 3.13 reflect the average \pm the standard deviation from each data set.

A direct comparison between the literature data and the results obtained at Purdue is not possible given the difference in density (only medium-loose samples were tested at Purdue versus dense in the three literature studies), and in the direction of flow (vertical flow in the

Purdue tests versus horizontal in two out of the three studies reviewed). Despite this, the literature data appears relatively consistent with the lab results collected as part of this research, with the vast majority of the tests exceeding the 350 ft/day threshold. Analysis of the literature data also highlights the significant variation in hydraulic conductivity that is measured for gradations falling within the same band (e.g., compare the results for fine, medium and coarse #304 (Randolph et al., 1996), which show a variation of one to two orders of magnitude for the same source material), and the role played by aggregate source (e.g., compare data for different sources of the fine aggregate in both the studies by Jones and Jones (1989) and Randolph et al. (1996), which both show a range of approximately one order of magnitude).

3.3.4 Comparison to Predictions from Empirical Correlations

Values of hydraulic conductivity collected during this project, as well as those reported by Randolph et al. (1996) and Jones and Jones (1989) were compared to

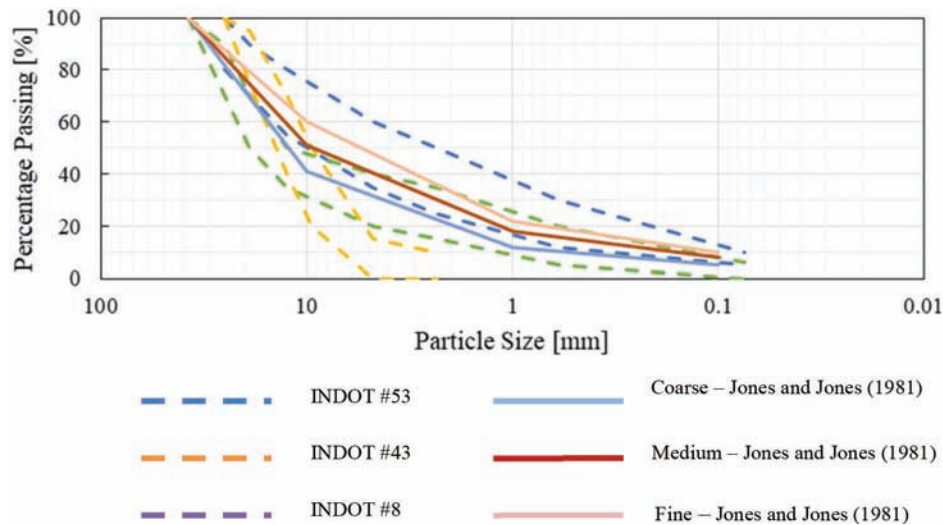


Figure 3.12 Comparison of particle size distributions of coarse, medium, and fine aggregates investigated by Jones and Jones (1989) to the gradation bands for INDOT #8, #43, and #53.

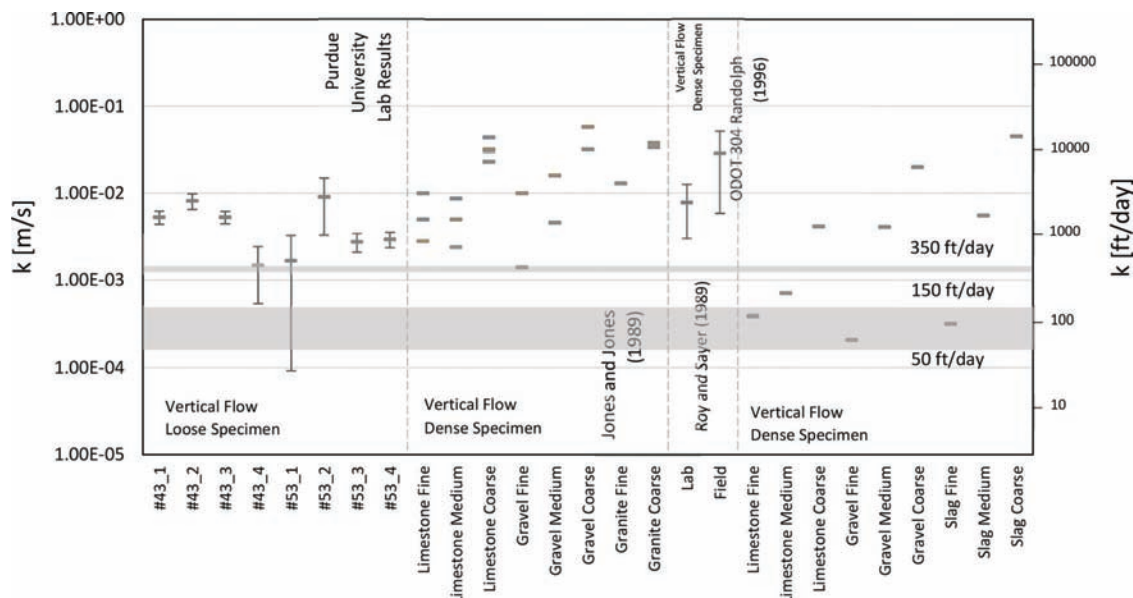


Figure 3.13 Comparison of hydraulic conductivity results from this study to literature data for similar aggregates (thresholds based on ACPA (2007)).

predictions derived from the empirical models listed above.

The first comparison is presented in Figure 3.14 for the prediction model by Moulton (1980/1990). For aggregates #43 and #53, the values of D_{10} , n and P_{248} measured on the specific samples tested in this project were used as input parameters (see Appendix D). The figure indicates that for all aggregates shown, the correlation by Moulton (1980/1990) does not provide reliable estimates, in most case underestimating k , by as much as five orders of magnitude. This is significant as this is the model employed in the DRIP software used by many agencies, including INDOT, for drainage design.

Similar comparisons are presented for the models by Hazen (1892), Kenney et al. (1984) and Kozeny

(1927)-Carman (1938, 1956) in Figure 3.15 (for reference the predictions by Moulton are also shown again). Again, the input parameters were derived from the particle size distributions obtained or reported for the specific aggregates tested (see Appendix C). These comparisons show that for materials similar to #43 and #53 the best predictions of the hydraulic conductivity are provided by the Kozeny-Carman model, with deviations generally less than one order of magnitude from the measured values, and no consistent tendency of the model to underestimate or overestimate k . The other two empirical models both tend to consistently underestimate k for this type of aggregate.

With regard to the material similar to #8 (ODOT #57 and #67), the prediction obtained using the

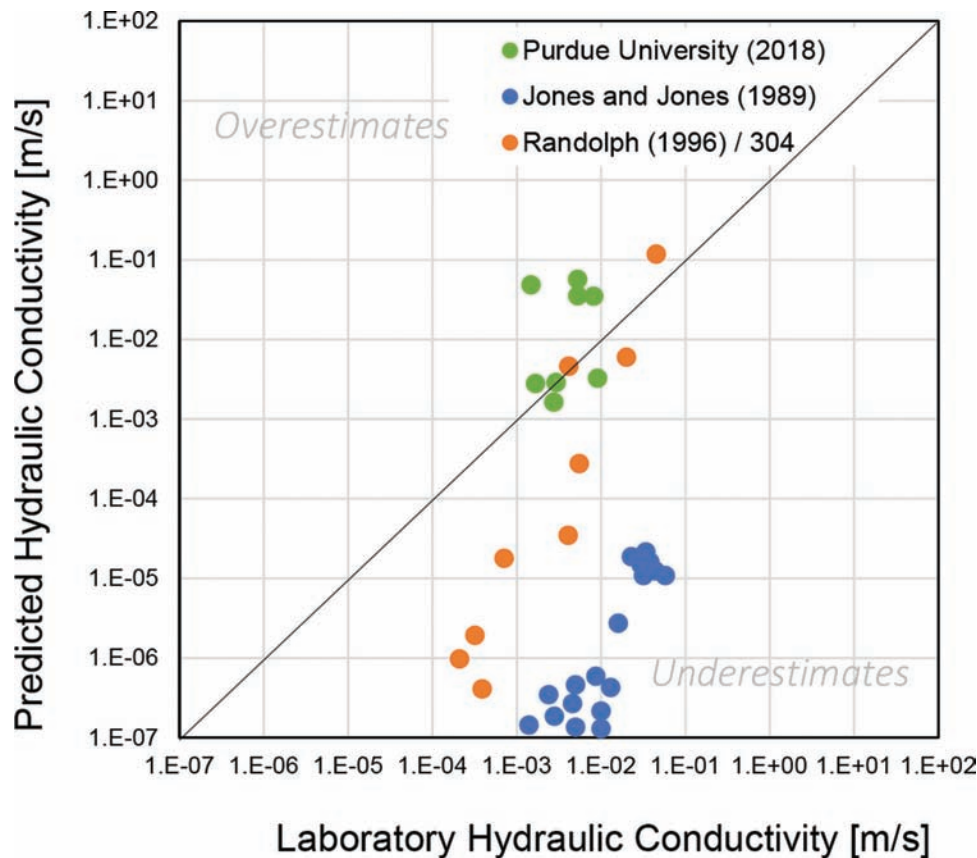


Figure 3.14 Comparison of hydraulic conductivity data for #43 and #53 and similar materials to predictions using the model by Moulton (1980/1990).

Hazen (1892) and Kenney et al. (1984) models show the best agreement with the laboratory results. Given that the data come from a single study, this conclusion requires further validation. Note also that, for both ODOT #57 and #67, D_{10} ranges between 0.4 and 0.8 cm, outside of the range for which the use of the expression by Hazen is generally recommended (Carrier, 2003).

3.4 Design and Construction of Horizontal Permeameter

Hydraulic conductivity is a key parameter in the performance of pavement coarse subbases. It speaks to the ability of the layer to drain water out of the structure. Measurement of this property in the lab requires that the testing conditions be representative of the field conditions where: the material is placed in a large and horizontally unbound domain, the aggregate is compacted to the maximum dry unit weight, flow is close to horizontal and perpendicular to the compaction direction, and the hydraulic gradients are small. It is acknowledged that in the field flow through the aggregate layer will be mostly under unsaturated conditions. However, as with other geomaterials, it is common to measure the saturated hydraulic conductivity of the material, which can be considered as an upper band to the values expected in the field.

As described above, as part of this project, preliminary measurements of the hydraulic conductivity were obtained from both constant head tests performed using a 6" Proctor mold and from falling head tests in a large acrylic permeameter. Both tests highlighted some of the challenges in measuring the hydraulic conductivity of aggregates such as those of interest to this study, including the following:

- the need to ensure that the measurements are not controlled by the permeability of the setup (e.g., porous stones, valves);
- the requirement to test large representative samples;
- the ability to control and quantify the compaction of the sample;
- the difficulty in ensuring and maintaining saturation of the sample during the test;
- the ability to apply and control small gradients;
- the uncertainty in deriving horizontal hydraulic k values from measurements in which the flow is vertical.

A new experimental set-up was designed and built to address these shortcomings. The design is inspired by the work by Hydraulics Research Limited (1985, 1986). This type of permeameter has also been used by select transportation agencies in the U.S., including the Ohio Department of Transportation. The setup is comprised of four major components:

- the permeameter cell,
- the water reservoirs,

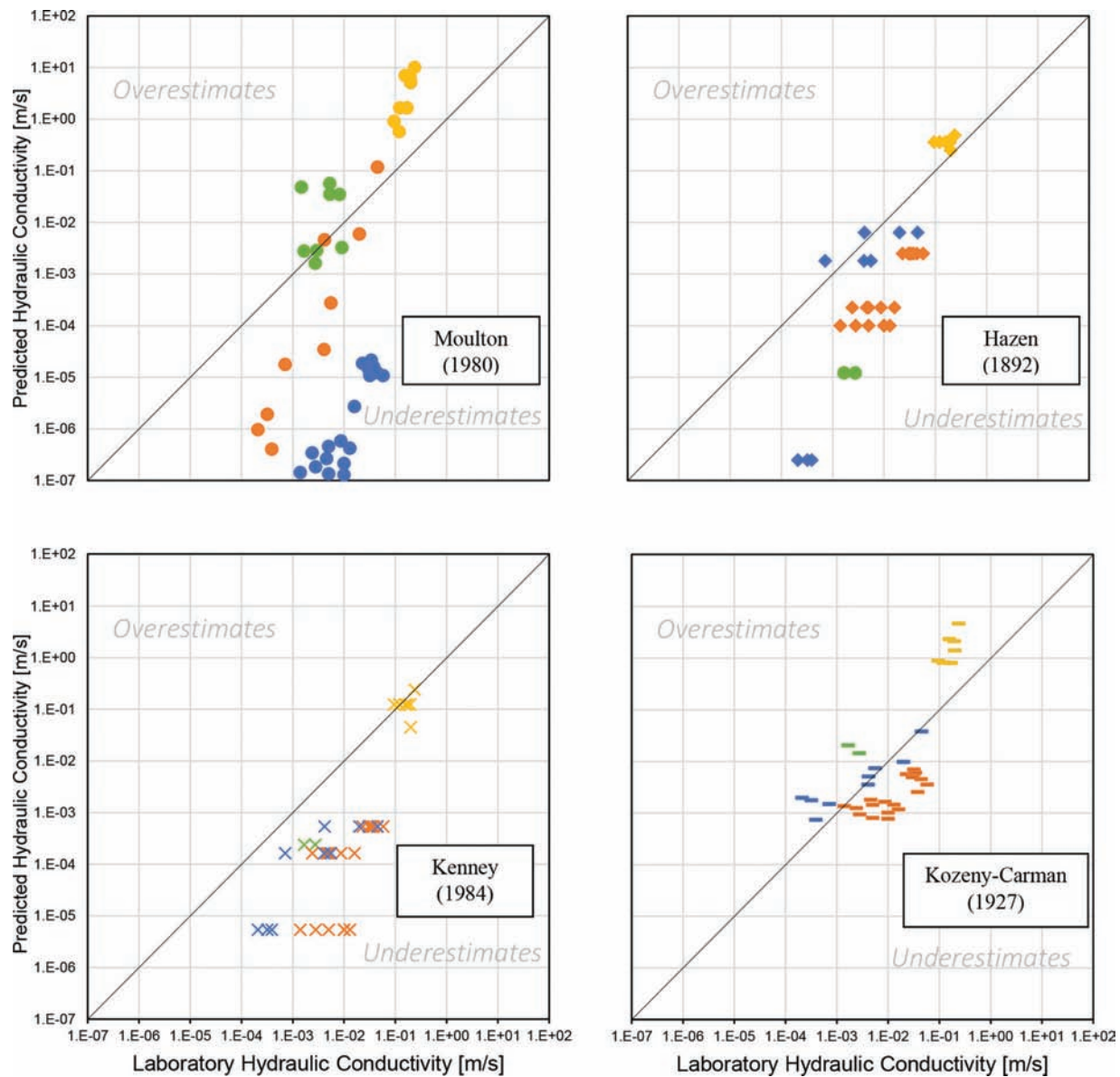


Figure 3.15 Comparison of hydraulic conductivity data to predictions using empirical models.

- the plumbing, and
- the instrumentation.

The first three components are shown assembled in Figure 3.16.

The cell is built from $\frac{1}{4}$ " thick stainless steel plates. The bottom part (12" [30.5 cm] \times 12" [30.5 cm] \times 43" [109.2 cm] inside dimensions) is designed to house a prismatic soil specimen with a 12" \times 12" cross section and a 36" [91.4 cm] length. The walls of the permeameter cell are welded. Both walls and joints are strong enough to resist the stresses induced during compaction. Twenty-eight bolts positioned at a spacing of 125 mm along the 6 cm wide top lip of the cell are used to connect the top cover. A rubber gasket ensures that the

enclosure is water tight. The cover of the cell is stiffened with three parallel rectangular (0.5" \times 1") reinforcing bars that extend over the entire length of the cover, with three orthogonal bars connecting them. A port is machined in the cover. It enables the application of vacuum during flushing with water. The location of the valve facilitates saturation from bottom to top and allows the air to be released at the top reducing the chances that it remains trapped in the void network. Two stainless steel handles are welded to the cover to facilitate its placement and lifting.

As shown in Figure 3.16, the permeameter design includes two rows of three ports in the side, for the installation of pressure transducers. These, in conjunction



Figure 3.16 Purdue horizontal flow permeameter.

with the GEOTAC data acquisition system available in Purdue's Geotechnical Laboratory, allow tracking the head loss along the specimen. Moreover, the two parallel rows provide the additional capability to track flow throughout layered materials. Drawings of the permeameter cell are provided in Appendix E.

For the gradation tested, the three major dimensions of the cell meet the requirement of being at least 10 times bigger than the maximum size of the particles. The size of the cell allows compaction to be performed using a method (vibratory hammer) that mimics conditions occurring in the field. Moreover, the large dimensions of the permeameter can accommodate representative samples of the coarse materials of interest to this work.

In this setup the material placement orientation as well as the direction of densification are vertical. As shown in Figure 3.16, the connections to the input and output water lines are placed at the ends of the longest dimension of the cell. Thus, the flow is essentially horizontal. Inside the permeameter, stiff ($\sim 0.1''$) mesh screens made of stainless steel bound the ends of the specimen at 3.75" from the ends, separating the specimen from the connections to the water input and output lines, and guaranteeing a unique flow direction throughout the entire specimen.

Two four-gallon square pails are used as water reservoirs to perform constant head tests, recording the mass of water flowing out of the sample during a known time frame. The total heads in the reservoirs are controlled through the pipes threaded into the sides, which function as weirs. Interpretation of the constant head tests is based on Darcy's law, which relies on laminar flow through the specimen. For the types of materials examined in this study this requires a hydraulic gradient smaller than approximately 0.05 (e.g., Jones & Jones, 1989). However, under field conditions, the hydraulic gradient is expected to be smaller by an order of magnitude or more. Different gradients can be achieved by controlling the difference in head between the two reservoirs. For the gradients at the

low end of the range of interest ($i < 0.485$), given the length of the sample, this requires maintaining a difference in total head between the reservoirs of less than for 5 mm. This requires careful control of the testing conditions.

Flexible tubing is used to connect the reservoirs to the cell. Four large diameter PVC valves are used to block the flow both at the reservoirs and at the two ends of the cell. The diameter of the valves and of all the tubing in the apparatus is 2". This size is necessary to (a) ensure that the head losses through the set-up do not control the results (as was observed in some preliminary tests performed using a Proctor mold); and (b) provide the required flow rate.

The aggregate can be placed in several layers. Each layer is compacted using a vibratory hammer as illustrated in Figure 3.17(a). A rectangular wooden tamper is positioned between the hammer and the aggregate surface. The size of the tamper (7.25" \times 11.75") was chosen to cover the entire surface of the specimen in six applications. Preliminary tests show that for #43 over 90% relative compaction is achieved using four layers, with one minute of vibration at each of the six locations for each layer. This will not necessarily be the case for other gradations. Figure 3.17(b) shows the surface of the specimen at the end of the compaction process. The exact height of the specimen is obtained measuring the distance from the top of the permeameter to the top of the aggregate layer using a depth micrometer. Several measurements are conducted to obtain an average value.

A foam sheet with thickness of $\sim 1''$, is placed on the compacted specimen before positioning the cover to avoid preferential flow along the top of the soil (Figure 3.18(a)). Figure 3.18(b) shows the indentation into the foam sheet after completion of a test. It suggests that the foam is effective in avoiding preferential flow at the cover-aggregate interface. Current modifications involve placing the same type of foam also on the sides of the permeameter to avoid preferential flow along these surfaces.

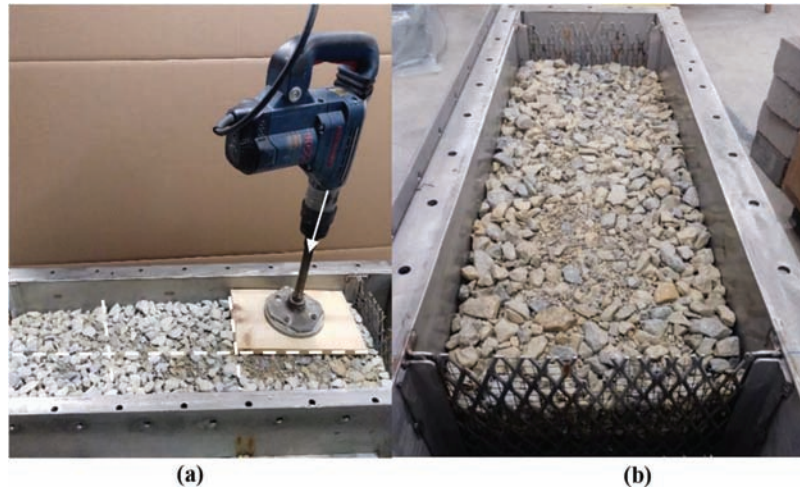


Figure 3.17 (a) Vibrating hammer and tamper used to compact each layer; (b) aggregate surface after compaction.

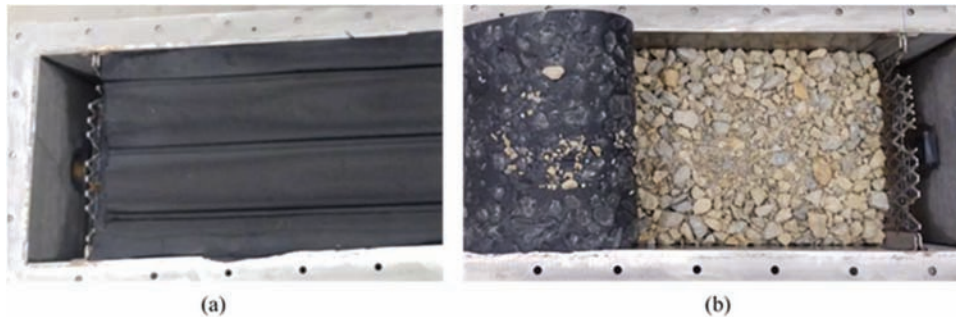


Figure 3.18 Foam sheet used to avoid preferential flow: (a) top view of specimen covered with the foam; (b) top view of the contact between foam and specimen after a test.

The following main conclusions can be drawn from the study of the compaction and hydraulic conductivity properties of aggregates #8, #43, and #53:

With regard to the compaction behavior:

- The data collected in this project support the conclusion from previous studies that the vibratory hammer method is the most effective method for the laboratory compaction of granular materials such as the aggregates of interest to this study. This method should be used as laboratory reference in compaction specifications when a value of the relative compaction must be prescribed.
- For the #8 aggregate the maximum dry unit weight is reached under dry conditions, whereas for #43 and #53 this occurs in correspondence to an optimum value which falls in the 4%–10% range. This value is aggregate specific and must be determined in the laboratory.

With regard to the hydraulic conductivity:

- Based on literature data for materials with similar gradation, values of the hydraulic conductivity in excess 10^4 ft/day should be expected for #8. This value falls well above the limit for permeable subbases (350 ft/day $\sim 1.2 \cdot 10^{-3}$ m/s), which, according to the ACPA (2007) “have had a problematic history in the field.”

- Also falling above this limit, are the vast majority of the values of k reported for aggregates similar to #43 and #53 (Jones & Jones, 1989; Randolph et al., 1996).
- Based on published data (e.g., see results from Randolph et al., 1996), small variations in particle size distribution can lead to changes in k as large as 2 orders of magnitude. Aggregate origin appears to play a lesser role (e.g., see data by Randolph et al., 1996 and Jones & Jones, 1989).
- Based on the tests performed and the analysis of literature data, the Moulton (1980/1990) model used in the DRIP software, may provide predictions that differ significantly from the measured values. Its use should be considered with care.
- The falling head apparatus employed in this study provides relatively consistent results. However, a few important shortcomings limit its applicability. Specifically, the method is limited to testing medium-loose samples; measures vertical hydraulic conductivity instead of the horizontal value which has more relevance to the drainage performance of aggregate layers in the field; and the sample preparation procedure yields non-homogeneities.
- The newly constructed horizontal permeameter addresses these shortcomings and provides the opportunity to measure the hydraulic conductivity of subbase aggregates under conditions more representative of the in situ conditions.

4. REVIEW OF LITERATURE SHEAR STRENGTH DATA

The peak friction angle (ϕ'_p) is the key parameter required to evaluate the stability of granular masses. In this research it was required as an input parameter for the analyses presented in Section 5 to evaluate the stability of the subbase layers under the weight of compaction and paving equipment. Measurements of the friction angle of the aggregates of interest to this study could not be performed given the particle size, the tests require large diameter triaxial cells, or large direct shear devices that are not available in Purdue's geotechnical engineering laboratories. Instead, a review of the literature was performed to identify data for similar materials obtained at confining stress levels relevant to this study (<148 kPa, and preferably <30 kPa). The database assembled through this effort is presented in Section 4.1. The results of the statistical analysis performed to investigate the factors controlling the measured peak friction angle are discussed in Section 4.2.

4.1 Peak Friction Angle Database

Shear strength data for aggregates having particle size distribution similar to that of the aggregates considered in this research (INDOT #8, #43, and #53) were obtained from studies by Nicks et al. (2015), Chow et al. (2014) and Aghaei Araei et al. (2010). The

materials and testing methods employed in these three studies are briefly reviewed below. Key information regarding the three studies is summarized in Table 4.1 as well as in Appendix F.

4.1.1 Nicks et al. (2015)

The study by Nicks et al. (2015) performed as part of a USDOT project involved both large triaxial (specimens 6" (152 mm) in diameter and 12" (305 mm) in height) and large (12" by 12" by 8") direct shear tests on loose ($D_r = 30\%$) aggregates. Only the data from the triaxial tests, which were conducted on saturated specimens isotropically consolidated to stresses between 5 and 30 psi (34 kPa–207 kPa), are used here. Aggregates all with the same mineralogy (diabase) were tested. Figure 4.1(a) shows the average of each of the particle size distributions tested. Of these, ten have relatively uniform particle size distributions ($C_u = 1.5$ –3), with five (N2–N6 in figure below) having distributions falling very close to or within the #8 band. A summary of the peak friction angles obtained from this study is shown in Figure 4.1(b). Even for the very low relative density examined in this study the peak friction angle at the lowest confining stress (35 kPa) exceeds 40° . Along with the expected decrease in friction angle with confining stress, the plot shows that at low confining stresses, the higher values are measured on the coarser materials.

TABLE 4.1
Testing conditions and parameters investigated in the three studies

Source	Gradation	Tests	Variable Set	Parameter	Test
Nicks et al. (2015)	INDOT #8	Large Triaxial (LT) $D_r = 30\%$	Confining Stress ~ [35-210] kPa	Confining Stress	Triaxial
			Angularity	Angular Index (AI)	Aggregate Imaging Measurement System (AIMS2) Gates et al. (2011)
			Sphericity	Sphericity	
			Roughness	Texture Index (TI)	
			Particle Size Distribution	C_u, C_c, D_{50}	ASTM D6913/D6913M-17 (2017)
Chow et al. (2014)	INDOT #43 INDOT #53	Large Triaxial (LT) $D_r \sim 100\%$	Confining Stress ~ [34-140] kPa	Confining Stress	Triaxial
			Angularity	Angular Index (AI)	Enhanced University of Illinois Aggregate Image Analyzer (E-UIAIA) Moaveni et al. (2013)
			Sphericity	Flat and Elongated Ratio (FER)	
			Roughness	Surface Texture Index (TI)	
			Particle Size Distribution	C_u, C_c, D_{50}	ASTM D6913/D6913M-17 (2017)
Aghaei Araei et al. (2010)	INDOT #43 INDOT #53	Large Triaxial (LT) $D_r \sim 100\%$	Confining Stress ~ [34-140] kPa	Confining Stress	Triaxial
			Hardness	Los Angeles	ASTM C131/C131M-14 (2006)
			Resistance	Point Load-Strength Index (Is)	ASTM D5731-16 (2016)
			Particle Size Distribution	C_u, C_c, D_{50}	ASTM D6913/D6913M-17 (2017)

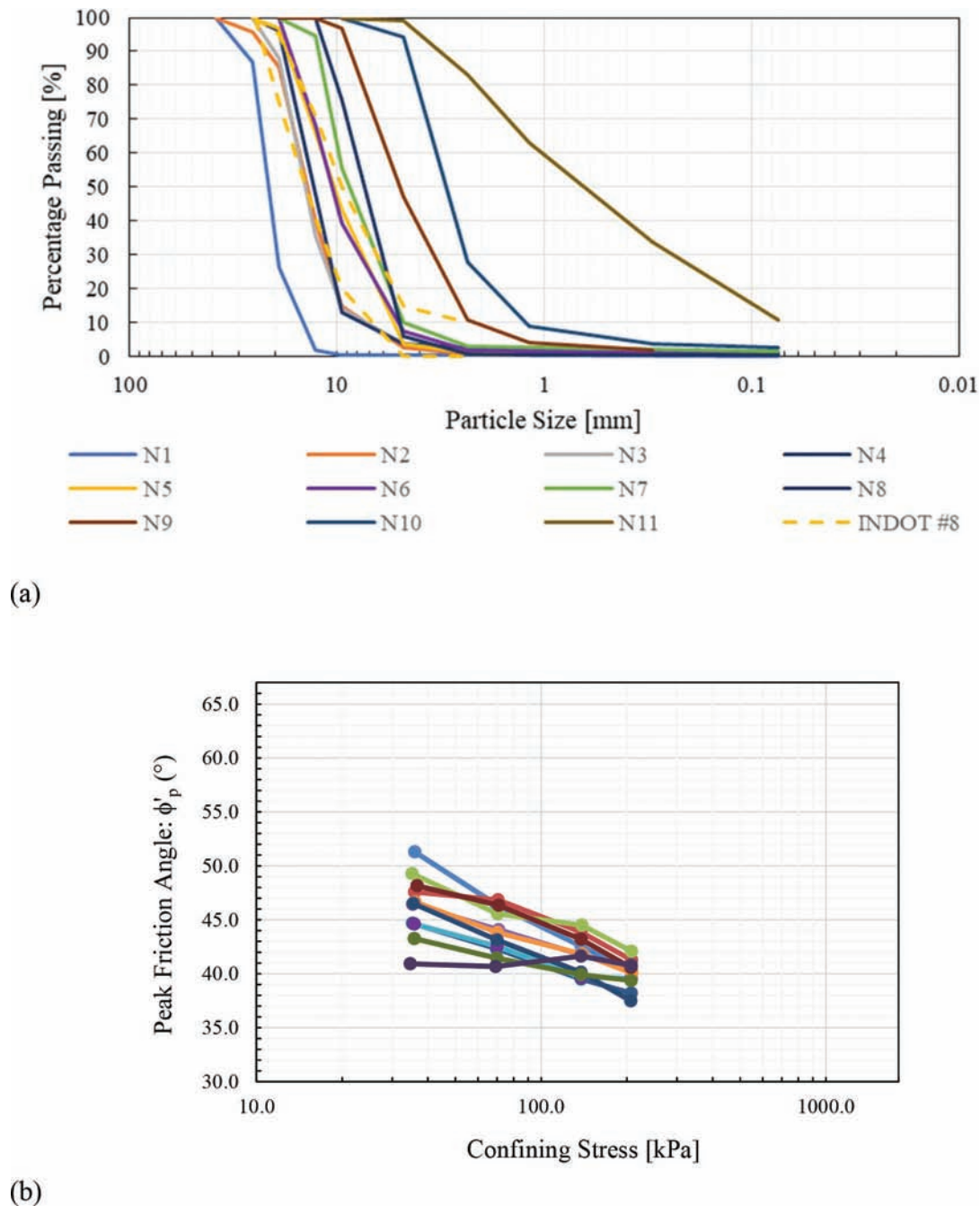


Figure 4.1 (a) Particle size distributions of aggregates; (b) peak friction angles measured on specimens with $Dr \sim 30\%$ (Nicks et al., 2015).

4.1.2 Chow et al. (2014)

The study by Chow et al. (2014) examined the behavior of 16 materials, differing in angularity, sphericity and roundness, all entirely passing the 1.5 in sieve, each blended to the same target particle size distribution, which, as shown in Figure 4.2(a), falls within the #53 band. All tests were performed using a large triaxial apparatus on specimens 6" (152 mm) in diameter and 12" (305 mm) in height. Specimens were compacted in six layers targeting a value of dry unit weight equal to

the maximum value measured in compaction tests performed according to AASHTO T-180 (2019) in a CBR mold (134.7–153.5 pcf range for the 16 aggregates). The compaction water content was equal to the optimum value (4.2%–7.4% w_{opt} range for the 16 aggregates) determined from the compaction tests. Note that the compaction tests used to determine γ_{dmax} and w_{opt} were performed on the original 16 aggregates (i.e., before blending to the target particle size distribution), and thus may not directly represent the behavior of the aggregates used in the triaxial tests. Following the

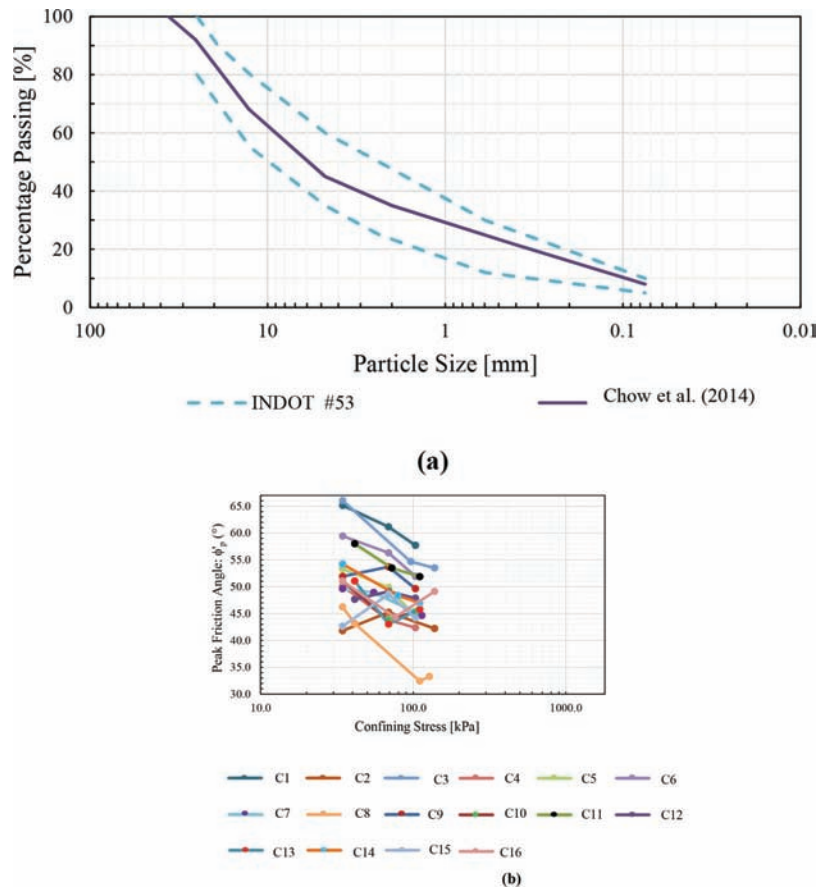


Figure 4.2 (a) Particle size distribution of aggregates; (b) peak friction angles measured on specimens with $Dr \sim 100\%$ (Chow et al., 2014).

application of a confining stress that varied between ~ 35 kPa and 140 kPa, specimens were sheared using a 1%/min axial loading rate.

Chow et al. (2014) report stress-strain curves for the majority of the tests performed. As recognized by the authors of the study, the curves exhibit a well-defined peak value, with post-peak softening. For this work, the stresses measured in correspondence to the peak deviator condition were used to derive values of the peak (secant) friction angle (ϕ'_p). Unfortunately, no volumetric data are reported by Chow et al. (2014), so dilation angles could not be calculated.

Peak friction angle data obtained from this study are plotted in Figure 4.2(b) versus confining stress for each of the 16 aggregates (Ch1–Ch16). For the low confinement stresses (≤ 30 kPa) of interest in this research the peak friction angles fall consistently above 45° and are as large as 65° . In general, for a given aggregate, the peak friction angle shows the expected decrease with increasing confining stress. Given the constant particle size distribution, the variability in the friction angle data at any given stress level reflect differences in angularity, sphericity and roundness of the aggregates. See more on the analysis of the data in the subsequent section.

4.1.3 Aghaei Araei et al. (2010)

The study by Aghaei Araei et al. (2010) provides shear strength data for 16 aggregates of different mineralogy, both rounded (alluvial origin) and angular (blasted). The nine different particle size distributions fall within or close to the band for #53 (Figure 4.3(a)). The data are from triaxial tests on 348-mm diameter specimens compacted using vibratory action to a dry density greater than 95% of the maximum value measured in compaction tests performed according to ASTM D1557-12e1 (2012), at the corresponding value of the optimum water content. The specimens were first saturated, then consolidated to the desired effective confining stress (50 kPa–1,548 kPa) and finally sheared in compression using an axial loading rate of 0.5 mm/min. The authors provide stress strain and volumetric data for all their tests.

Figure 4.3(b) summarizes the peak friction angle data obtained from these tests. As expected, the peak friction angle decreases with increasing confining stress. Consistent with the results from the other studies, the limited values of friction angle derived from tests at stress levels relevant to this study (< 148 kPa) exceed 45° .

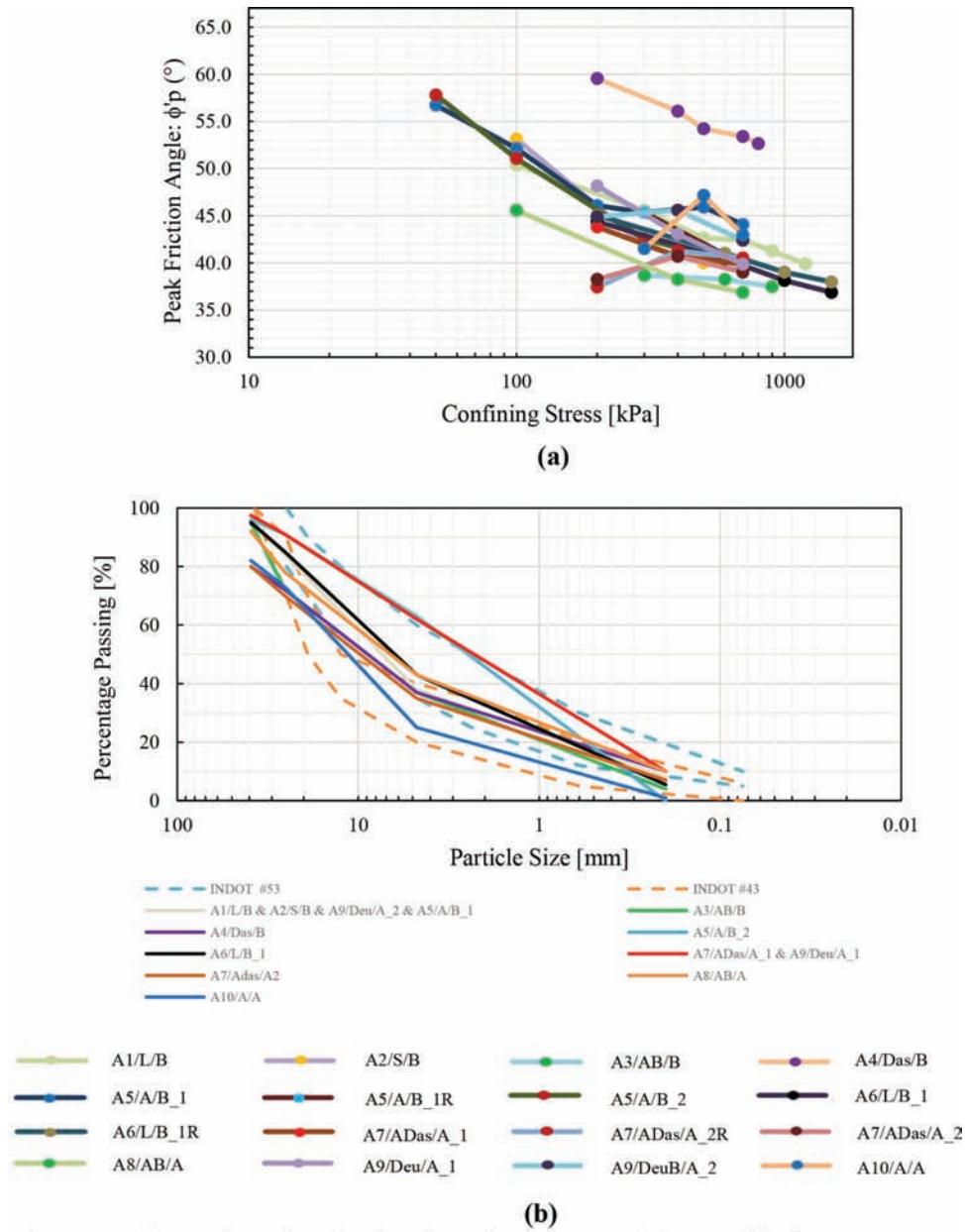


Figure 4.3 (a) Particle size distribution of aggregates; (b) peak friction angles measured on specimens with $Dr \sim 100\%$ (Aghaei Araei et al., 2010).

4.2 Statistical Analysis of Peak Friction Angle Data

As seen in Figure 4.1 through Figure 4.3, there is considerable variability in the ϕ'_p data at all confining stresses. It can be hypothesized that this relates to variations in parameters such as particle size distribution, mineralogy, particle resistance and shape. The existence of empirical relationships between these parameters and ϕ'_p was investigated by means of a statistical analysis of correlations between these parameters and the material shear strength. Considering the different definitions and scales used to characterize particle angularity, sphericity and roughness in the three studies forming the database, data from each

source were treated separately, as three distinct statistical samples.

Steps of the analysis were performed using the software, Origin/OriginPro (OriginLab Corporation, 2018), and included the following:

- Computation of linear (Pearson's) correlation coefficients between the material properties provided in the database and the shear strength parameters (peak values of the normalized stress deviator and peak angle of internal friction).*

The Pearson Correlation Coefficient is a measure of the linear relationship between two variables represented in a sample of their population. The coefficient can take values between -1 and +1. An absolute value close to 1

indicates a very close relationship whereas a value of zero indicates no linear relationship. The correlation coefficient is positive when the two variables simultaneously decrease or simultaneously increase and is negative otherwise.

(b) *Repeating the computations after logarithmic transformation of the parameters.*

Since the correlation analysis only quantifies linear relationships, it can ignore or understate relationships that are non-linear. This shortcoming is usually addressed by transforming the variables, prior to the analysis, through an appropriate non-linear function. The coefficient of correlation then measures how linearly related the transformed variables are. To this effect, a logarithmic transformation was used in this work.

(c) *Testing of null-hypothesis, using Student's t-distribution, in order to identify and then discard dubious correlations present in the (statistical) sample but not representative of the population.*

Irrespective of its value, a computed coefficient of correlation reflects only the data present in the sample which may not be a fair image of the population, especially when a sample contains a relatively small number of data, as is often the case in geotechnical engineering. Probability theory provides means to assess the degree of confidence we can grant to a correlation analysis result. In the present study a method of hypothesis testing was used to determine if a computed coefficient of correlation can be trusted or is only the result of chance in the data. The test uses Student's t-distribution to quantify the likelihood that, when a particular non-zero coefficient of correlation was found, its actual value in the variable population is rather zero (hence the Null-Hypothesis name). The conventional threshold probability for rejecting the Null-Hypothesis is 5% (or $P = 0.05$), i.e., when P is smaller than 5%, the hypothesis that the correlation is zero is rejected, and when P is larger than 5%, the hypothesis is accepted and the computed coefficient of correlation will not be trusted.

For a discussion of these techniques in the context of geotechnical engineering see, for instance, Harr (1977).

As shown earlier in this report, the peak friction angle decreases significantly with increasing confining stress, which is consistent with known behavior of granular materials (e.g., Lambe & Whitman, 1969). Logically, this relationship should translate statistically into a significant correlation with a negative coefficient, which will be verified in the following sections. However, because the relationship between peak shear strength and confining stress could interfere in relationships with other properties, the correlation analysis was performed on separate data sets corresponding to small ranges of confining stress.

Detailed results of the analysis are presented in Appendix G.

In summary, only a few empirical relationships emerge from this study, quantified by medium to high values of correlation coefficients and which can be trusted after hypothesis testing.

- For a material (Nicks et al., 2015), similar in particle size to INDOT #8, there is strong positive correlation

between the peak angle of internal friction and the average particle size D_{50} .

- For materials (Chow et al., 2014; Aghaei Araei et al., 2010) that are similar in particle size to INDOT #43 and INDOT #53, weak or medium-range correlations exist between peak shear strength and roughness (positive correlation) and sphericity (negative correlation), both under low or medium confining stresses.
- Always for materials similar in particle size to INDOT #43 and INDOT #53, and also within weak to medium range, and not systematic at all confining stresses, are correlation coefficients between peak shear strength and coefficient of uniformity (positive), coefficient of curvature (positive), abrasion (negative) and hardness (positive).
- There is no clear indication of differences between blasted and alluvial aggregates tested by Aghaei Araei et al., 2010, as the corresponding coefficients of correlation are weak and inconsistent.

These outcomes of the correlation analysis reflect the information inherent to the available database. Other, or stronger, relationships may exist between material shear strength and other properties, but no statistical evidence of such relationships was found. As to the correlations that have been identified, these are generally not strong enough to allow the development of empirical formulas applicable in engineering practice.

5. MECHANICAL STABILITY OF AGGREGATE LAYERS

5.1 Principle

Instability of granular material during its compaction and/or subsequent stages of construction was described to these investigators as excessive horizontal displacement under the effect of the compactor's or other construction equipment's moving loads. Although the mechanism of compactor-soil interaction is extremely complex (see, for instance, the discussion by Zambrano et al., 2006, as part of an earlier JTRP research project), this issue has similarity with bearing capacity problems observed with off-road vehicles (Ageïkin, 1987). Figure 5.1 shows two cases: (a) compactor cylinder (or wheel) able to move on a lift of granular material with adequate bearing capacity and (b) the situation where shear failure develops, making compaction impossible. With asphaltic concrete pavements, bearing capacity problems may also be experienced at a later construction stage if the granular base course has not been adequately compacted due to: failure of the base course under the tracks or the wheels of the paving machine (as these rest directly on the yet-unpaved area of the road), and failure during compaction of the asphaltic concrete.

Bearing capacity analyses of the granular base course—a simplified model for its potential instability—were performed for the situations described above, using the general bearing capacity equation (Meyerhof, 1963) under a static vertical load, distributed over a rectangular area and applied on the granular base surface (see Appendix H). In each case, the resulting

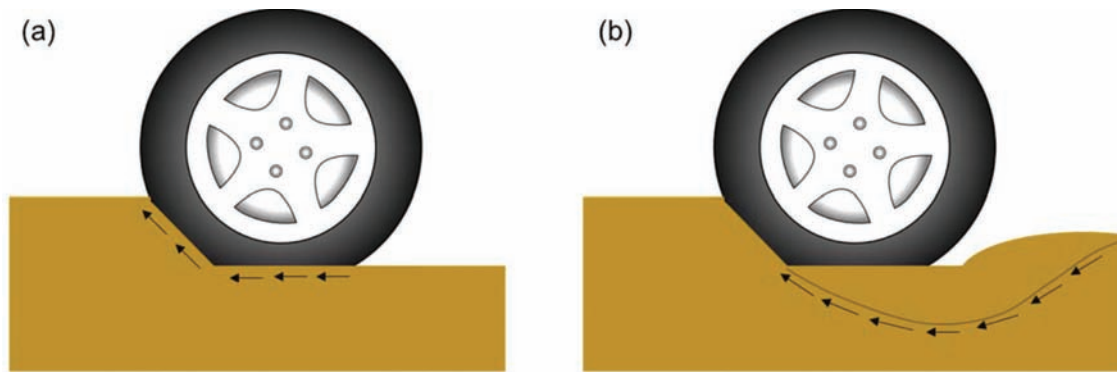


Figure 5.1 Conceptual model of wheel-granular layer interaction: (a) stability, and (b) instability caused by bearing capacity failure (adapted from Ageïkin, 1987).

ultimate load (i.e., the bearing capacity of the granular layer) was then compared to the load applied by a compactor or an asphalt paver.

Compactor vibratory effects were accounted for by means of an additional (equivalent) static force. According to the definition by Duncan et al. (1991) the total applied force is

$$Q_t = (FR) \times Q \quad (\text{Equation 5.1})$$

where (FR) is the Force Ratio and Q is the static load due to self-weight of the machine. The Force Ratio varies widely from one machine to another and, for some machines it can also be modulated by adjusting the oscillating centrifuge force. Data of FR are reported by manufacturers and cited in literature, ranging between 2 and 6, with a value of 4 being fairly common (Duncan et al., 1991; Ingold, 1987).

It is noted that current INDOT practice is to compact granular layers with no vibration whereas vibration is applied during compaction of the asphaltic concrete; implications will be discussed later. In spite of its simplifications, the model shows how sensitive the stability is to the material shear strength and density.

Computations were performed using software originally developed by Wolff (1995) for shallow foundation analysis and later modified for EXCEL by Bourdeau (2016). Software documentation is provided in Appendix H.

5.2 Geometry and Load Configurations for Sensitivity Analysis

Characteristics of representative construction equipment were selected, based on site visits and manufacturers' documentation (Table 5.1). The following cases were analyzed: (a) an individual rear tire wheel of a Caterpillar CS56 vibratory soil compactor (Figure 5.2), (b) the smooth drum of a Caterpillar CS56 vibratory soil compactor (Figure 5.2), (c) a single track of a Weiler P385B asphalt paver (Figure 5.4), and (d) a rear tire of a CAT AP1480F asphalt paver (Figure 5.3). Each case was modeled as a uniformly loaded rectangular area of dimensions B (width) and L (length). These dimensions are presented in Table 5.2.

Dimension B of the loaded area, i.e., the contact surface of a compactor wheel or roller, depends on local deformation of the material being compacted; its precise determination would be extremely complex and is beyond the scope of the present research study. The value of $B = 6''$, which represents a reasonably conservative estimate and is consistent with contact pressures of 0.1 to 0.5 MPa (14 to 69 psi) reported in the literature (Duncan et al., 1991; Zambrano et al., 2006), was generally used for the computations, but in the case of the INDOT #8 base layer, a more critical situation was also analyzed where $B = 3''$. It is noted that, with $B = 3''$, according to bearing capacity theory the instability mechanism would be confined to the base layer #8 while with $B = 6''$, the underlying material may be involved, which would be a more favorable situation.

With asphalt pavers, the machine tracks or wheels are supported directly by the (compacted) granular base layer while asphalt concrete is poured. In the case of a paver equipped with tracks, the contact surface dimension is well determined, but in the case of tire wheels the contact width, B , depends on the relative deformability of granular material and tire. A value of $B = 8''$ was estimated, consistent with a realistic contact pressure on the order of 100 psi.

In all cases considered, as manufacturers do not provide weight distribution data but only the equipment total weight, it was assumed the distribution between axles is even, e.g., each wheel of the compactor supports 25% of the operating weight.

5.3 Material Data for Sensitivity Analysis

As part of this study, literature sources (Nicks et al., 2015; Chow et al., 2014; Aghaei Araei et al., 2010), were used to assemble a database of the shear strength of aggregates similar in particle size distribution, mineralogy and angularity to INDOT's #8, #43, and #53 (see Section 4.1). This provided a range for the peak angle of internal friction (ϕ) to be used in the analysis. For the state of compaction represented by the aggregates, laboratory test results obtained in this project were used. The corresponding ranges are summarized in Table 5.3.

TABLE 5.1
Example loads used for comparison

(a) Compactors/Rollers	Source	Operating Weight		Working (Roller) Width	
		kips	kN	ft	m
BOMAG BW 900-50 (small) Tandem Roller	BOMAG Fayat Group (2009)	2.6	11.6	2.95	0.9
BOMAG BW 138 AD-5 (large) Tandem Roller	BOMAG Fayat Group (2009)	9.4	41.8	4.5	1.4
Caterpillar CS56 Vibratory Soil Compactor	AC Business Media (2019)	27.6	122.8	7	2.1
Dynapac CA12D Vibratory Roller	Duncan et al. (1991)	13.4	60	4.25	1.3

(b) Asphalt Pavers	Source	Operating Weight		Individual Track Width		Individual Track Length	
		kips	kN	ft	m	ft	m
Caterpillar AP300F Paver	AC Business Media (2019)	18	80	1–2 ^a	0.3–0.6 ^a	16.5 ^b	5 ^b
Caterpillar AP1000F Paver	AC Business Media (2019)	45.4	202	1–2 ^a	0.3–0.6 ^a	22.5 ^b	6.9 ^b
Weiler P385B Commercial Paver	Weiler (n.d.)	37.5	166.8	1.2	0.36	5.7	1.74

^aNo width of wheel defined in specs.

^bLength of closely spaced tires.

Caterpillar CS56 Vibratory Soil Compactor



Operating Weight: 27.57 kips

→ Estimated weight on one tire ~ 6.9 kips (1/4 the operating weight)

→ Estimated weight on roller ~ 13.8 kips (1/2 the operating weight)

Figure 5.2 Caterpillar CS56 vibratory soil compactor.

The sensitivity analysis was performed by keeping all geometric parameters constant while varying the two material parameters, friction angle and dry unit weight, one at a time, within the ranges indicated in Table 5.3. When one of these two parameters was varied, the other was kept equal to its average value within the range (Table 5.4).

5.4 Results of Analysis and Discussion

Plots of the results obtained for geometric and loading configurations (a), (b), (c), and (d) are presented in the following four pairs of figures. For each case, the first figure shows the influence of the granular material's friction angle on the bearing capacity while the second figure shows the influence of the material unit weight. In addition to the curves of ultimate bearing

load (Q_{ult}) in function of friction angle (ϕ) and dry unit weight (γ_d), drawn for the three types of granular material, the applied loads (dotted horizontal lines) are also shown for comparison.

All of these results exhibit common trends: bearing capacity increases with increasing friction angle as well as with increasing unit weight; this variation is extremely sensitive and nonlinear with respect to friction angle (as N_γ in the bearing capacity equation increases exponentially with ϕ) whereas the variation in function of γ_d is linear and slower. Another general observation is the bearing capacity of INDOT #8 is systematically inferior to that of both INDOT #43 and #53, because of #8's lesser density and shear strength. Computed performances of #43 and #53, in terms of bearing capacity, are generally close. Particulars to each loading case are discussed next.

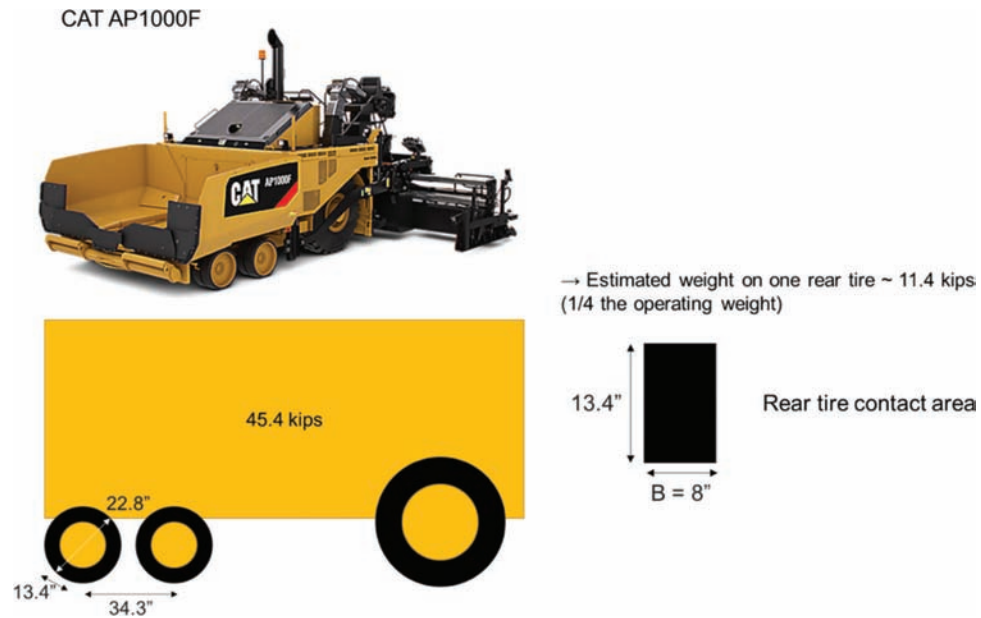


Figure 5.3 Caterpillar CAT AP1000F asphalt paver with wheels.

Weiler P385B Commercial Paver



Operating Weight: 19.5 kips + 18 kips
→ Estimated weight on one track ~ 18.8 kips (1/2 the operating weight)

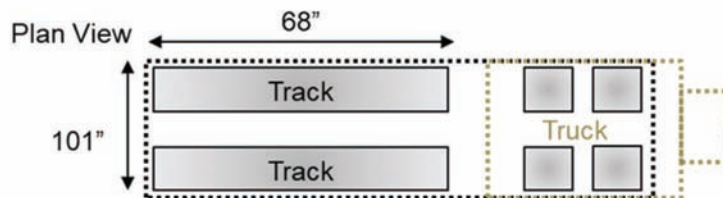


Figure 5.4 Weiler P385B asphalt paver with tracks.

TABLE 5.2
Geometry constants used for different equipment in sensitivity analysis

	B (ft)	B (m)	L (ft)	L (m)
Individual Wheel for Vibratory Soil Compactor	0.25 ^a , 0.5	0.08 ^a , 0.15	1.9	0.58
Vibratory Soil Compactor Roller	0.25 ^a , 0.5	0.08 ^a , 0.15	7	2.1
Asphalt Paver Track (Weiler P385B)	1.2	0.4	5.7	1.7
Rear Wheel of Asphalt Paver (CAT AP1000F)	0.7	0.2	1.1	0.34

^aOnly for #8 due to limiting thickness of layer.

TABLE 5.3
Dry unit weight and friction angle ranges used in analysis

	γ_{d_max} (lb/ft ³)	γ_{d_max} (kN/m ³)	Source for Friction Angle	ϕ_{peak} (°)
INDOT #8	110–112	15.7–17.6	Nicks et al. (2015)	45–50
INDOT #43	108–152	17.0–23.9	Chow et al. (2014) and Aghaei Araei et al. (2010)	40–65
INDOT #53	128–144	20.1–22.6	Chow et al. (2014) and Aghaei Araei et al. (2010)	40–65

TABLE 5.4
Average values of material parameters for sensitivity analysis

	γ_{d_max} (lb/ft ³)	γ_{d_max} (kN/m ³)	ϕ_{peak} (°)
INDOT #8	106	16.7	47.5
INDOT #43	130	20.4	52.5
INDOT #53	136	21.4	52.5

5.4.1 Stability of Granular Layer Under a Rear Wheel of Compactor

The rear wheel of the compactor is considered a static (i.e., non-vibratory) loading case (Figure 5.5 and Figure 5.6). It is not likely to represent the most critical condition for the aggregate stability. This is confirmed as friction angle and unit weight of INDOT #43 and #53 are such that their bearing capacity exceeds the applied load. However, the model indicates INDOT #8 could be close to failure if its angle of internal friction is still in its low range (45°), when it has not yet been densified by compaction, and the situation for this material is even worse if the bearing mechanism is confined to the top layer ($B = 3$ in).

5.4.2 Stability of Granular Layer Under Vibratory Drum of Compactor

This is the case (Figure 5.7 and Figure 5.8) most critical for assessing the granular material stability during compaction. In the static condition (i.e., no vibratory effect) which represents INDOT's current practice for the compaction of base and subbase, all three materials are likely to remain stable, as their ultimate bearing capacity is greater than the compactor drum load, even in loose state and with minimal shear strength.

If vibration was induced with force ratios, FR, in the range of 4 and above—values common to modern machines—then stability would be an issue, for INDOT #8 certainly, but even for INDOT #43 and #53, considering the relatively high values of the friction required for Q_{ult} to be greater than the total applied force. For instance, with $FR = 4$, values of $\phi = 49^\circ$ and 48° would be required for INDOT #8 and INDOT #43 and #53, respectively. With the full force ratio of 5.7 developed by the CAT CS56 compactor, the required friction angle would be out of range for INDOT #8 and at least 49° for #43 and #53. Angles of internal friction above 49° for #43 and #53 materials are achievable, as suggested by the database,

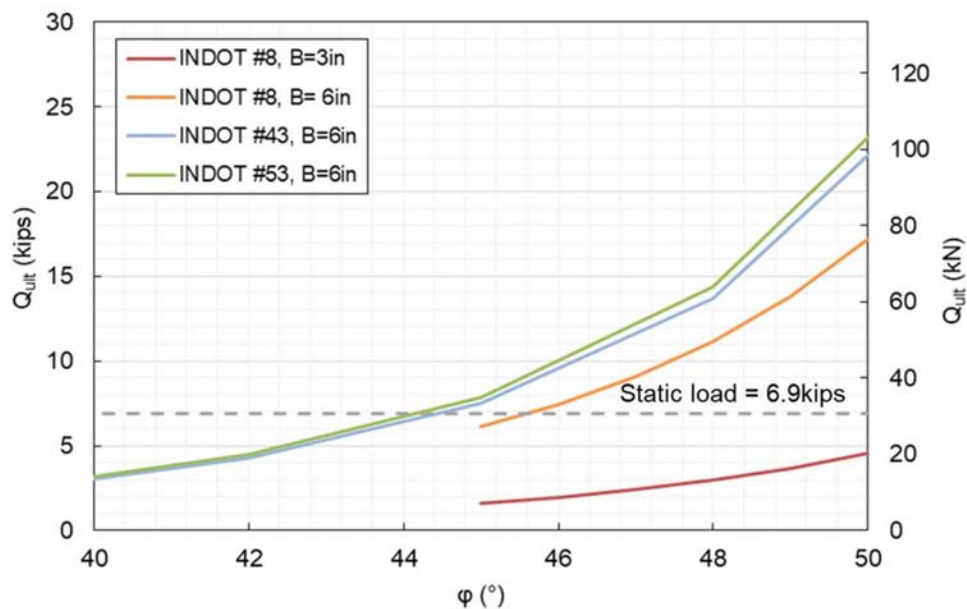


Figure 5.5 Effect of aggregate friction angle on ultimate bearing load, under a wheel of compactor.

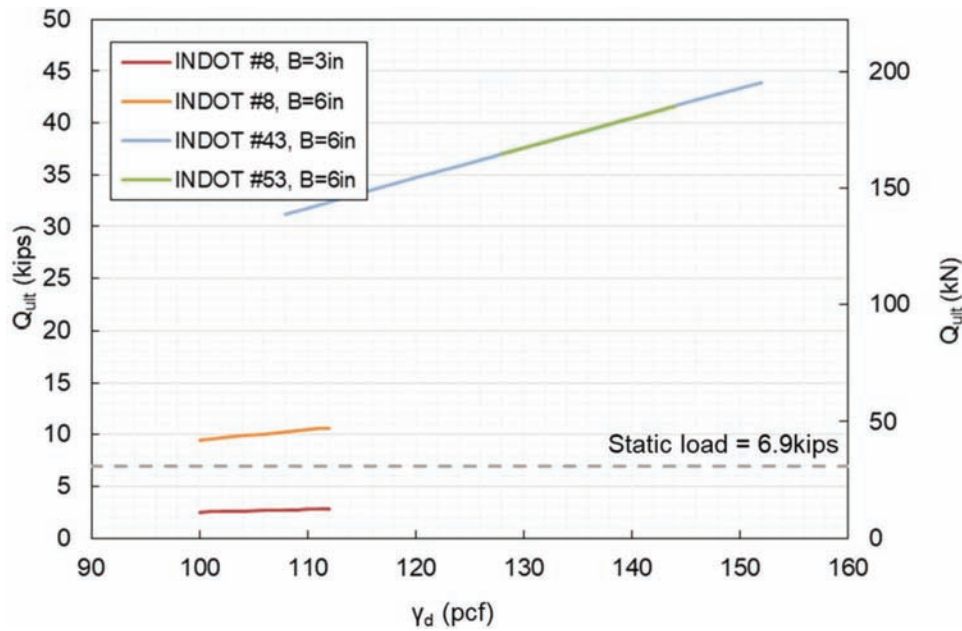


Figure 5.6 Effect of aggregate unit weight on the ultimate bearing load, under a wheel of compactor.

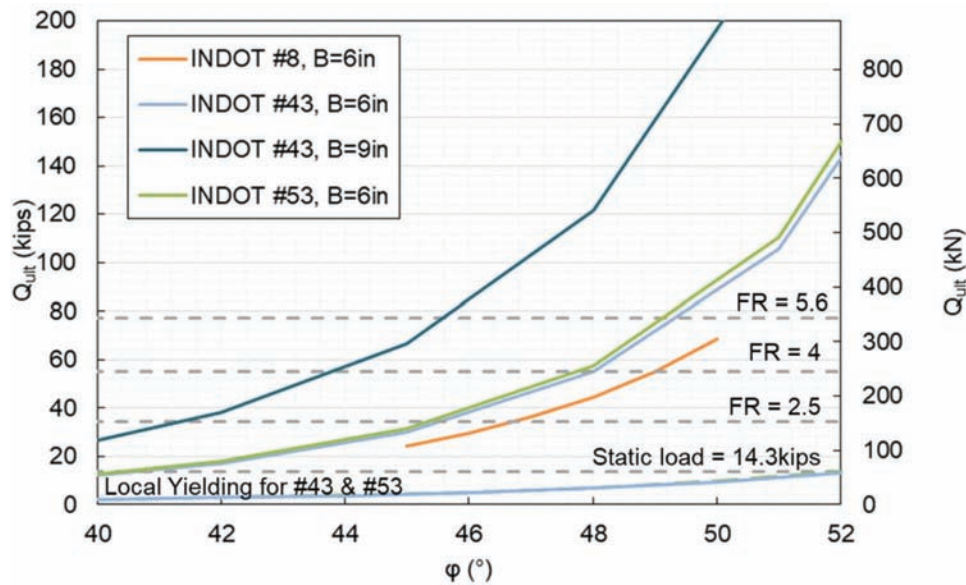


Figure 5.7 Effect of aggregate friction angle on ultimate bearing load, under compactor drum (horizontal dotted lines represent the static and total applied force with force ratio FR).

but not in the materials loose states, at the start of the compaction process. This might justify the noted reluctance to apply vibration in INDOT construction sites. However, high density and shear strength that are required from in-service base and subbase courses are very difficult to obtain without using the vibratory effect of the compactor. An effective procedure, in order to achieve thorough compaction, could be to perform the first passes with the compactor in static mode, so that sufficient densification and shear strength would be gained for the following and final passes to be performed in vibratory mode.

Two additional curves are shown in Figure 5.7 to provide further verification. The lowest curve, at the bottom of Figure 5.7, represents the local yielding load in function of the angle of internal friction for materials #43 and #53. Local yielding is a state of plastic deformation, without failure of the granular layer, which develops at locations of intense shear during loading. During compaction, local yielding is a necessary condition for permanent densification to occur. The local yielding loads were computed, following Terzaghi's (1943) method, using the same bearing capacity equation than the ultimate load where only 2/3 of the ultimate

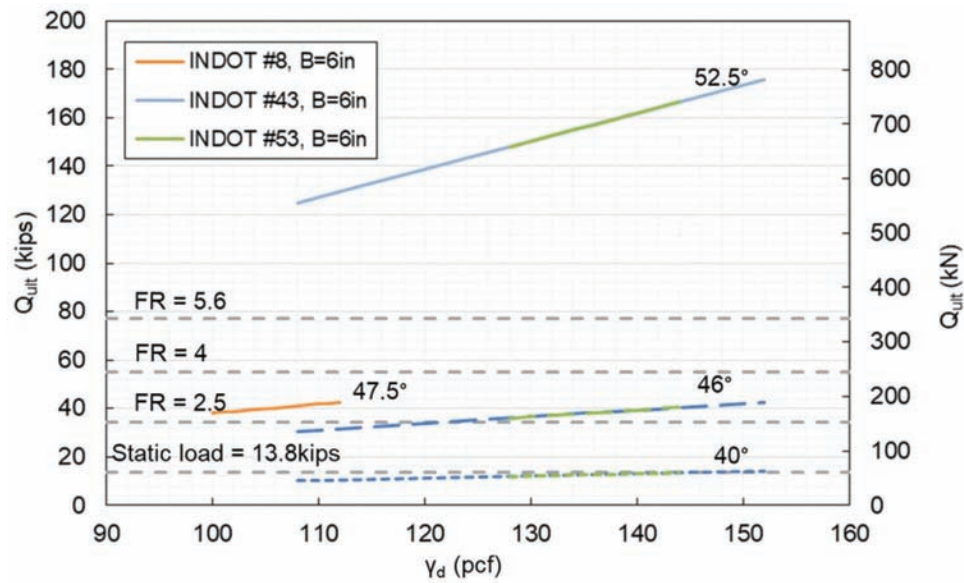


Figure 5.8 Effects of aggregate unit weight on ultimate bearing load, under roller of compactor (horizontal dotted lines represent the static and total applied force with force ratio FR).

shear strength is mobilized. As can be seen, applied loads from the compactor, even in static mode, are larger than the local yielding load through the whole range of ϕ values. This confirms the mechanical condition is met for starting compaction in static mode.

The uppermost curve in the Figure 5.7 addresses a final stage of construction, when an asphaltic pavement layer has been placed over the granular base and is being compacted with a vibratory compactor. It was assumed the compactor characteristics are similar to those of the granular base compactor but, as the drum load acts on the surface of the asphaltic concrete layer, its magnitude is attenuated by diffusion through that layer. In Figure 5.9 it is shown how this is modeled, by distributing the load on the granular base, over a width B' instead of B . With a diffusion angle of 45° , $B = 6''$ and the thickness of asphaltic concrete, $3''$, then $B' = 9''$. The ultimate bearing load of the granular base was re-computed, assuming the base course is made of INDOT #43. It is verified that the stability condition of the base course during vibratory compaction of the asphaltic concrete is more critical than during static compaction of the granular material itself: for a force ratio, $FR = 4$, the required friction angle, for the base course to remain stable, would be approximately 44° as compared to 40° during its static compaction. On the other hand, this value (44°) is significantly smaller than 49° required during vibratory compaction of the granular base. It can be concluded that, if the granular base course has been thoroughly compacted with vibratory action and was stable during the process, then it will remain stable during vibratory compaction of the asphaltic concrete pavement.

This is a case of static loading, where the tracks of the paver rest on the granular base while asphaltic concrete is poured. As shown in Figure 5.10 and Figure 5.11, this loading situation is not critical for the stability of

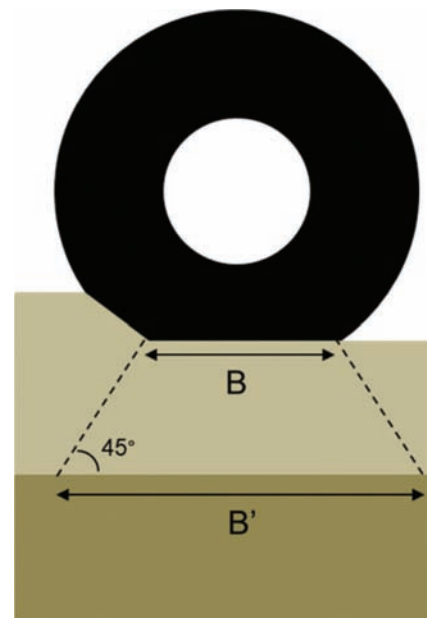


Figure 5.9 Load transfer through asphaltic concrete pavement layer during compaction.

the granular course, as the applied load is always much smaller than the ultimate bearing capacity.

5.4.4 Stability of Granular Layer Under a Wheel of Asphalt Paver

Under the weight of an asphalt paver on wheels, the situation is more severe than with a machine equipped with tracks. As seen in Figure 5.12 and Figure 5.13 stability of the granular base requires a friction angle of approximately 48° for INDOT #43 and #53, close to values that were required during vibratory compaction.

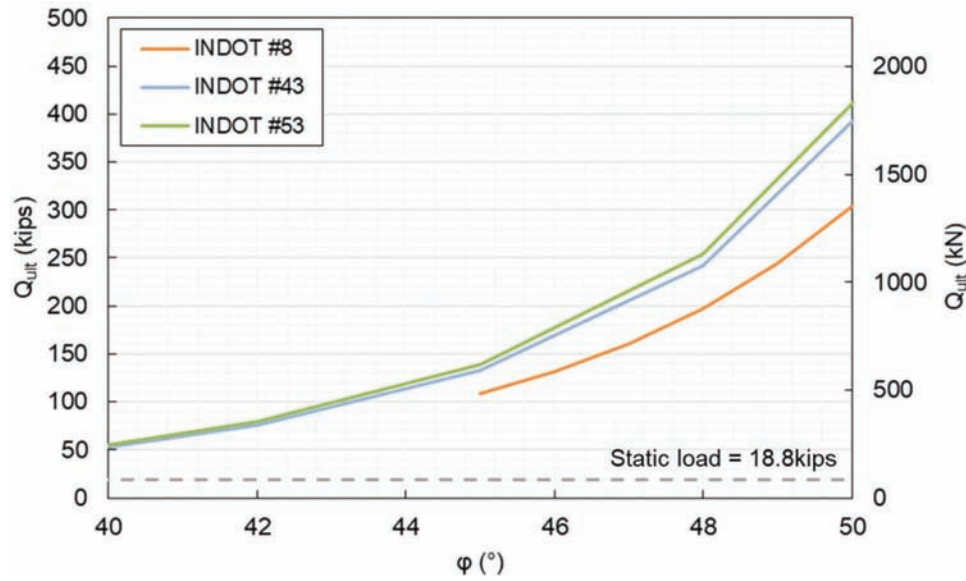


Figure 5.10 Effect of aggregate friction angle on ultimate bearing load, under track of asphalt paver.

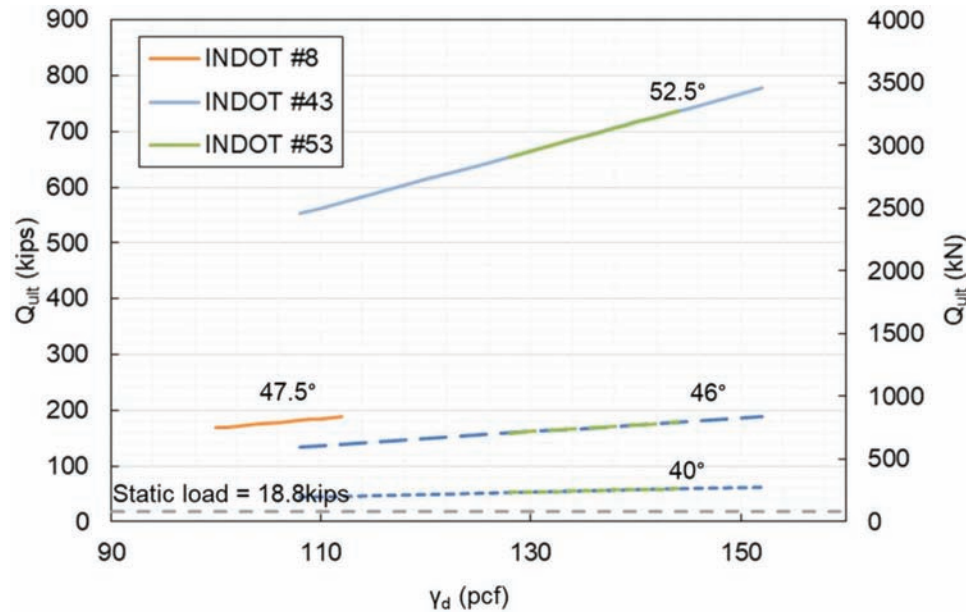


Figure 5.11 Effects of aggregate unit weight on ultimate bearing load, under track of asphalt paver.

This observation stresses again the need for thorough vibratory compaction of the granular materials.

As mentioned above, the general bearing capacity equation is applicable to homogeneous, semi-infinite medium below the loaded area. The influence of this simplification was assessed in the case where a weaker material, #8, only 3" thick, is being compacted above a layer of more resistant material, #53. The approximate, semi-empirical method for layered soils proposed by Meyerhof and Hanna (1978) was used for this purpose. The results indicate this approach is less conservative (i.e., larger values of bearing capacity are obtained) than the simplified model used in this study.

In summary, for all the loading cases considered in the study, the stability of INDOT #8 seems highly problematic.

Stability of INDOT #43 and #53 requires density and frictional resistance that are achievable with thorough compaction. Static compaction alone is likely to be insufficient to this purpose, thus vibratory compaction is highly desirable. An adequate procedure could include first passes of static compaction for gaining strength so that the material could sustain further passes in vibratory mode.

Static loading by an asphaltic concrete paver on wheels is one of the critical situations for stability of the granular

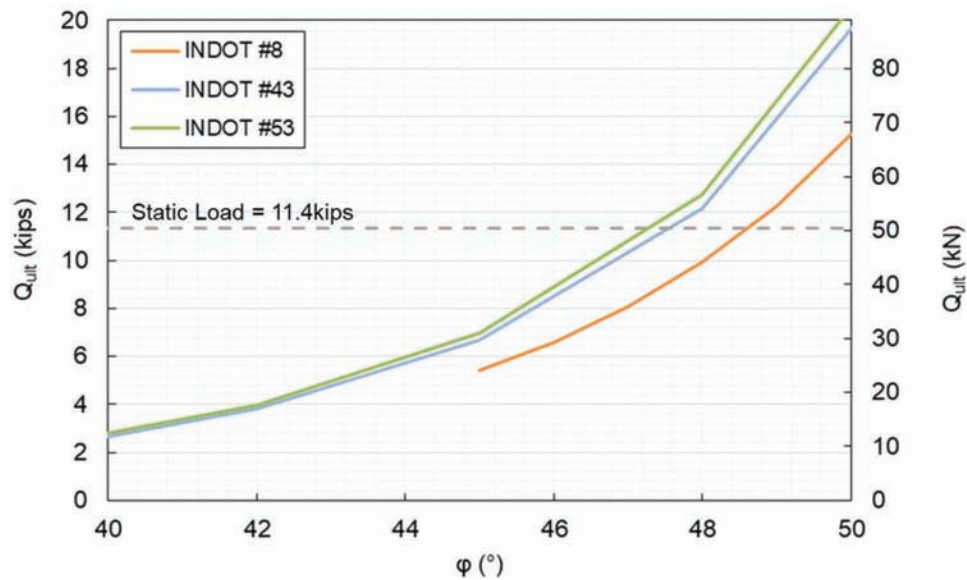


Figure 5.12 Effect of aggregate friction angle on ultimate bearing load, under a wheel of asphalt paver.

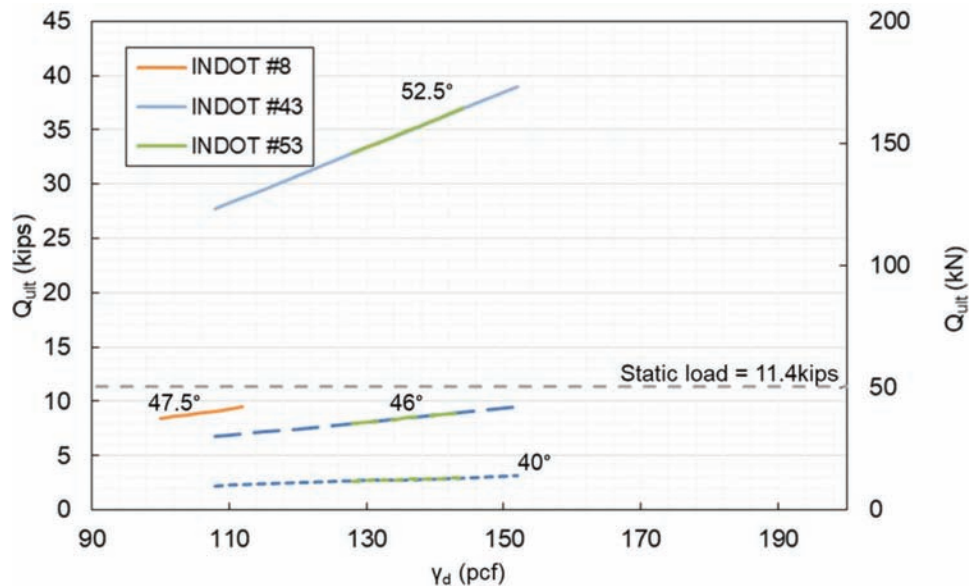


Figure 5.13 Effects of aggregate unit weight on the ultimate bearing load, under a wheel of asphalt paver, for different friction angles.

base. Instead, it would be advisable to use asphalt pavers on tracks which have a much lighter effect.

6. COMPATIBILITY BETWEEN MATERIALS AND USE OF GEOTEXTILES

In this section, compatibility requirements between materials in the roadway structure are discussed, and the need for separator and filter layers is addressed. The materials involved in these considerations include subgrade soil and granular drainage and sub-base layers. Separator and filter layers can be made of granular material or geotextile fabric.

The topic is better understood if one considers, at first, the nature and definition of incompatibility. In the present context, material incompatibility is observed in two forms, both highly detrimental to the long-term structural integrity of the roadway; the first is penetration or intrusion of a coarse material layer into a finer material layer (e.g., drainage material intruding subgrade), and the second is contamination of a coarse layer by fine particles of the material it is in contact with (e.g., fines from the subgrade into the drainage layer). Intrusion is a mechanical effect of forces induced by traffic or compaction, while contamination is of hydrodynamic origin, the fine particles being

transported in pore water under the action of seepage forces as observed, for instance, with the phenomenon of “pumping of fines.” These two mechanisms are conceptually represented in Figure 6.1 and Figure 6.2.

Prevention of the intrusion mechanism requires a separator layer, while prevention of contamination requires a filter layer. However, the two functions of separation and filtration are generally combined as, to be effective, a separator must not be contaminated by—or contaminate—materials it is in contact with. This translates in the guidelines for material selection being a combination of both types of criteria.

Throughout this discussion, reference will be made to software DRIP, in comparison to current FHWA guidelines for separator and filter layers, and discrepancies between these documents will be highlighted.

DRIP (Drainage Requirements in Pavement) is user-friendly software, frequently used by INDOT and other transportation agencies. It was developed by Applied Research Associates, Inc., (2014) on the basis of guidelines FHWA-TS-80-224 *Highway Subdrainage Design* (Moulton, 1980/1990) supplemented with content from two subsequent documents, *Demonstration Project 87* (FHWA, 1992) and *Pavement Subsurface Drainage*

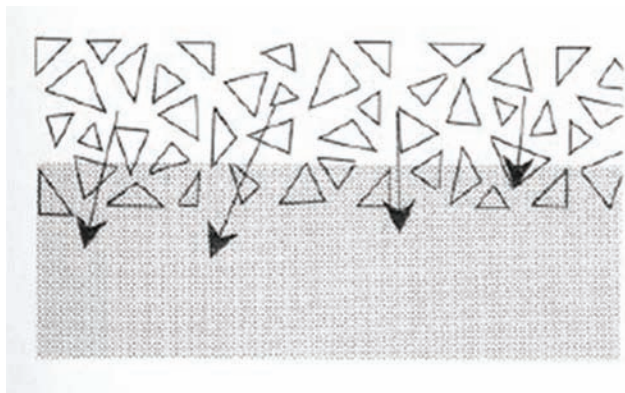


Figure 6.1 Incompatibility by intrusion—requires a separator (after Koerner, 2005).

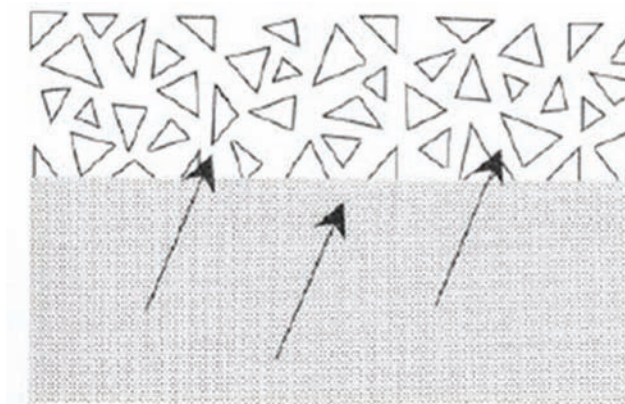


Figure 6.2 Incompatibility by contamination—requires a filter (after Koerner, 2005).

Design NHI Course No 131026 (FHWA, 1999). The current version, DRIP v2 (Applied Research Associates, 2014), is documented by Mallela et al. (2002) and can be downloaded from the AASHTO website. The software addresses both water infiltration and compatibility between materials; it allows designing granular or geotextile separators. In the present section about compatibility only the “Sieve Analysis” and “Separator” functions of the program were needed.

Independently of DRIP, current guidelines for granular separators are the result of a long evolution since the 1940s. Early steps in this history are retraced by Huang (1993), including works by Betram (1940), the U.S. Army Corps of Engineers (1955), Sherard et al. (1963), and Moulton (1980/1990). In all the proposed criteria compatibility is expressed as a desirable ratio between the materials respective particle sizes—or fractions thereof. Underlying this concept is the relation between particle size and pore size. Current FHWA guidelines include granular filter criteria from FHWA-TS-80-224 *Highway Subdrainage Design* (Moulton, 1980/1990) and additional material requirements in FHWA NHI-05-037 *Geotechnical Aspects of Pavements* (Christopher et al., 2006).

Geotextile separators and filters have a more recent history, going back only a few decades. An overview can be found in Koerner (2005). The current guideline is FHWA NHI-07-092 *Geosynthetic Design & Construction Guidelines* (Holtz et al., 2008). Here the separation and filtration functions are addressed separately: separation is a matter of mechanical survivability of the geotextile fabric during installation and relies on a set of material index properties, whereas filtration criteria are inspired from the granular models in relating the fabric opening size to the retained soil particle size.

6.1 Need for Separator Between Drainage Layer and Subgrade

The first question is whether a separator is needed between subgrade and drainage layer, for a particular project at a particular site.

If a drainage layer or granular base was placed directly in contact with the subgrade without separator, FHWA-TS-80-224 (Moulton, 1980/1990) evaluates compatibility between this aggregate and the subgrade by considering whether the properties that are required from a granular separator are already met by the drainage layer. The general requirements are:

$$(D_{15})_{\text{aggregate}} \leq 5(D_{85})_{\text{subgrade}} \quad (\text{Equation 6.1})$$

$$(D_{15})_{\text{aggregate}} \geq 5(D_{15})_{\text{subgrade}} \quad (\text{Equation 6.2})$$

$$(D_{50})_{\text{aggregate}} \leq 25(D_{50})_{\text{subgrade}} \quad (\text{Equation 6.3})$$

$$(D_5)_{\text{aggregate}} \geq 0.074\text{mm} \quad (\text{Equation 6.4})$$

$$(C_u)_{\text{aggregate}} \leq 25 \quad (\text{Equation 6.5})$$

If these are not satisfied, a protective layer (separator) must be included between drainage layer and subgrade.

In DRIP, only two of these requirements, Equations (6.1) and (6.3), are used to perform this verification. No justification for this simplification is provided in the *User's Guide* (Mallela et al., 2002) but some explanation can be found in the origin of the general requirements and how they apply to the situation considered here. Both requirements used by DRIP are filter criteria: Equation (6.1) from Betram (1940) aims at the aggregate being fine enough to prevent the subgrade finer material from piping or migrating into it, a requirement to which Equation (6.3) was added by the USACE (U.S. Army Corps of Engineers, 1955). Equation (6.2), also from Betram (1940), is to guarantee the aggregate is significantly coarser than the subgrade and, as a result, more permeable. This condition would be automatically met if the aggregate was by itself a drainage layer placed on a finer-grained subgrade. Equation (6.4) from Moulton (1980/1990) aims at limiting the amount of fines in the aggregate so that they do not contaminate upper layers, a condition which is not relevant in this case. The omission of Equation (6.5) by DRIP is more problematic, as it is the only one to be specifically relevant to a separation function: limiting the Coefficient of Uniformity was proposed by the USACE (U.S. Army Corps of Engineers, 1955) in order to minimize segregation and penetration of the aggregate into the subgrade.

The above criteria were used to assess the need of separator layers with INDOT design options summarized in Table 6.1. Following guidance from INDOT (T. Nantung, personal communication, 2019), example subgrade conditions were selected from an earlier JTRP study (Jung & Bobet, 2008). Data on these subgrades are provided in Appendix I, Table I.1. Particle size information for the aggregates is also provided in Appendix I, Table I.2.

In absence of separator, the drainage layer, INDOT #8 or INDOT #43, would be directly in contact with the subgrade; the compatibility analysis is summarized in Table 6.2. As the compatibility criteria do not apply to HMA drainage layers, Options 4 and 5 were not considered.

It is observed that, in three of the subgrade situations being considered, a separator layer would not be required with INDOT#8 aggregate, while INDOT#43 would require a separator in every case. What makes INDOT #43 incompatible with the example subgrades is its Coefficient of Uniformity (C_u) which is too large according to Equation 6.5. In other terms, its broad gradation would make it prone to segregation and penetration into the subgrade if one relies on the USACE (U.S. Army Corps of Engineers, 1955) recommendation. As will be seen in Section 6.2, this particular requirement that C_u be smaller than 25 has been amended in the latest separator guidelines which prescribe values between 20 and 40. If this was considered here, two of

the subgrade situations would not require separators from INDOT #43, while all cases would require a separator from INDOT#8. It is also noted that, in absence of requirement on C_u , the decisive criteria would be those implemented in DRIP. However, this observation should not be generalized, as different subgrade conditions may lead to different conclusions.

Independently of these considerations, inclusion of a separator layer seems to be the preferred design for INDOT projects as well as in other states, as it provides a clean, stable and self-draining working platform. Furthermore, in the case of a granular separator material, this layer contributes mechanically to the pavement structure (even if it is not explicitly accounted for in design calculations).

The case of treated subgrade may call for further examination. Intuitively, it seems that lime- or cement-treated subgrade would provide an adequate working platform without the help of a separator layer and that the chemical bounding would limit the ability of fine particles to migrate into the drainage layer. However, according to Christopher et al. (2006), "Lime- or cement-treated subgrades alone are not acceptable as separator layers over fine-grained soils. There have been some classic failures of lime-treated soils used as separator layers in which pumping into the permeable base caused excessive settlements." The cited document does not include supporting documentation for the reported observation. Further study would be needed for clarifying the case of fines migration from treated subgrades.

6.2 Granular Separators

When a granular separator layer is included, the proposed material must be compatible with both materials it is in contact with, i.e., the subgrade and the drainage layer. This is done by applying a set of criteria, similar types to Equations 6.1 to 6.5, to the lower and upper interfaces.

If the notations in the previous equations are adjusted to the present cases, the criteria should be, for compatibility between separator layer and subgrade (Moulton, 1980/1990),

$$(D_{15})_{\text{separator}} \leq 5(D_{85})_{\text{subgrade}} \quad (\text{Equation 6.6})$$

$$(D_{15})_{\text{separator}} \geq 5(D_{15})_{\text{subgrade}} \quad (\text{Equation 6.7})$$

$$(D_{50})_{\text{separator}} \leq 25(D_{50})_{\text{subgrade}} \quad (\text{Equation 6.8})$$

and for compatibility between the separator and drainage layer,

$$(D_{15})_{\text{drainage}} \leq 5(D_{85})_{\text{separator}} \quad (\text{Equation 6.9})$$

$$(D_{15})_{\text{drainage}} \geq 5(D_{15})_{\text{separator}} \quad (\text{Equation 6.10})$$

$$(D_{50})_{\text{drainage}} \leq 25(D_{50})_{\text{separator}} \quad (\text{Equation 6.11})$$

TABLE 6.1
Summary of proposed options by INDOT (2/17/17)

Asphalt or Concrete Pavement						
	Option 1	Option 2	Option 3	Option 4	Option 5	Option 6
Drainage	#8	#43	#43	HMA open-graded	HMA open-graded	#8
Separator	#53	NJDOT	Geotextile woven	NJDOT	Geotextile woven	NJDOT
Soil Treatment			14" 4-6%			
Subgrade		Examples from Jung and Bobet (2008): A-7-6, A-6, A-4				

TABLE 6.2
Summary of INDOT design options without separator layer, according to criteria from FHWA-TS-80-224 (Moulton, 1980/90) and DRIP, with subgrade examples from Jung and Bobet (2008)

No Separator	Base: #8 Cu = 2.6 (Pass) ^b				Base: #43 Cu = 46.6 (Fail) ^b			
	D ₁₅ ^{base} ≥ 5D ₁₅ ^{subgrade} ^a	D ₅ ^{base} ≥ 0.074 mm ^a	D ₁₅ ^{base} ≤ 5D ₈₅ ^{subgrade}	D ₅₀ ^{base} ≤ 25D ₅₀ ^{subgrade}	D ₁₅ ^{base} ≥ 5D ₁₅ ^{subgrade} ^a	D ₅ ^{base} ≥ 0.074 mm ^a	D ₁₅ ^{base} ≤ 5D ₈₅ ^{subgrade}	D ₅₀ ^{base} ≤ 25D ₅₀ ^{subgrade}
	Subgrade: A-7-6 untreated							
	Pass	Pass	Fail	Fail	Pass	Pass	Pass	Fail
	Subgrade: A-7-6 Treated (site 3)							
	Pass	Pass	Pass	Pass	Pass	Pass	Pass	Pass
	Subgrade: A-4 Treated (site 2)							
	Pass	Pass	Pass	Fail	Pass	Pass	Pass	Fail
	Subgrade: A-4 Treated (site 4)							
	Pass	Pass	Pass	Pass	Pass	Pass	Pass	Fail
	Subgrade: A-6 Treated (site 5)							
	Pass	Pass	Pass	Fail	Pass	Pass	Pass	Fail
	Subgrade: A-6 Treated (site 6)							
	Pass	Pass	Pass	Pass	Pass	Pass	Pass	Pass

Note: D₅ not available from tests was estimated using D₁₀ values.

^aCriteria considered in DRIP *User's Guide* (Mallela et al., 2002) but not implemented in software.

^bCriterion not considered in DRIP.

to which should be added

$$(D_5)_{separator} \geq 0.074mm \quad (\text{Equation 6.12})$$

$$(C_u)_{separator} \leq 25 \quad (\text{Equation 6.13})$$

However, DRIP differs from these rules in several instances:

- Equations 6.7 and 6.10 are disregarded; this is consistent with disregarding Equation 6.2 as previously noted.
- The allowable amount of fines in the separator is increased to 12%, from 5% in equation 6.12. The equation becomes

$$(D_{12})_{separator} \geq 0.074mm \quad (\text{Equation 6.14})$$

This is in agreement with document, *Geotechnical Aspects of Pavements Reference Manual FHWA NHI-05-037* (Christopher et al., 2006; a web-based version of this document, dated 2017, differs in format but is identical in content to the 2006 original). The purpose of this guideline is to design a separator layer with relatively low permeability, as compared to the drainage layer (the expectation is that the separator hydraulic conductivity (k) will not exceed 5 m/day or 15 ft/day), so that water in the drainage layer will flow horizontally toward the edge drains instead of infiltrating into the separator.

- As indicated in the User's Guide, Technical Background section (Mallela et al., 2002), but not implemented in the software, the separator coefficient of uniformity should now be between 20 and 40. Equation 6.13 is thus replaced by

$$20 \leq (C_u)_{separator} \leq 40. \quad (\text{Equation 6.15})$$

It should be noted that Equation 6.15 is an important departure from the traditional notion that granular separators and filters should be uniformly graded as indicated by Equation 6.13 (see, for instance USBR, 1987). It had earlier been recognized that broadly graded separators were prone to segregation and penetration in the subgrade. The origin of Equation 6.15 is to be found in Demonstration Project 87 (FHWA, 1992), the synthesis of a survey conducted among 10 states DOTs about their practices. The document does not provide a strong rationale to support these values besides the convenience of possibly using the same material than for the base course. Since the criterion is apparently not checked by the DRIP program separator design function, its application is left, up to the user.

Additional guidelines, not addressed in DRIP, are indicated by Christopher et al. (2006) about the selection of separator aggregates.

- Aggregates should have at least two fractured faces, as determined by the material retained on the No. 4 sieve (preferably, it should consist of 98% crushed stone).

- L.A. abrasion wear (as per AASHTO T 96-02, 2019) should not exceed 50%.
- Soundness loss percent (as per AASHTO T 104-99, 2016) should not exceed 12% or 18%, as determined by the sodium sulfate or magnesium sulfate tests, respectively.
- Material passing the No. 40 sieve should be non-plastic (as per AASHTO T 90-16, 2016).

All the aggregates being considered in this study are made of crushed stone and their coarse fraction generally presents several fractured faces. No verification was made for the other recommendations; the present discussion focuses on particle size requirements.

Again, using the subgrade examples from Jung and Bobet (2008), the adequacy of the separators in INDOT design options 1, 2, and 6 was assessed on the basis of the above set of equations and DRIP. Design options 4 and 5 were not assessed because of lack of criteria when a HMA layer is present. Option 3, which includes a geotextile separator, is discussed later.

The analysis is summarized in Table 6.3, Table 6.4, and Table 6.5 for options 1, 2, and 6, respectively. The following are important observations:

- If, at first, the coefficient of uniformity guidelines is not considered (these are not implemented in DRIP), INDOT #53 and NJDOT separators are always compatible with the drainage aggregate INDOT #8 or #43, but in some of the example subgrade situations, they do not meet the requirements at the lower interface, whether the subgrade is treated or untreated. This stresses

the importance of considering the separator design, case by case, in function of the subgrade conditions.

- The guidelines about the separator coefficient of uniformity require further attention. If the traditional notion of a uniformly graded separator is still valid, the NJDOT aggregate would meet the criterion ($C_u < 25$), but the INDOT #53 would not. In turn, if the more recent guideline ($20 < C_u < 40$) is followed, neither the NJDOT nor the #53 would be acceptable, the NJDOT material because it is too uniformly graded, the INDOT #53 because it is too broadly graded. Key to this discussion is the tendency of #53 to segregate during placement on the subgrade and how severe is the problem.

6.3 Geotextile Separators

An alternative to using aggregate separators is provided by geotextiles (Figure 6.3). Geotextile separators are applicable to soft, fine-grained subgrade conditions with $CBR > 3$. Geotextiles, a category of geosynthetic materials, are highly permeable woven or non-woven fabrics made of plastic polymer fibers or threads. They are delivered on construction sites in rolls (generally 50-ft wide) and are laid down on the subgrade with overlaps or seams between strips to ensure continuity. No structural contribution is expected from geotextile separators, in contrast with geosynthetics used as basal reinforcement such as geogrid or high-modulus geotextiles. Great care must be taken for the geotextiles not to be contaminated with dirt while they

TABLE 6.3
Summary of separator analysis for Design Option 1 (subgrade examples from Jung and Bobet, 2008)

Option 1		Drainage/Base: #8				
Separator: #53		$D_{15}^{\text{drainage}} \leq 5D_{85}^{\text{separator}}$	$D_{50}^{\text{drainage}} \leq 25D_{50}^{\text{separator}}$	$D_{15}^{\text{separator}} \leq 5D_{85}^{\text{subgrade}}$	$D_{50}^{\text{separator}} \leq 25D_{50}^{\text{subgrade}}$	$D_{12}^{\text{separator}} \geq \#200$
Cu = 69.4 (Fail) ^a						
Subgrade: A-7-6 Untreated						
Separator	#53 Modified	Pass	Pass	Pass	Fail	Pass
	#53 Mod_6	Pass	Pass	Pass	Pass	Pass
	#53 Mod_7	Pass	Pass	Fail	Fail	Pass
Subgrade: A-7-6 Treated (site 3)						
Separator	#53 Modified	Pass	Pass	Pass	Pass	Pass
	#53 Mod_6	Pass	Pass	Pass	Pass	Pass
	#53 Mod_7	Pass	Pass	Pass	Pass	Pass
Subgrade: A-4 Treated (site 2)						
Separator	#53 Modified	Pass	Pass	Pass	Pass	Pass
	#53 Mod_6	Pass	Pass	Pass	Pass	Pass
	#53 Mod_7	Pass	Pass	Pass	Pass	Pass
Subgrade: A-4 Treated (site 4)						
Separator	#53 Modified	Pass	Pass	Pass	Pass	Pass
	#53 Mod_6	Pass	Pass	Pass	Pass	Pass
	#53 Mod_7	Pass	Pass	Pass	Pass	Pass
Subgrade: A-6 Treated (site 5)						
Separator	#53 Modified	Pass	Pass	Pass	Pass	Pass
	#53 Mod_6	Pass	Pass	Pass	Pass	Pass
	#53 Mod_7	Pass	Pass	Pass	Fail	Pass
Subgrade: A-6 Treated (site 6)						
Separator	#53 Modified	Pass	Pass	Pass	Pass	Pass
	#53 Mod_6	Pass	Pass	Pass	Pass	Pass
	#53 Mod_7	Pass	Pass	Pass	Pass	Pass

^aCriterion considered in DRIP *User's Guide* (Mallela et al., 2002) but not implemented in software.

TABLE 6.4
Summary of separator analysis for Design Option 2 (subgrade examples from Jung and Bobet, 2008)

Option 2 Separator: NJDOTCu = 4.8 (Fail) ^a	Drainage/Base: #43				
	$D_{15}^{\text{drainage}} \leq 5D_{85}^{\text{separator}}$	$D_{50}^{\text{drainage}} \leq 25D_{50}^{\text{separator}}$	$D_{15}^{\text{separator}} \leq 5D_{85}^{\text{subgrade}}$	$D_{50}^{\text{separator}} \leq 25D_{50}^{\text{subgrade}}$	$D_{12}^{\text{separator}} \geq \#200$
Separator: NJDOT	Pass	Subgrade: A-7-6 Untreated Pass	Fail	Fail	Pass
Separator: NJDOT	Pass	Subgrade: A-7-6 Treated (site 3) Pass	Pass	Pass	Pass
Separator: NJDOT	Pass	Subgrade: A-4 Treated (site 2) Pass	Pass	Pass	Pass
Separator: NJDOT	Pass	Subgrade: A-4 Treated (site 4) Pass	Pass	Pass	Pass
Separator: NJDOT	Pass	Subgrade: A-6 Treated (site 5) Pass	Pass	Fail	Pass
Separator: NJDOT	Pass	Subgrade: A-6 Treated (site 6) Pass	Pass	Pass	Pass

^aCriterion considered in DRIP *User's Guide* (Mallela et al., 2002) but not implemented in software.

TABLE 6.5
Summary of separator analysis for Design Option 6 (subgrade examples from Jung and Bobet, 2008)

Option 6 Separator: NJDOTCu = 4.8 (Fail) ^a	Base: #8				
	$D_{15}^{\text{drainage}} \leq 5D_{85}^{\text{separator}}$	$D_{50}^{\text{drainage}} \leq 25D_{50}^{\text{separator}}$	$D_{15}^{\text{separator}} \leq 5D_{85}^{\text{subgrade}}$	$D_{50}^{\text{separator}} \leq 25D_{50}^{\text{subgrade}}$	$D_{12}^{\text{separator}} \geq \#200$
Separator: NJDOT	Pass	Subgrade: A-7-6 Untreated Pass	Fail	Fail	Pass
Separator: NJDOT	Pass	Subgrade: A-7-6 Treated (site 3) Pass	Pass	Pass	Pass
Separator: NJDOT	Pass	Subgrade: A-4 Treated (site 2) Pass	Pass	Pass	Pass
Separator: NJDOT	Pass	Subgrade: A-4 Treated (site 4) Pass	Pass	Pass	Pass
Separator: NJDOT	Pass	Subgrade: A-6 Treated (site 5) Pass	Pass	Fail	Pass
Separator: NJDOT	Pass	Subgrade: A-6 Treated (site 6) Pass	Pass	Pass	Pass

^aCriterion considered in DRIP *User's Guide* (Mallela et al., 2002) but not implemented in software.

are stored on construction sites, and not to be damaged during their installation and construction of subsequent layers of the pavement.

Similar to their granular counterparts, both separation and filtration functions are expected from geotextile separators. However, because of the physical nature of geotextile fabrics there is no possibility for the separator to contaminate the granular drainage/base layer—only the compatibility between subgrade and geotextile has to be assessed. In addition, geotextile separators should be more permeable than the subgrade, in order to prevent accumulation of excess pore pressure (this requirement is easily met on low-permeability, fine-grained subgrades, given the open pore structure of the textile fabrics).

Separation requirements are based on the ability of the geotextile to survive installation and subsequent pavement construction without damage, i.e., the criteria are based on a set of mechanical index properties which

must be met in order for the geotextile structural integrity to be preserved. Minimal requirements for these parameters depend on the severity of construction conditions: ratings from 1 (most severe) to 3 (least severe) have been established as a result of AASTO joint committees' work (AASHTO, 1990), and are shown for roadway separation applications in Table 6.6. It is seen, for instance, that for subgrades with CBR > 3, the rating would be 2 (medium severity). Minimal required values for the mechanical index properties are shown in Table 6.7 for severity of construction conditions 1 and 2. It is noted that, in its geotextile design function for separators, the DRIP software does not address survivability.

Filtration compatibility between the geotextile and the subgrade is based on the size of the fabric pores, characterized by the Apparent Opening Size (AOS) and representative of the larger opening range, as compared to the larger fraction of the subgrade particles,

TABLE 6.6
Construction survivability ratings (after AASHTO, 1990; AASHTO, 2006)

Subgrade CBR ^a	<1	<1	1 to 2	1 to 2	>3	>3
Equipment Ground Contact Pressure	>50 psi (>350 kPa)	<50 psi (<350 kPa)	>50 psi (>350 kPa)	<50psi (<350 kPa)	>50 psi (>350 kPa)	<50 psi (<350 kPa)
Cover Thickness ^b (compacted)	Required Geotextile Class (construction severity rating: 1 = most severe, 2 = moderate severity)					
4 in ^{c,d} (100 mm)	NR ^e	NR	1 ^e	1	2 ^e	2
6 in (150 mm)	NR	NR	1	1	2	2
12 in (300 mm)	NR	1	2	2	2	2
18 in (450 mm)	1	2	2	2	2	2

^aAssume saturated CBR unless construction scheduling can be controlled.

^bMaximum aggregate size not to exceed one-half the compacted cover thickness.

^cFor low-volume, unpaved roads (ADT < 200 vehicles).

^dThe 4" (100 mm) min. cover is limited to existing road bases and not intended for use in new construction.

^eNR = NOT RECOMMENDED; 1 = high survivability Class 1 geotextiles per AASHTO M-288 (2006), and 2 = moderate survivability Class 2

TABLE 6.7
Geotextile survivability requirements (based on Holtz et al., 2008)

Property	Pertinent Standard	Required Values, (N, [lb])			
		Geotextile Class 1		Geotextile Class 2	
		Elongation <50% (typical of woven)	Elongation ≥50% (typical of nonwoven)	Elongation <50%	Elongation ≥50%
Grab Strength	ASTM D 4632/D4632M-15a (2015)	1400 [315]	900 [200]	1100 [250]	700 [157]
Sewn Seam Strength	ASTM D 4632/D4632M-15a (2015)	1260 [280]	810 [180]	990 [220]	630 [140]
Tear Strength	ASTM D 4533/D4533M-15 (2015)	500 [110]	350 [80]	400 [90]	250 [56]
Puncture Strength	ASTM D 6241-14 (2014)	2750 [620]	1925 [433]	2200 [495]	1375 [309]

characterized by its D_{85} value. The main concept of geotextile filtration is that, if the larger particles of the subgrade are prevented from entering the geotextile fabric, a bridging mechanism will develop at the interface where smaller particles will be also retained. According to document FHWA NHI-07-092 (Holtz et al., 2008; per B. R. Christopher's personal communication to Amy Getchall on February 20, 2019, this document should be preferred to Christopher et al., 2006, and FHWA NHI-05-037, 2017, for the design of geotextile separators and filters), the criterion is also a function of the manufacturing type of geotextile, i.e., woven or non-woven fabric; this is because woven fabrics have a uniform opening size distribution whereas non-woven fabric have a broadly distributed opening size distribution:

$$AOS < (D_{85})_{\text{subgrade}} \text{ for woven geotextiles} \quad (\text{Equation 6.16})$$

$$AOS < 1.8(D_{85})_{\text{subgrade}} \text{ for non-woven geotextiles} \quad (\text{Equation 6.17})$$

In its section on the Technical Background of the software, the DRIP User's Guide (Mallela et al., 2002)

also acknowledges the use of Equations 6.16 and 6.17, but in its operation the program uses a different criterion based on the fine fraction of the subgrade particle size distribution (irrespective of the type of geotextile):

$$AOS > 3(D_{15})_{\text{subgrade}} \quad (\text{Equation 6.18})$$

No explanation is provided for this discrepancy.

The list of geotextiles approved by INDOT (see Appendix J) was reviewed and a database of their index properties, according to the manufacturers' documentation, was created. It was noted that this list seems to be outdated as, among the 55 products, 8 have been discontinued, 9 of the manufacturing companies no longer exist, and 9 of the companies could not be reached for documentation requests. For the remaining products, an assessment was made of their applicability as separator in the case of INDOT Design Option 3 (see Table 6.1) with the subgrade example type A-7-6 (untreated) from Jung and Bobet (2008). Results are presented in Table 6.8 and Table 6.9 for survivability criteria, filtration criterion based on D_{85} of the subgrade (Holtz et al., 2008) and filtration criterion based on D_{15} (DRIP). In Table 6.8 it is Table 6.8 Compiled data for list of INDOT approved geotextiles and

TABLE 6.8
Compiled data for list of INDOT approved geotextiles and assessment of separator and filter functions for Design Option 3 with untreated A-7-6 subgrade from Jung and Bobet (2008), assuming Class 1 geotextiles are needed

Geotextile			Characteristics Used for Assessment (based on Holtz et al. 2008)					Retention Criterion (based on Holtz et al., 2008)		Separator Criterion DRIP
Manufacturer	Product Name	Woven or Nonwoven	Grab Strength [N]	Tear Strength [N]	Puncture Strength [N]	Permittivity [s-1]	AOS [mm]	AOS < BD ₈₅ ^{subgrade} B = 1 Woven B = 1.8 Nonwoven		AOS > 3D ₁₅ ^{subgrade}
Amoco Fabrics and Fibers Co	Propex 4553	Nonwoven	900	355	533	1	0.15	Yes	Yes	Yes
	4535	Nonwoven	355	155	200	2	0.21	Yes	Yes	Yes
	4545	Nonwoven	400	175	240	1.8	0.21	Yes	Yes	Yes
	FX-70HS	Nonwoven	800	330	2000	1.4	0.21	Yes	Yes	Yes
Carthage Mills	FX-80HS	Nonwoven	910	360	2230	1.35	0.18	Yes	Yes	Yes
Carthage Mills	Poly-Filter X (6% monofilaments)	Woven	1650 × 1110	450 × 270	4230	0.28	0.21	Yes	Yes	Yes
Carthage Mills	FX-30HS	Nonwoven	360	130	760	2.1	0.3	Yes	Yes	Yes
Carthage Mills	FX-35HS	Nonwoven	400	180	1110	2	0.3	Yes	Yes	Yes
Crown Resources	Style R080	Nonwoven	911	356	2330	1.4	0.18	Yes	Yes	Yes
Dalco Nonwovens	Daltex 1080	Nonwoven	911.8	378.1	578.3	1.4	0.18	Yes	Yes	Yes
Dalco Nonwovens	Daltex 1031	Nonwoven	350	110	934	2.2	0.3	Yes	Yes	Yes
Hanes Geo Components	Terratex EP	Woven	1647	445	4228	0.28	0.21	Yes	Yes	Yes
Hanes Geo Components	Terratex N08	Nonwoven	911	378	2380	1.35	0.18	Yes	Yes	Yes
Hanes Geo Components	Terratex N03	Nonwoven	350	130	760	2.2	0.3	Yes	Yes	Yes
Linq	GTF 180EX	Nonwoven	912	356	2380	1.5	0.15	Yes	Yes	Yes
Propex Inc	Propex Geotext 801	Nonwoven	912	356	2380	1.4	0.18	Yes	Yes	Yes
Propex Inc	Propex Geotext 311	Nonwoven	356	133	934	2.2	0.3	Yes	Yes	Yes
Skaps	GT 180	Nonwoven	911.9	378.1	533.8	1.35	0.18	Yes	Yes	Yes
Skaps	GT 131	Nonwoven	355	133	778	2.2	0.33	Yes	Yes	Yes
Skaps	GT 135	Nonwoven	401	178	1180	2	0.3	Yes	Yes	Yes
Tencate	Fillerweave 700	Woven	1647	445	4228	0.28	0.21	Yes	Yes	Yes
Tencate	Geo-Mirafi 180N	Nonwoven	912	356	2224	1.4	0.18	Yes	Yes	Yes
Tencate	135N	Nonwoven	365	134	79	2.1	0.3	Yes	Yes	Yes
Tencate	140 NI	Nonwoven	401	178	1113	2	0.3	Yes	Yes	Yes
Thrace-Linq	120EX	Nonwoven	356	133	934	2.2	0.21	Yes	Yes	Yes
US Fabrics Inc	US 205NW	Nonwoven	912	378	579	1.35	0.18	Yes	Yes	Yes
US Fabrics Inc	US 80NW	Nonwoven	365	133	799	2.2	0.3	Yes	Yes	Yes
US Fabrics Inc	US 90NW	Nonwoven	401	178	1179	2	0.3	Yes	Yes	Yes
US Fabrics Inc	US 120NW-C	Nonwoven	533	222	1513	1.7	0.21	Yes	Yes	Yes
Thrace-Linq	GTF 125EX	Nonwoven	400	178	1179	2.1	0.21	Yes	Yes	Yes

Notes:

Bold font identifies geotextiles meeting all requirements.

Red shows failure to meet a requirements.

TABLE 6.9
Compiled data for list of INDOT approved geotextiles and assessment of separator and filter functions for Design Option 3 with untreated A-7-6 subgrade from Jung and Bobet (2008), assuming Class 2 geotextiles are needed

Geotextile		Characteristics Used for Assessment (based on Holtz et al. 2008)					Retention Criterion (based on Holtz et al. 2008)		Separator Criterion
Manufacturer	Product Name	Woven or Nonwoven	Grab Strength [N]	Tear Strength [N]	Puncture Strength [N]	Permittivity [S-I]	AOS [mm]	AOS < BD _{gs} subgrade B = 1 Woven B = 1.8 Nonwoven	AOS ≥ 3D ₁₅ subgrade
Amoco Fabrics and Fibers Co	Propex 4553	Nonwoven	900	355	533	1	0.15	Yes	Yes
Amoco Fabrics and Fibers Co	4535	Nonwoven	355	155	200	2	0.21	Yes	Yes
Amoco Fabrics and Fibers Co	4545	Nonwoven	400	175	240	1.8	0.21	Yes	Yes
Carthage Mills	FX-70HS	Nonwoven	800	330	2000	1.4	0.21	Yes	Yes
Carthage Mills	FX-80HS	Nonwoven	910	360	2230	1.35	0.18	Yes	Yes
Carthage Mills	Poly-Filter X (6% monofilaments)	Woven	1650 × 1110	450 × 270	4230	0.28	0.21	Yes	Yes
Carthage Mills	FX-30HS	Nonwoven	360	130	760	2.1	0.3	Yes	Yes
Carthage Mills	FX-35HS	Nonwoven	400	180	1110	2	0.3	Yes	Yes
Crown Resources	Style R080	Nonwoven	911	356	2330	1.4	0.18	Yes	Yes
Dalco Nonwovens	Daltex 1080	Nonwoven	911.8	378.1	578.3	1.4	0.18	Yes	Yes
Dalco Nonwovens	Daltex 1031	Nonwoven	350	110	934	2.2	0.3	Yes	Yes
Hanes Geo Components	Terratex EP	Woven	1647	445	4228	0.28	0.21	Yes	Yes
Hanes Geo Components	Terratex N08	Nonwoven	911	378	2380	1.35	0.18	Yes	Yes
Hanes Geo Components	Terratex N03	Nonwoven	350	130	760	2.2	0.3	Yes	Yes
Linq	GTF 180EX	Nonwoven	912	356	2380	1.5	0.15	Yes	Yes
Propex Inc	Propex Geotext 801	Nonwoven	912	356	2380	1.4	0.18	Yes	Yes
Propex Inc	Propex Geotex 311	Nonwoven	356	133	934	2.2	0.3	Yes	Yes
Skaps	GT 180	Nonwoven	911.9	378.1	533.8	1.35	0.18	Yes	Yes
Skaps	GT 131	Nonwoven	355	133	778	2.2	0.33	Yes	Yes
Skaps	GT 135	Nonwoven	401	178	1180	2	0.3	Yes	Yes
Tencate	Filterweave 700	Woven	1647	445	4228	0.28	0.21	Yes	Yes
Tencate	Geo-Mirafi 180N	Nonwoven	912	356	2224	1.4	0.18	Yes	Yes
Tencate	135N	Nonwoven	365	134	79	2.1	0.3	Yes	Yes
Tencate	140 N1	Nonwoven	401	178	1113	2	0.3	Yes	Yes
Thrace-Linq	120EX	Nonwoven	356	133	934	2.2	0.21	Yes	Yes
US Fabrics Inc	US 205NW	Nonwoven	912	378	579	1.35	0.18	Yes	Yes
US Fabrics Inc	US 80NW	Nonwoven	365	133	799	2.2	0.3	Yes	Yes
US Fabrics Inc	US 90NW	Nonwoven	401	178	1179	2	0.3	Yes	Yes
US Fabrics Inc	US 120NW-C	Nonwoven	533	222	1513	1.7	0.21	Yes	Yes
Thrace-Linq	GTF 125EX	Nonwoven	400	178	1179	2.1	0.21	Yes	Yes

Notes:

Bold font identifies geotextiles meeting all requirements.

Red shows failure to meet a requirements.

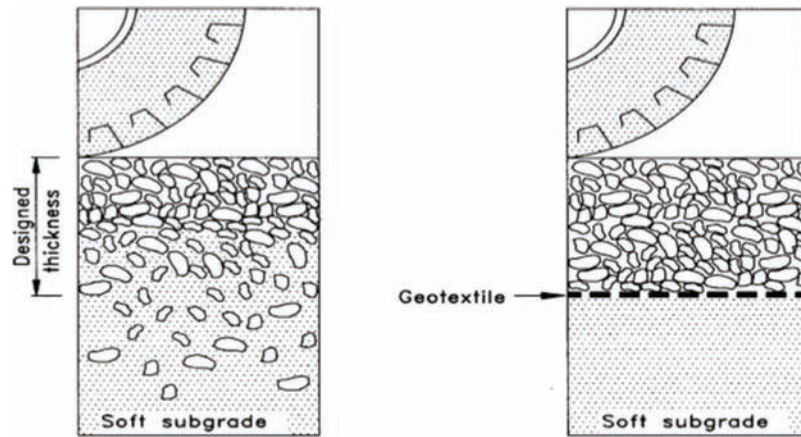


Figure 6.3 Concept of geotextile separation in roadways (Holtz et al., 2008).

assessment of separator and filter functions for Design Option 3 with untreated A-7-6 subgrade from Jung and Bobet (2008), assuming Class 1 geotextiles are needed, and in Table 6.9, more favorable construction conditions, where Class 2 geotextiles would be sufficient, are assumed.

With this example, it is observed that a number of the approved geotextiles would not pass the survivability requirements (failing values are shown in red) as separators, while all the products meet the filter criteria. Of the products deemed adequate (highlighted in green), a majority are non-woven geotextiles.

In summary, geotextile separators can be considered as an economic alternative to aggregate separator layers. The following important points should be noted:

- Design of geotextile separators requires, at first, the assessment of the construction condition severity for the survivability of the fabric.
- Characterization of the subgrade, in particular of its particle size distribution, is necessary.
- In a number of situations, non-woven geotextiles would be better candidates than woven fabrics.
- The INDOT list of approved geotextiles should be updated.
- The DRIP software shows significant discrepancies in its implementation of filter criteria, it does not address geotextile survivability. Unchecked outputs from the software for the design of separators can be misleading and result in unconservative designs.

7. CONCLUSIONS AND RECOMMENDATIONS

7.1 Introduction

This project addressed the design of the subbase of pavements. The work performed included a review of existing practices for subbase design in Indiana and in other states; laboratory evaluation of the compaction and hydraulic conductivity properties of select aggregates, complemented by additional data for similar materials collected from the literature; the analysis of

the stability of the aggregates under the weight and the action of construction equipment; a review of the guidelines for establishing the compatibility between aggregate layers, and analysis of the compatibility between select aggregates using the software DRIP; assessment of the applicability of select geotextiles as separators in place of an aggregate layer.

The following section summarizes the main conclusions drawn from this work. Recommendations for implementation as well as for additional research are presented in Section 7.3.

7.2 Conclusions

The study yielded a number of conclusions, which are summarized below in seven categories that cover general principles, material selection, use of geotextiles, construction methods, use of the DRIP software, laboratory aggregate characterization methods and the relationship between strength parameters and aggregate characteristics.

General conclusions on subbase design

- Inclusion of a separator layer seems to be the preferred design for INDOT projects as well as in other states, as it provides a clean, stable and self-draining working platform. Furthermore, in the case of a granular separator material, this layer contributes mechanically to the pavement structure, even if it is not explicitly accounted for in design calculations.
- In principle, it is possible to design subbase design solutions that are common to both asphalt and concrete pavements. This is already being done in two of the states (Ohio and Kentucky) interviewed as part of this project.
- The compatibility analyses performed in this study suggest that a separator may not always be necessary for pavements on cement-treated subgrades. Additional research on the mechanisms for fine particle migration through treated subgrades is required to support this conclusion.

- Geotextile separators can be considered as an economic alternative to aggregate separator layers (see more on this below).
- Of the aggregate-only design options specifically examined in this study, compatibility analyses suggest that the use of #43 as drainage layer over a material such as NJDOT functioning as separator layer appears promising, provided both layers are compacted appropriately. Additional data on the hydraulic conductivity of these types of aggregates is required before a conclusive recommendation can be made.

Selection of aggregates for drainage layer and separator layer

- For all the loading cases considered, the stability of #8 is found to be highly problematic. This is consistent with experience reported by field engineers and contractors both in Indiana and elsewhere. Additionally, while no hydraulic conductivity experimental data could be obtained for this material as part of this project, literature data available for aggregates of similar gradation indicate that values of k in excess of 10^4 ft/day should be expected. Aggregates with such a high value of k have traditionally had performance problems in the field. Note also that none of the state agencies interviewed as part of this research effort consider the use of a material such as #8.
- Aggregates with particle size distribution falling within the bands for Indiana #43 and #53 have the potential to be used for the drainage layer. Data from preliminary tests as well as results from the literature indicate that with appropriate aggregate particle size selection and compaction, values of k between 150 and 1,480 ft/day (depending on gradation, aggregate source and level of compaction) can be achieved. Additional data for aggregates with different particle size distributions falling in these ranges are required.
- The use of #43 and #53 for drainage is also consistent with practice in other states which utilize aggregate with particle size distribution falling in comparable ranges.
- Specifications prescribing narrow intervals of k of the compacted aggregate that contractors are required to achieve in the field appear problematic to verify/enforce, due to the challenges in measuring this property both in the field and in the laboratory and the documented variability of this property.
- Published data (e.g., Randolph et al., 1996) demonstrate that relatively small variations in particle size distribution can lead to changes in hydraulic conductivity as large as 2 orders of magnitude. This signifies that prescribing the use of aggregates simply based on their particle size distribution falling within a broad band (such as those that characterize #43 and #53) may not be sufficient, even with adequate compaction in the field, to achieve a target value or range of k .
- Selection of aggregates for the separator layer requires site specific consideration of the subgrade conditions. The analyses performed show that lack of compatibility with the subgrade at the lower interface is the primary reason for considering a material inadequate as a separator.
- There are some inconsistencies in the criteria employed by different agencies for evaluating aggregates used for the

separator layer. In particular, the guidelines on the separator coefficient of uniformity require further attention.

- Aggregates used for the separator layer in the states interviewed as part of this project have particle size distributions comparable to #43 and #53, or finer.

Use of geotextiles

While, as stated above, geotextile separators can be considered as an economic alternative to aggregate separator layers, the following important points should be noted:

- The design of geotextile separators requires assessment of the construction condition severity for the survivability of the fabric and consideration of the site-specific subgrade characteristics including particle size distribution.
- In a number of situations, non-woven geotextiles are likely to be better candidates than woven fabrics. Of the products on the list of geotextiles approved by INDOT that were found to be adequate, a majority are non-woven geotextiles.
- The DRIP software does not address geotextile survivability, and, alone, cannot be used for geotextile selection.
- The INDOT list of approved geotextiles should be updated.

Construction methods

- Existing INDOT specifications to avoid segregation should be enforced when placing aggregates in the field, in particular materials such as #43 and #53, as experience from other states indicates that best handling procedures are key to obtaining optimal performance in the field. The use of a spreader box is strongly encouraged.
- For aggregates such as #43 and #53, maximum values of dry density are reached at optimum water contents that typically fall in the 5%–10% range. Values of optimum water content are aggregate specific and should be assessed in the laboratory and controlled in the field.
- The stability of materials such as INDOT #43 and #53 requires density and frictional resistance that are achievable with thorough compaction. Static compaction alone is unlikely to be sufficient to this purpose, thus vibratory compaction is highly desirable. An adequate procedure could include *first* passes of static compaction for gaining strength so that the material can sustain further passes in vibratory mode.
- Static loading by an asphaltic concrete paver on wheels is one of the critical situations for stability of the granular base. Where possible, it would be advisable to use asphalt pavers on tracks which impose greatly reduced stresses.

Use of DRIP software for design of drainage and separator layers

- DRIP cannot be used alone for the selection of aggregates as it provides no assessment of the soundness/abrasion characteristics of these materials.

- Caution should be exercised in using DRIP for separator design, as DRIP does not account for the coefficient of uniformity of the aggregate. As noted in the main body of this report, this can in some cases lead to considering a material viable, where guidelines for example by the FHWA would deem it inadequate as a separator due to the excessively large value of Cu.
- Caution should also be exercised when using DRIP to evaluate a geotextile as separator, as the software does not include survivability criteria. These criteria were found to be the most stringent when evaluating geotextiles and controlled the design.
- Predictions of the hydraulic conductivity of aggregate layers generated through DRIP should be considered with care, as the software relies on the model by Moulton (1980/1990), which was shown in this work to yield generally unreliable estimates of k for all the aggregates examined.
- There are several important inconsistencies between the documentation provided in the DRIP manual and the software implementation.

Laboratory methods for aggregate characterization

- The data collected in this project support the conclusion from previous studies that the vibratory hammer method is the most effective method for the laboratory compaction of granular materials. This method should be used as laboratory reference in compaction specifications when a value of the relative compaction must be prescribed.
- Laboratory measurement of the hydraulic conductivity of aggregates under field-relevant conditions (compaction and drainage) is problematic in the laboratory using traditional equipment due to the size and the high k of the aggregates. The newly constructed horizontal permeameter addresses these shortcomings.

Relationships between strength and aggregate characteristics

- Only a few empirical relationships between strength parameters and aggregate characteristics emerge from this study, quantified by medium to high values of correlation coefficients, and which can be trusted after hypothesis testing. These are generally not strong enough to allow the development of empirical formulas applicable in engineering practice. These outcomes of the correlation analysis reflect the information inherent to the available database. Other, or stronger, relationships may exist between material shear strength and other properties, but no statistical evidence of such relationships was found in this study.

7.3 Recommendations

Based on the work performed the following recommendations for implementation are provided:

- Indiana #8 should no longer be used for the base drainage layer. This recommendation is based on the excessively high hydraulic conductivity and the inadequate

stability of this material under the expected field loading conditions and is supported by field experience in Indiana and in other states.

- The use of geotextiles, including non-woven, should be encouraged as an economic and potentially lower carbon footprint alternative for the separator layer. The design should rely on both survivability and filtration criteria, with consideration of the site-specific subgrade conditions. As noted above, this evaluation *should not* be conducted using DRIP alone.
- Construction methods to limit segregation of the aggregates in the field should be enforced. Limiting segregation will ensure that the material placed in the field consistently exhibits the expected (design) behavior, while also reducing short range variability in the engineering properties, which may ultimately be responsible for pavement distress.
- Compaction of aggregates in the field should be performed using vibratory rollers, which provide the most effective compaction, with potentially early passes using static compaction to address stability problems.
- When placing materials such as #43 and #53 verification of the water content should be required to ensure the maximum values of dry density. As stated above, values of optimum water content are aggregate specific and should be assessed in the laboratory.
- Where available asphalt paving machines *on tracks* should be considered preferable to pavers on wheels due to the greatly reduced stresses imposed on the aggregate layers.

The study also highlighted areas where additional research is warranted. In particular, it is suggested that future efforts be directed to the following:

- Obtaining both shear strength and hydraulic conductivity data for #43 and #53 aggregates under a range of field-relevant testing conditions. This should be done for different sources of the aggregates (e.g., limestone versus slag), with consideration of different gradations. This type of information appears critical both for developing future specifications and for conducting more in-depth analyses.
- Identifying/developing techniques for measuring the in situ hydraulic conductivity of compacted aggregates. This is a necessary step as INDOT continues to move towards the development of performance-based specifications.
- Investigating the migration of fines through and from treated subgrades. This could lead to significant savings in the construction of subbases, if specific conditions not requiring the use of a separator layer are identified.
- Incorporating survivability and filtration criteria in a software that would be used for geotextile separator selection in place of DRIP. This would address the shortcomings of the DRIP software identified in this work.
- Extending the statistical analysis of shear strength data to a broader database.

REFERENCES

AASHTO. (1990). *Guide specifications and test procedures for geotextiles* (AASHTO-AGCARTBA Task Force 25 Report). Subcommittee on New Highway Materials,

- American Association of State Transportation and Highway Officials.
- AASHTO M-147. (2017). *Standard specification for materials for aggregate and soil-aggregate subbase, base, and surface courses*. American Association of State Highway and Transportation Officials.
- AASHTO M-288. (2006). *Standard specification for geosynthetic specification for highway applications*. American Association of State Highway and Transportation Officials.
- AASHTO T 90-16. (2016). *Standard method of test for determining the plastic limit and plasticity index of soils*. American Association of State Highway and Transportation Officials.
- AASHTO T 96-02. (2019). *Standard method of test for resistance to degradation of small-size coarse aggregate by abrasion and impact in the Los Angeles machine*. American Association of State Highway and Transportation Officials.
- AASHTO T 104-99. (2016). *Standard method of test for soundness of aggregate by use of sodium sulfate or magnesium sulfate*. American Association of State Highway and Transportation Officials.
- AASHTO T-180. (2019). *Standard method of test for moisture-density relations of soils using a 4.54-kg (10-lb) rammer and a 457-mm (18-in) drop*. American Association of State Highway and Transportation Officials.
- AC Business Media. (2019, November). Asphalt paver spec guide. *Asphalt Contractor*, 20–22. <https://issuu.com/forconstructionpros.com/docs/acon1119>
- ACPA. (2007). *Subgrades and subbases for concrete pavements* (Engineering Bulletin EB204P). American Concrete Pavement Association. <http://www.acpa.org/wp-content/uploads/2019/02/EB204P-Subgrades-and-Subbases-for-Concrete-Pavements.pdf>
- ACPA. (2010). *Subbase specification trends* (Concrete Pavement Technology Series TS204.12P). American Concrete Pavement Association. <http://1204075.sites.myregisteredsite.com/downloads/TS/EB204P/TS204.12P.pdf>
- Ageikin, I. S. (1987). *Off-the Road Mobility of Automobiles*, Amerind Publishing Co., New Delhi (translated from 1981 Russian book).
- Aghaei Araei, A., Soroush, A., & Rayhani, M. H. T. (2010, June). Large-scale triaxial testing and numerical modeling of rounded and angular rockfill materials. *Scientia Iranica*, 17(3), 169–183. http://scientiairanica.sharif.edu/article_3149_983e8148022e553f1d61a02e9ecb315c.pdf
- Applied Research Associates, Inc., (2014, October 27). *Drainage requirements in pavements (DRIP 2.0)*. <https://me-design.com/MEDesign/DRIP.html?AspxAutoDetectCookieSupport=1>
- ASTM C131/C131M-14. (2006). *Standard test method for resistance to degradation of small-size coarse aggregate by abrasion and impact in the Los Angeles machine* (Annual Book of ASTM Standards). ASTM International. <http://www.astm.org/cgi-bin/resolver.cgi?C131C131M-14>
- ASTM C127-15. (2015). *Standard test method for relative density (specific gravity) and absorption of coarse aggregate* (Annual Book of ASTM Standards). ASTM International. <https://www.astm.org/Standards/C127>
- ASTM D7382-08. (2008). *Standard test methods for determination of maximum dry unit weight and water content range for effective compaction of granular soils using a vibrating hammer* (Withdrawn 2017; Annual Book of ASTM Standards). ASTM International. <https://www.astm.org/Standards/D7382.htm>
- ASTM D1557-12e1. (2012). *Standard test methods for laboratory compaction characteristics of soil using modified effort (56,480 ft-lbf/ft³ (2,748 kN-m/m³))* (Annual Book of ASTM Standards). ASTM International. <https://www.astm.org/Standards/D1557>
- ASTM D6241-14. (2014). *Standard test method for static puncture strength of geotextiles and geotextile-related products using a 50-mm probe* (Annual Book of ASTM Standards). ASTM International. <https://www.astm.org/Standards/D6241.htm>
- ASTM D4718/D4718M-15. (2015). *Standard practice for correction of unit weight and water content for soils containing oversize particles* (Annual Book of ASTM Standards). ASTM International. <https://www.astm.org/Standards/D4718.htm>
- ASTM D5856-15. (2015). *Standard test method for measurement of hydraulic conductivity of porous material using a rigid-wall, compaction-mold permeameter* (Annual Book of ASTM Standards). ASTM International. <https://www.astm.org/Standards/D5856.htm>
- ASTM D4632/D4632M-15a. (2015). *Standard test method for grab breaking load and elongation of geotextiles* (Annual Book of ASTM Standards). ASTM International. <https://www.astm.org/Standards/D4632>
- ASTM D4533/D4533M-15. (2015). *Standard test method for trapezoid tearing strength of geotextiles*. (Annual Book of ASTM Standards). ASTM International. <https://www.astm.org/Standards/D4533.htm>
- ASTM D5731-16. (2016). *Standard test method for determination of the point load strength index of rock and application to rock strength classifications* (Annual Book of ASTM Standards). ASTM International. <https://www.astm.org/Standards/D5731.htm>
- ASTM D6913/D6913M-17. (2017). *Standard test methods for particle-size distribution (gradation) of soils using sieve analysis* (Annual Book of ASTM Standards). ASTM International. <https://www.astm.org/Standards/D6913>
- Bergeron, K., Jahren, C., Wemager, M., & White, D. (1998, May). *Embankment quality phase I report* (CTRE Management Project 97-8). Center for Transportation Research and Education, Iowa State University. <https://pdfs.semanticscholar.org/9c14/bd404e7b1eb4ebca926d453ac3a04c6b08b7.pdf>
- BOMAG Fayat Group. (2009, February). *Basic principles of asphalt compaction: Compaction methods, compaction equipment, and rolling technique*. BOMAG GmbH. <https://yumpu.com/en/document/read/6035545/basic-principles-of-asphalt-compaction-bomag>
- Bourdeau, P. L. (2016, March). *BEARING1, EXCEL Application Software* (March 2016 version). Lyles School of Civil Engineering, Purdue University.
- Betram, G. E. (1940). *An experimental investigation of protective filters* (Publication No. 267), Graduate School of Engineering, Harvard University.
- Carman, P. C. (1938). The determination of the specific surface of powders. *Journal of the Society of Chemical Industries Transactions*, 57, 225–234.
- Carman, P. C. (1956). *Flow of gases through porous media*. Butterworths Scientific.
- Carrier, W. D., III. (2003). Goodbye, Hazen; Hello, Kozeny-Carman. *Journal of Geotechnical and Geoenvironmental Engineering*, 129(11), 1054–1056. [https://doi.org/10.1061/\(ASCE\)1090-0241\(2003\)129:11\(1054\)](https://doi.org/10.1061/(ASCE)1090-0241(2003)129:11(1054))
- Cedergren, H. R. (1974). *Drainage of highway and airfield pavements*. John Wiley & Sons.
- Chow, L. C., Mishra, D., & Tutumluer, E. (2014, December). *Aggregate base course material testing and rutting model development* (Report No. FHWA/NC/2013-18). Illinois

- Center for Transportation. <https://connect.ncdot.gov/projects/research/RNAProjDocs/2013-18FinalReport.pdf>
- Christopher, B. R., Schwartz, C., & Boudreau, R. (2006, May). *Geotechnical aspects of pavements*. (Report No. NHI-05-037). Federal Highway Administration, U.S. Department of Transportation. <https://www.fhwa.dot.gov/engineering/geotech/pubs/05037/index.cfm>
- Drnevich, V. P., Evans, A. C., & Prochaska, A. B. (2007). *A study of effective soil compaction control of granular soils* (Joint Transportation Research Program Report No. FHWA/IN/JTRP-2007/12). West Lafayette, IN: Purdue University. <https://doi.org/10.5703/1288284313357>
- Duncan, J. M., Williams, G. W., Sehn, A. L., & Seed, R. B. (1991). Estimation of earth pressures due to compaction. *Journal of Geotechnical Engineering*, 117(12), 1833–1847. [https://doi.org/10.1061/\(ASCE\)0733-9410\(1991\)117:12\(1833\)](https://doi.org/10.1061/(ASCE)0733-9410(1991)117:12(1833))
- Evans, A. C. (2006). *Compaction control of large-sized granular soils/laggates: The vibrating hammer method of compaction and time domain reflectometry* (Master's thesis, Purdue University).
- FHWA. (1992, March). *Drainable pavement system participant notebook: Demonstration project no. 87* (Publication No. FHWA-SA-92-008). Federal Highway Administration, U.S. Department of Transportation. <https://www.fhwa.dot.gov/pavement/pubs/013226.pdf>
- FHWA. (1999). *Pavement subsurface drainage design* (FHWA-HI-99-028, NHI Course No. 131026). Federal Highway Administration, U.S. Department of Transportation.
- FHWA. (2016, September, rev. 2017). *Bases and subbases for concrete pavements* (Tech Brief HIF-16-485) Federal Highway Administration, U.S. Department of Transportation <https://www.fhwa.dot.gov/pavement/concrete/pubs/hif16485.pdf>
- Forssblad, L. (1981). *Vibratory soil and rock fill compaction*. Dynapac Maskin AB.
- Gates, L., Masad, E., Pyle, R., & Bushee, D. (2011, January). *Aggregate Image Measurement System 2 (AIMS2): Final report* (Report No. FHWA-HIF-11-030). Highways for LIFE Program Office. <https://www.fhwa.dot.gov/hfl/partnerships/aims2/hif11030/hif11030.pdf>
- Harr, M. E. (1977). *Mechanics of particulate media*. McGraw-Hill Education.
- Hazen, R. A. (1892). *Some physical properties of sands and gravels, with special reference to their use in filtration, 24th annual report* (Publication Document No. 34). Massachusetts State Board of Health. 539–556.
- Hilf, J. W. (1991). Compacted fill. In: H.-Y. Fang (Ed.), *Foundation engineering handbook*. Springer, Boston, MA.
- Holtz, R. D., Christopher, B. R., & Berg, R. R. (2008, August). *Geosynthetic design & construction guidelines: Reference manual* (Publication No. FHWA NHI-07-092). Federal Highway Administration.
- Huang, Y. H. (1993). *Pavement analysis and design*. Prentice Hall.
- Hydraulics Research Limited. (1985). *A permeameter for road drainage layers* (Report EX 1313).
- Hydraulics Research Limited. (1986). *Performance tests on a permeameter for road drainage layers* (Report EX 1518).
- INDOT. (2020). *Indiana Department of Transportation standard specifications 2020*.
- Ingold, T. S. (1987, November). Discussion of “Compaction-induced earth pressures under K0-Conditions” by Duncan, J. M. and R. B. Seed. *Journal of Geotechnical Engineering*, 113(11), 1403–1405. [https://doi.org/10.1061/\(ASCE\)0733-9410\(1987\)113:11\(1403\)](https://doi.org/10.1061/(ASCE)0733-9410(1987)113:11(1403))
- Jones, H. A., & Jones, R. H. (1989). Horizontal permeability of compacted aggregates. In R. H. Jones and A. R. Dawson (Eds.), *Proceedings of the 3rd International Symposium on Unbound Aggregates in Roads* (pp. 70–77). Butterworths Scientific.
- Jung, C., & Bobet, A. (2008). *Post-construction evaluation of lime-treated soils* (Joint Transportation Research Program Report No. FHWA/IN/JTRP-2007/25). West Lafayette, IN: Purdue University. <https://doi.org/10.5703/1288284313443>
- Kenney, T. C., Lau, D., & Ofoegbu, G. I. (1984). Permeability of compacted granular materials. *Canadian Geotechnical Journal*, 21(4), 726–729. <https://www.nrcresearchpress.com/doi/pdf/10.1139/t84-080>
- Koerner, R. M. (2005). *Designing with geosynthetics* (5th Ed.). Pearson/Prentice Hall.
- Kozeny, J. (1927). *Ueber kapillare Leitung des Wassers im Boden*. Wien, Akad. Wiss., 136(2a), 271–306.
- Lambe, T. W., & Whitman, R. V. (1969) *Soil Mechanics*. John Wiley & Sons.
- Mallela, J., Larson, G., Wyatt, T., Hall, J., & Barker, W. (2002, July). *User's guide for drainage requirements in pavements—DRIP 2.0 microcomputer program*. ERES Consultants.
- Meyerhof, G. G. (1963). Some recent research on the bearing capacity of foundations. *Canadian Geotechnical Journal*, 1(1), 16–26. <http://dx.doi.org/10.1139/t63-483>
- Meyerhof, G. G., & Hanna, A. M. (1978). Ultimate bearing capacity of foundations on layered soil under inclined load. *Canadian Geotechnical Journal*, 15(4), 565–572.
- Moaveni, M., Wang, S., Hart, J. M., Tutumluer, E., & Ahuja, N. (2013). Evaluation of aggregate size and shape by means of segmentation techniques and aggregate image processing algorithms. *Transportation Research Record*, 2335(1), 50–59. <https://doi.org/10.3141/2335-06>
- Moulton, L. K. (1980, August; reprinted, July 1990). *Highway subdrainage design* (Report No. FHWA-TS-80-224C). Federal Highway Administration. <https://www.fhwa.dot.gov/pavement/pubs/489633.pdf>
- Nicks, J. E., Gebrenegus, T., & Adams, M. T. (2015, June). *Strength characterization of open-graded aggregates for structural backfills* (Report No. FHWA-HRT-15-034). U.S. Department of Transportation Federal Highway Administration.
- OriginLab Corporation. (2018). OriginPro, Version 2018 [Computer Software]. <https://www.originlab.com/index.aspx?go=Support&pid=3301>
- Parsons, A. W. (1992). *Compaction of soils and granular materials: A review of research performed at the transport research laboratory*. HMSO.
- Pike, D. C. (1972) *Compaction of graded aggregates: 1. Standard laboratory tests* (TRRL Laboratory Report LR447). Transport Road Research Laboratory, Department of the Environment. <https://trl.co.uk/sites/default/files/LR447.pdf>
- Prochaska, A. B. (2004). An alternative method for effective compaction control of granular soils. (Master's Thesis, Purdue University).
- Randolph, B. W., Cai, J., Heydinger, A. G., & Gupta, J. D. (1996). Laboratory study of hydraulic conductivity for coarse aggregate bases. *Transportation Research Record: Journal of the Transportation Research Board*, 1519(1), 19–27. <https://doi.org/10.1177/0361198196151948103>
- Roy, M., & Sayer, S. K. (1989). Technical note. In-situ permeability testing of sub-bases on the M5 motorway. In R. H. Jones and A. R. Dawson (Eds.), *Proceedings of the*

- 3rd International Symposium on Unbound Aggregates in Roads* (pp. 86–93). Butterworths Scientific.
- Sherard, J. L., Woodward, R. J., Gizienski, S. F., & Clevenger, W. A. (1963). *Earth and Earth-rock Dams: Engineering problems of design and construction*. John Wiley & Sons.
- Terzaghi, K. (1943). *Theoretical soil mechanics*. Wiley & Sons.
- U.S. Army Corps of Engineers. (1955, June). Part XIII: Drainage and erosion control, Chapter 2: Subsurface drainage facilities for airfields. In *Engineering manual: Military construction*.
- USBR. (1987). *Design of small dams—A water resources technical publication* (3rd ed.). U.S. Department of the Interior Bureau of Reclamation. <https://www.usbr.gov/tsc/techreferences/mands/mands-pdfs/SmallDams.pdf>
- Vesic, A. S. (1973). Analysis of ultimate loads of shallow foundations. *Journal of the Soil Mechanics and Foundations Division*, ASCE, 99(1), 45–73.
- Weiler. (n.d.). *P385B commercial paver spec sheet*. <https://www.weilerproducts.com/upl/downloads/dealer/sales/p385b-spec-sheet-3.pdf>
- Wolff, T. F. (1995). *Spreadsheet applications in geotechnical engineering*. PWS Publishing Co.
- Zambrano, C., Drnevich, V. P., & Bourdeau, P. L. (2006). *Advanced compaction quality control* (Joint Transportation Research Program Research Report No. FHWA/IN/JTRP-2006/10). West Lafayette, IN: Purdue University. <https://doi.org/10.5703/1288284313408>

APPENDICES

Appendix A. Purdue University Survey on Pavement Subbase Design

Appendix B. State Survey Summaries

Appendix C. Particle Size Data

Appendix D. Details on Empirical Correlations Used to Estimate k

Appendix E. Technical Drawings of Permeameter

Appendix F. Shear Strength Database

Appendix G. Details of Statistical Analyses

Appendix H. Overview of Bearing Capacity Analysis

Appendix I. Supporting Data for Compatibility Analyses

Appendix J. List of Geotextiles Approved by INDOT

APPENDIX A. PURDUE UNIVERSITY SURVEY ON PAVEMENT SUBBASE DESIGN

We are conducting this survey in collaboration with the Indiana Department of Transportation (INDOT) to evaluate the current design of the subbase layer of both concrete and asphalt pavements. Our goal in conducting this survey is to summarize the work being done in other states, and specifically identify design solutions that have proven successful and that could find application in Indiana. At the same time, we are also interested in gathering information on options that have not proven successful.

Date:

Name:

State and Affiliation:

Job Title:

Years of Experience:

Questions:

Current Design

1. What types of pavements does your agency typically design or build? What design period is used for concrete pavements? What about for asphalt pavements?
2. What design method are you using (i.e., MEPDG, AASHTO 93)?
3. What performance measures do you use in the design of concrete pavements? What condition levels define failure conditions?
4. Please describe the current structure used in your state for concrete pavements. What types of stabilized and unstabilized subbases are used? Please provide typical thickness values for this layer (and sublayers, if applicable). If more than one subbase design alternative is available, please describe each separately.
5. How does the design change in the case of asphalt pavements? Again, please provide details on thickness values for the different layers and sublayers.
6. Are these designs available in an agency document that we could access?
7. Focusing on the subbase, if more than one design alternative is available, how is the decision to select a specific one made?
 - a. If more than one option, the following questions should be answered separately for each, focusing exclusively on solutions that comprise unbound layers and/or geosynthetics:

8. Are you aware of the history of the current design(s)?
9. The subbase is considered responsible for fulfilling the following four functions:
 - provide a stable and uniform construction platform;
 - protect the pavement from the *effects of frost* heave;
 - mitigate pumping of the subgrade fines;
 - facilitate drainage.
 - a. Would you agree with this statement, and does your subbase design specifically address any or all of these functions?
10. Focusing on the subbase layer, has the current design proven effective in the field based on pavement performance, post construction inspection, etc.?
11. What types of aggregates are used for the subbase layer(s)? What are the quality requirements for aggregates used in subbases (e.g., particle size distribution, toughness, etc.)? What are the permeability requirements (free draining or permeable)? How does the pavement type influence the selection of the aggregate?
12. If applicable, what type of geosynthetics do you use in subbases? What type of requirements do you use for these materials?
 - a. Do you use geotextiles in the horizontal layer as part of the structure? If yes, what is the function (or purpose) of the geotextile?
 - i. If reinforcement or stabilization, are you sure? What design method are you using? Do you mean separation?
 1. If you mean separation, are you considering drainage or filtration (to avoid clogging) or multifunction? Which mechanical properties do you consider? What type of geotextile, woven or nonwoven? How do you select the geotextile (i.e., approved list or case by case)? What is the design process?
 - ii. If drainage, will this replace the drainage layer in the structure? What type of geotextile, woven or nonwoven? How do you select the geotextile (i.e., approved list or case by case)? What is the design process? What other properties are considered to guarantee serviceability?
 - b. Do you expect the geotextile to serve several functions?
13. How do you determine compatibility between the layers in the subbase (standard filter requirements or other criteria)?
14. Are you satisfied with the current design of subbases? If so, what do you see as the major shortcoming?

Construction and Field Testing

15. In the case of unstabilized subbases, is the aggregate delivered to the site dry? If not, is the water content checked on site or prior to delivery? Is any procedure employed to limit

segregation during placement of the aggregate? Which aggregate manufacturers do you work with?

16. What is the typical construction process for the subbase, and how is it monitored? Do you know how this process was determined?
17. How are the various layers compacted? What compaction specifications are used? What level of compaction is typically targeted?
18. Is compaction routinely controlled? If so, how (e.g., LWD, proof rolling)?
19. Do you check for segregation of the aggregates after placement and compaction?
20. If using a non-aggregate layer (i.e., geotextile), how is it delivered and placed? Do you have specific manufacturers you typically purchase from?
21. During our construction process, there appears to be segregation of the aggregate and little monitoring of the compaction efforts. Is there anything about the construction process that you think we should know for our investigation?

Post Construction

22. After construction, is the site inspected? If so, how regularly, what methods and who performs the inspection?
23. What type of repairs are performed and how often?
24. What are the typical pavement failure modes you encounter in the field?

Other

25. What are the natural soil conditions found in your state? Is there anything about the geology you must consider?
26. What environmental factors must you consider in your design (i.e., temperature, rainfall events, etc.)?
27. Do you use any soil stabilization techniques for the subgrade?
28. Can you describe any previous design solutions that were ultimately not found to be effective? Do you know what caused the failure of these designs? How was the failure addressed?

APPENDIX B. STATE SURVEY SUMMARIES

A series of interviews were performed with DOT personnel in neighboring states and other countries using the questionnaire found in Appendix A. A modified questionnaire was used to interview a representative of the Concrete Paving Association of Minnesota. A list of all interviews is presented in Figure B.1. Interviewees were selected based on recommendations from colleagues at INDOT, Purdue University and other academic institutions.


State	Affiliation	Name(s)	Date	
Indiana	INDOT	KS	7/6/17	
Kentucky	KY Transportation Cabinet	AR	11/17/17	
Minnesota	MnDOT	JS	11/28/17	
	Concrete Paving Association of MN	MZ	12/11/17	
Ohio	ODOT	AM & SS	11/30/17 12/5/17	
Pennsylvania	PennDOT	RP	1/24/18	
Michigan	Michigan Department of Transportation	AI	2/23/18	
Ontario	Ontario Ministry of Transportation	SL	3/20/18	

Figure B.1 Interviews conducted between July 2017 and March 2018.

The complete list of questions posed to the interviewees is included in Appendix A. The design of the pavement structure can vary from state to state and depends on the pavement type (asphalt or concrete), geology, climate and traffic. The first set of questions focused on the design of the pavement structure. Table B.1 summarizes the main findings from this set of questions, while the respective pavement structure and aggregate information for each state are presented later.

A detailed review of the findings for each state is reported in Table B.1.

Table B.1 State interview pavement structure summary

State	Is Pavement Structure Same for Concrete and Asphalt?	Is There More Than One Option Considered?	Is There a Subbase Layer?	Are There Options with Geotextiles?	What Type of Pavement is Most Common?
KY	Yes	Yes	Not always	Yes	Asphalt
MN	No	Yes	Not always	No	Asphalt
OH	Yes	No	No	No	Asphalt
PA	No	Yes	Not always	No—geogrid between subgrade and subbase	Both
MI	No	Yes	Yes	No	Both
Ontario	No	Yes	Yes	No	Both

B.1 Kentucky

As seen in Table B.1, Kentucky utilizes the same structure for both concrete and asphalt pavements and is the only state among those interviewed that considers an option with geotextiles. Different pavement structures are used in different parts of the state due to the different subgrade conditions. Eastern Kentucky is mostly sandstone and western/central Kentucky has a soil subgrade. Figure B.2 shows the structure used in eastern Kentucky where a separator layer is not considered necessary and a Dense Graded Aggregate (DGA) or Crushed Stone Base (CSB) act as a drainage layer. The particle size distribution for DGA and CSB are plotted with INDOT #8, #43 and #53 in Figure B.3. Note that the drainage layer (DGA or CSB) has a similar gradation to both #43 and #53, where #53 is used as a separator layer in Indiana. DGA and CSB also have a bit of overlap and it was mentioned that the manufacturers of these materials use them interchangeably.

8-13" concrete layer OR min. 5.5" to 18" asphalt layer
4-6" aggregate (DGA or CSB)
2ft shot rock bed
Subgrade

Figure B.2 Eastern Kentucky pavement structure.

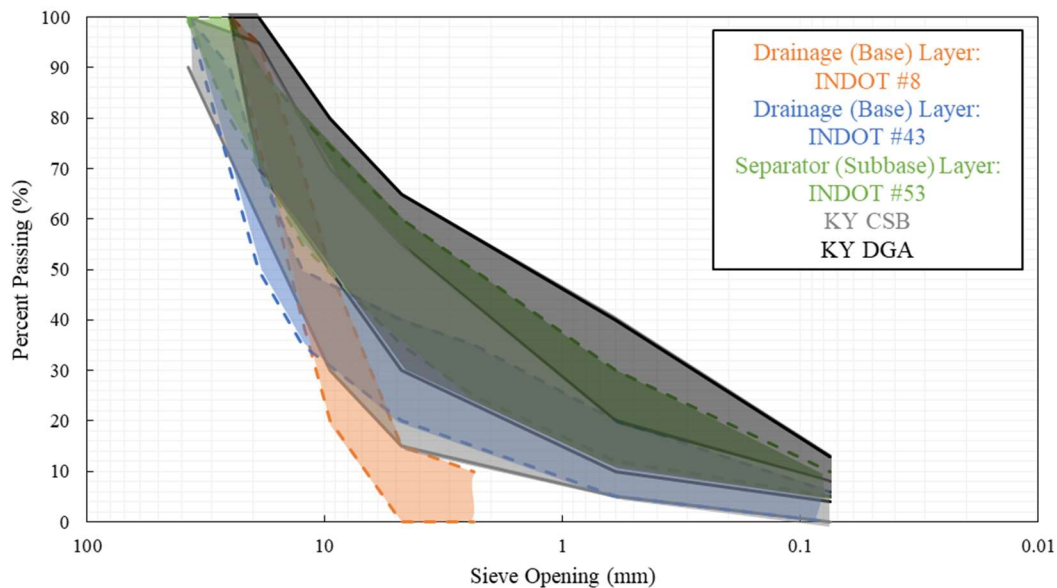


Figure B.3 Kentucky aggregate particle size distribution comparison.

In western/central Kentucky, three pavement structures are used. Figure B.4 is the preferred option for western/central Kentucky and is very similar to that used in eastern Kentucky with a stabilized subgrade in place of the shot rock layer and a drainage layer on top. Figure B.5 and Figure B.6 show two alternatives considered in western/central Kentucky where the separation function is performed by a geotextile or an aggregate wrapped in geotextile. Option 2 (Figure B.5) also includes a geogrid between the aggregate layers to provide a structural component.

8-13" concrete layer OR min. 5.5" to 18" asphalt layer
4-6" aggregate (DGA or CSB)
8" lime or cement stabilized subgrade
Subgrade

Figure B.4 Western/Central Kentucky pavement structure (Option 1).

8-13" concrete layer OR min. 5.5" to 18" asphalt layer
5-9" DGA or CSB
Geogrid (reinforcement)
2-3" DGA or CSB
Geotextile (separator)
Subgrade

Figure B.5 Western/Central Kentucky pavement structure (Option 2).

8-13" concrete layer OR min. 5.5" to 18" asphalt layer
DGA
Geotextile
18" quarry processed limestone (1-4")
Geotextile
Subgrade

Figure B.6 Western/Central Kentucky pavement structure (Option 3).

B.2 Minnesota

In Minnesota, the pavement structure is slightly different for concrete and asphalt. The pavement structure for concrete is presented in Figure B.7. A drainable or aggregate base is placed on top of a granular subbase. If an aggregate base (class 5, class 5Q, or class 6) is used, the granular base is a non-defined select material determined by the contractor. The particle size distributions for class 5, class 5Q and class 6 are graphed in Figure B.8 and are comparable to Indiana #43 and #53. If a drainable base is used (Open Graded Aggregate Base (OGAB) and Drainable Stable Base (DSB)), the granular base is either class 5, class 5Q, or class 6. The particle size distributions for OGAB and DSB are found in Figure B.9 and are comparable to Indiana #43 and #53. OGAB is more uniform in size and less stable than DSB.

The pavement structure for asphalt in Minnesota is presented in Figure B.10 where the base layer is 2" thicker than that used for concrete. The base layer consists of class 5, class 5Q, class 6 or

DSB. OGAB is not used in asphalt due to poor performance in terms of stability. The aggregate base layer sits on top of either class 3 or class 4 aggregate or a compacted subgrade. The gradations for class 3 and class 4 are presented in Figure B.11. The lower limit of class 3 and class 4 is very similar to INDOT #53, but the overall band is much more variable in size. The subbase layer for asphalt pavements in Minnesota assist in the structural capacity.

PCC Pavement	6.0-inch minimum thickness
Drainable or Aggregate Base	<ul style="list-style-type: none"> • 4.0-inch minimum thickness aggregate base (class 5, Class 5Q, Class 6). • Or 4.0 inches of drainable base (OGAB or DSB).
Granular Subbase	<ul style="list-style-type: none"> • When using aggregate base: <ul style="list-style-type: none"> ○ For non-granular existing soils use a minimum of 12.0 inches of select granular materials. ○ For granular soils (percent passing ratio [no. 200 (75 μm)/1.0 inch (25 mm)] sieve \leq 20), mix and compact the upper 12.0 inches (minimum) of the existing granular soils. • When using a drainable base, place it on a minimum of 4.0 inches of aggregate base (class 5, class 5Q or class 6).
Existing Soil	Any construction beneath the granular subbase shall be at the discretion of the District Materials/Soils Engineer.

Figure B.7 Minnesota concrete pavement structure.

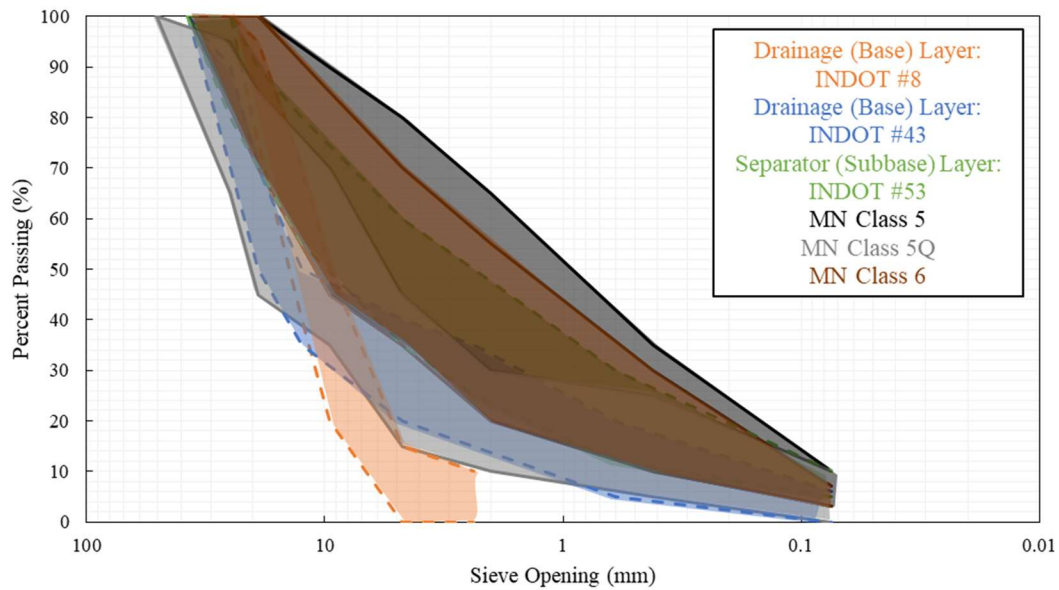


Figure B.8 Minnesota class 5, class 5Q, class 6 aggregate particle size distribution comparison.

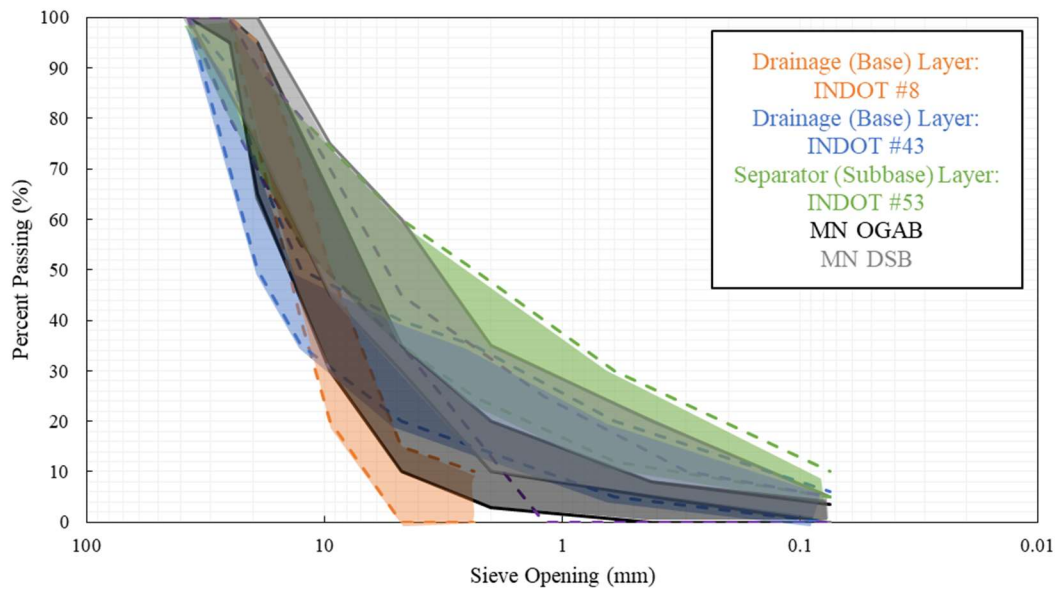


Figure B.9 Minnesota drainable aggregate particle size distribution comparison.

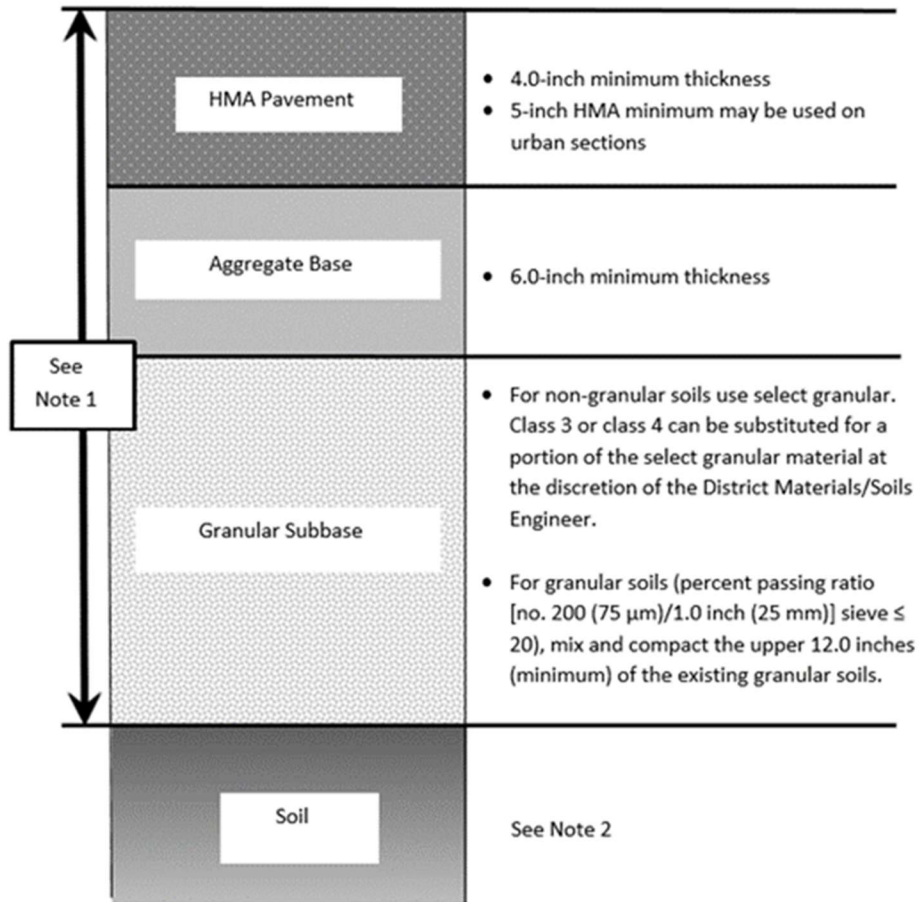


Figure B.10 Minnesota asphalt pavement structure.

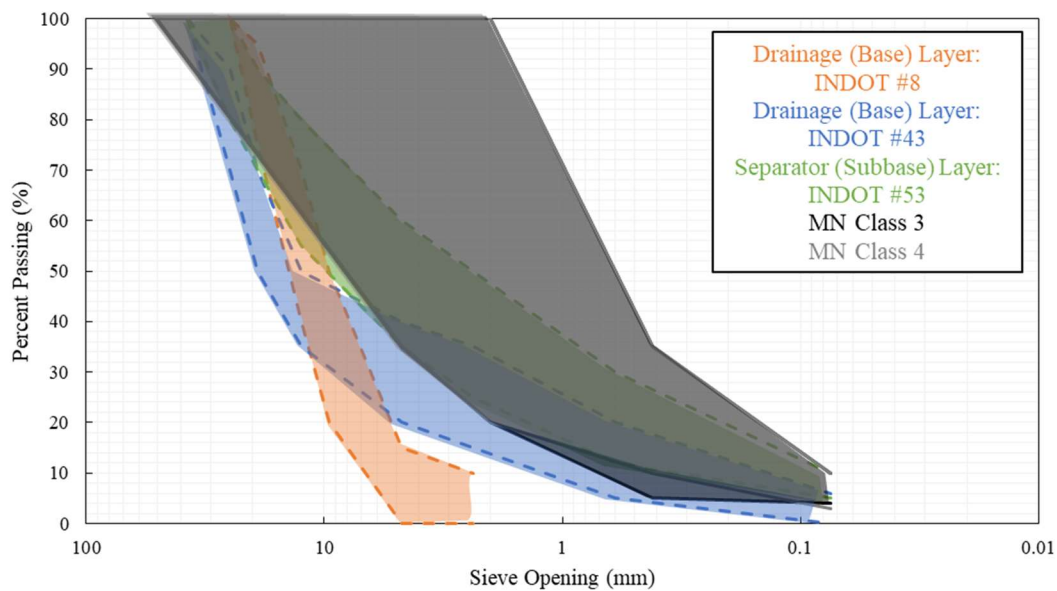


Figure B.11 Minnesota Class 3, Class 4 aggregate particle size distribution comparison.

B.3 Ohio

Ohio uses the same pavement structure for both asphalt and concrete, and only one option is considered (Figure B.12). The particle size distribution for Ohio 304 is shown in Figure B.13 and falls along the middle of INDOT #43 and the entirety of #53. In the past, Ohio had tried using a free draining base, but experienced stability issues.

Concrete or Asphalt Pavement
6" 304 aggregate base
Stabilized Subgrade

Figure B.12 Ohio pavement structure.

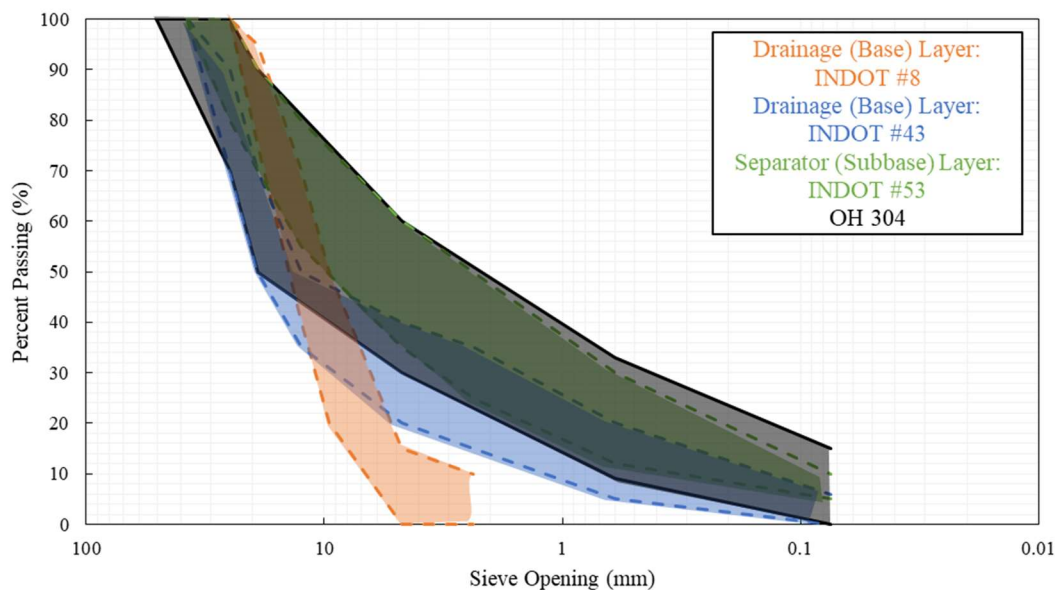


Figure B.13 Ohio aggregate particle size distribution comparison.

B.4 Pennsylvania

Again, different structures are used for concrete and asphalt pavements in Pennsylvania. According to the PennDOT specifications, a drainable layer is necessary below concrete pavement. The primary structure used for concrete pavements is presented in Figure B.14, where the treated permeable base course (TPBC) serves as a drainage layer below the pavement. For low volume or local roads, the TPBC layer can be excluded and the 2A aggregate subbase layer is sufficient (Figure B.15). As observed in Figure B.16, the 2A aggregate is similar in particle size distribution to INDOT #43 and #53.

Concrete Pavement
3-4" TPBC
4-6" 2A aggregate subbase
Subgrade

Figure B.14 Pennsylvania concrete pavement structure (primary).

Concrete Pavement
6" 2A aggregate subbase
Subgrade

Figure B.15 Pennsylvania concrete pavement structure (low-volume/local roads).

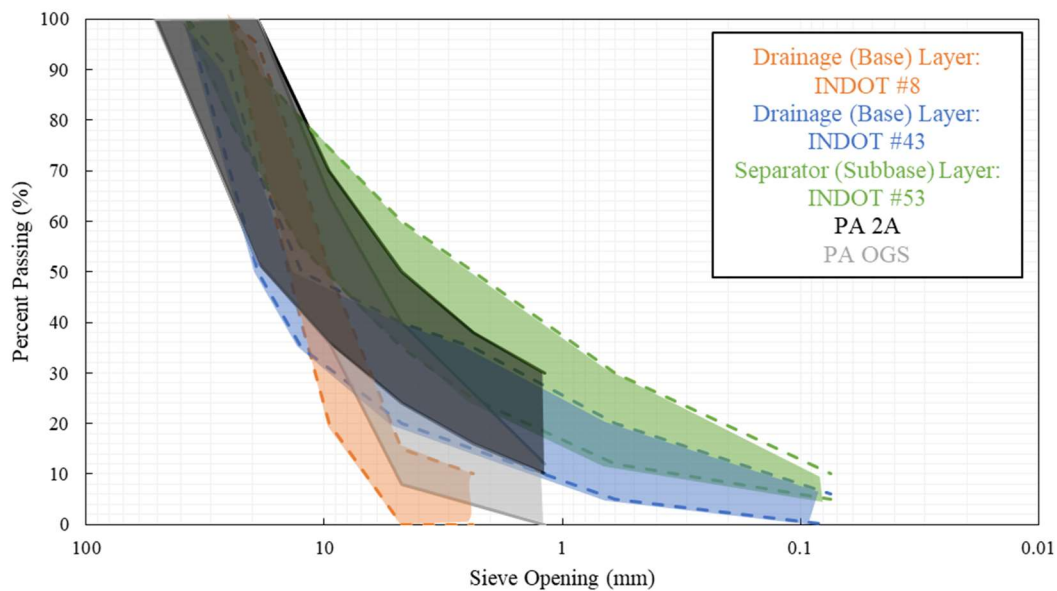


Figure B.16 Pennsylvania aggregate particle size distributions comparison.

Four different options are used for asphalt pavement in Pennsylvania (Figure B.17) where the 2A aggregate is the primary aggregate used as the subbase layer. In the past, open graded subbase (OGS) was used as a drainage layer for both concrete and asphalt pavements and is now prohibited in concrete pavement projects due to the associated clogging and is only applicable in limited situations for asphalt pavements. As observed in Figure B.16, the particle size

distribution band for OGS falls between INDOT #8 and #43. All four options make use of a stabilized base layer.

Asphalt Pavement	Asphalt Pavement
6-16" CABC or CABC-DG	3-15" Superpave Base Courses
≥6" 2A or OGS aggregate subbase	≥6" 2A or OGS aggregate subbase
Subgrade	Subgrade

Asphalt Pavement	Asphalt Pavement
5-12" Agg/Cement/Bituminous Base Courses	5-12" Plain Cement Concrete Base Courses
≥6" 2A or OGS aggregate subbase	≥6" 2A or OGS aggregate subbase
Subgrade	Subgrade

Figure B.17 Pennsylvania asphalt pavement structures.

B. 5 Michigan

Michigan specifications also require different structures for concrete and asphalt pavements in terms of thickness, but the layers are composed of the same aggregate type. The concrete pavement structures are presented in Figure B.18, where a drainage base layer rests on top of a sand subbase layer or the sand subbase layer is removed, and a thicker base layer is used. Both the dense graded aggregate base and open graded drainage course fall between INDOT #43 and #53 (see Figure B.19). The asphalt pavement structures are presented in Figure B.20 and are the same as the concrete with different thickness of the base and subbase layers.

8-13" Concrete Pavement	8-13" Concrete Pavement	8-13" Concrete Pavement
6" Dense Graded Aggregate Base	6" Open Graded Drainage Course (OGDC)	16" Open Graded Drainage Course (OGDC)
10" Sand Subbase	10" Sand Subbase	
Subgrade	Subgrade	Subgrade

Figure B.18 Michigan concrete pavement structures.

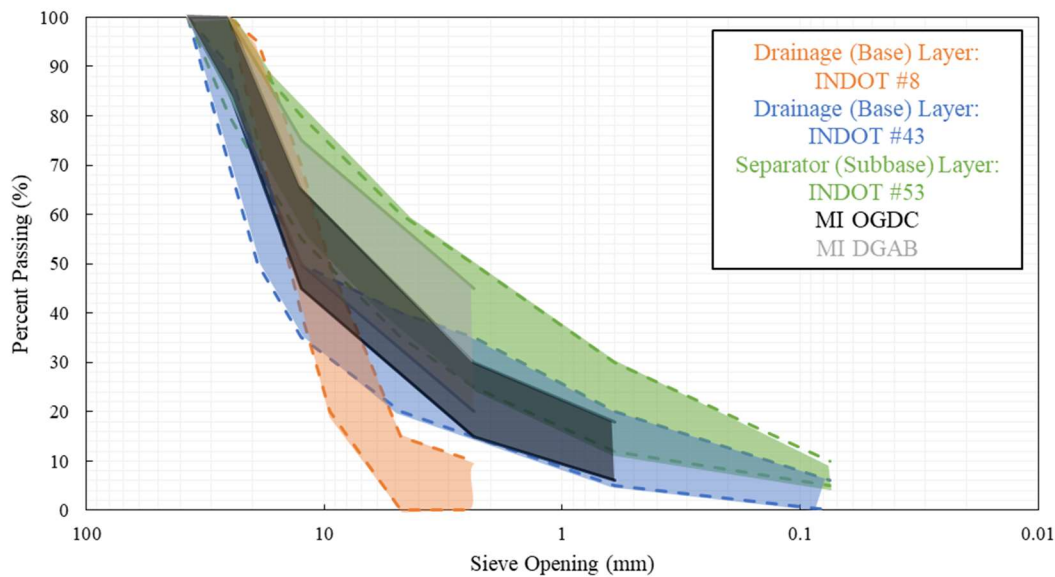


Figure B.19 Michigan OGDC and DGAB particle size distribution comparison.

Asphalt Pavement	Asphalt Pavement
6" Dense Graded Aggregate Base	16" Open Graded Drainage Course (OGDC)
18" Sand Subbase	8" Sand Subbase
Subgrade	Subgrade

Figure B.20 Michigan asphalt pavement structures.

B.6 Ontario

Lastly, Ontario utilizes a treated open graded drainage layer on top of a granular subbase for its concrete pavement structure as observed in Figure B.21. The granular subbase (A or O) is similar to INDOT #43 and #53 (Figure B.22) in terms of gradation. As for the asphalt pavement structure, a 6" granular base layer rests on top of a less than 12" granular subbase layer (Figure B.23). The granular B layer has a very broad range in potential particle size distributions as observed in Figure B.24 that does overlap the INDOT materials.

9" Joint Plain Concrete Pavement
4" Open Graded Drainage Layer (asphalt or cement treated)
8" Granular A or O
Subgrade

Figure B.21 Ontario concrete pavement structure.

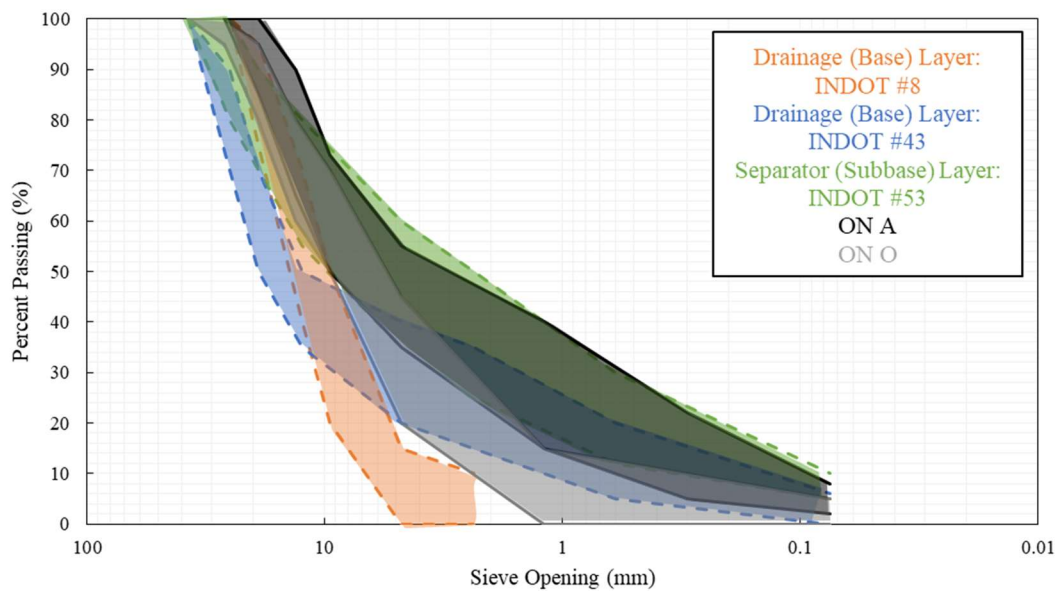


Figure B.22 Ontario aggregate A and O particle size distribution comparison.

6" Asphalt Pavement
6" Granular A
>12" Granular B Type I, Type II or Type III
Subgrade

Figure B.23 Ontario asphalt pavement structure.

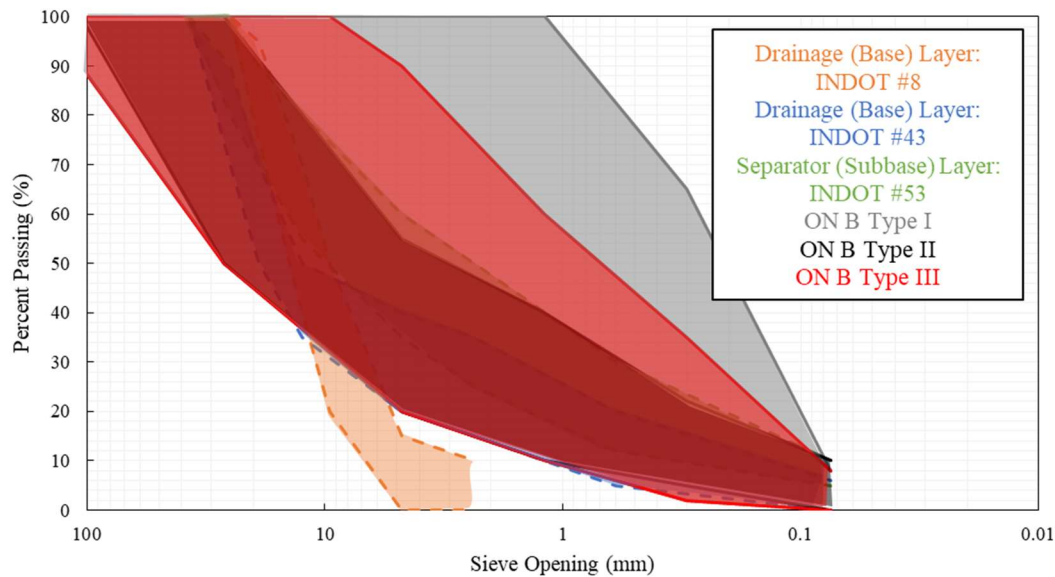


Figure B.24 Ontario B aggregates particle size distribution comparison.

The second main focus of the survey was on the method of construction and a brief summary of these findings can be found in Table B.2. In all instances, the aggregate is delivered to the site wet. None of those interviewed reported problems with segregation of the aggregate. Note that Indiana, however, does not require the aggregate to be delivered wet and does observe segregation issues. As far as the method of compaction, each state seems to use a type of vibratory roller. In all cases, compaction is controlled by use of a test section. Minnesota and Ontario do not identify a prescribed method in their specifications; instead, it is dependent on the project and the contractors must prove the method is sufficient.

Table B.2 State interview construction method summary

State	Is Aggregate Delivered to Site Wet?	Is Segregation an Issue?	How Are Layers Compacted?	How is Compaction Controlled?
KY	Yes	No	Single or double drum flat roller (vibrating)	Control strips and test sections
MN	Yes	No	Dependent on project, contractor must prove method is sufficient	
OH	Yes	No	Vibratory smooth drum roller	
PA	Yes	No	Roller or vibratory compaction equipment	Control strip and nuclear density reading
MI	Yes	No	Various types of rollers	Test strip and nuclear density gauges

Ontario	Yes	No	Dependent on project, contractor must prove method is sufficient
---------	-----	----	--

In summary, the unbound material used for the base layer by other states is comparable to #43 and #53. None of the other states seem to use anything comparable to #8 as a base layer. The aggregate used for the subbase or separator layer is also comparable to #43 and #53, or smaller in size (Ontario, Pennsylvania OGS, Minnesota class 3 and class 4). Kentucky also considers geotextiles for the separator function. The agencies interviewed do not report problems with segregation of unbound materials and test sections are used to determine the adequate amount of passes for best compaction results.

APPENDIX C. PARTICLE SIZE DATA

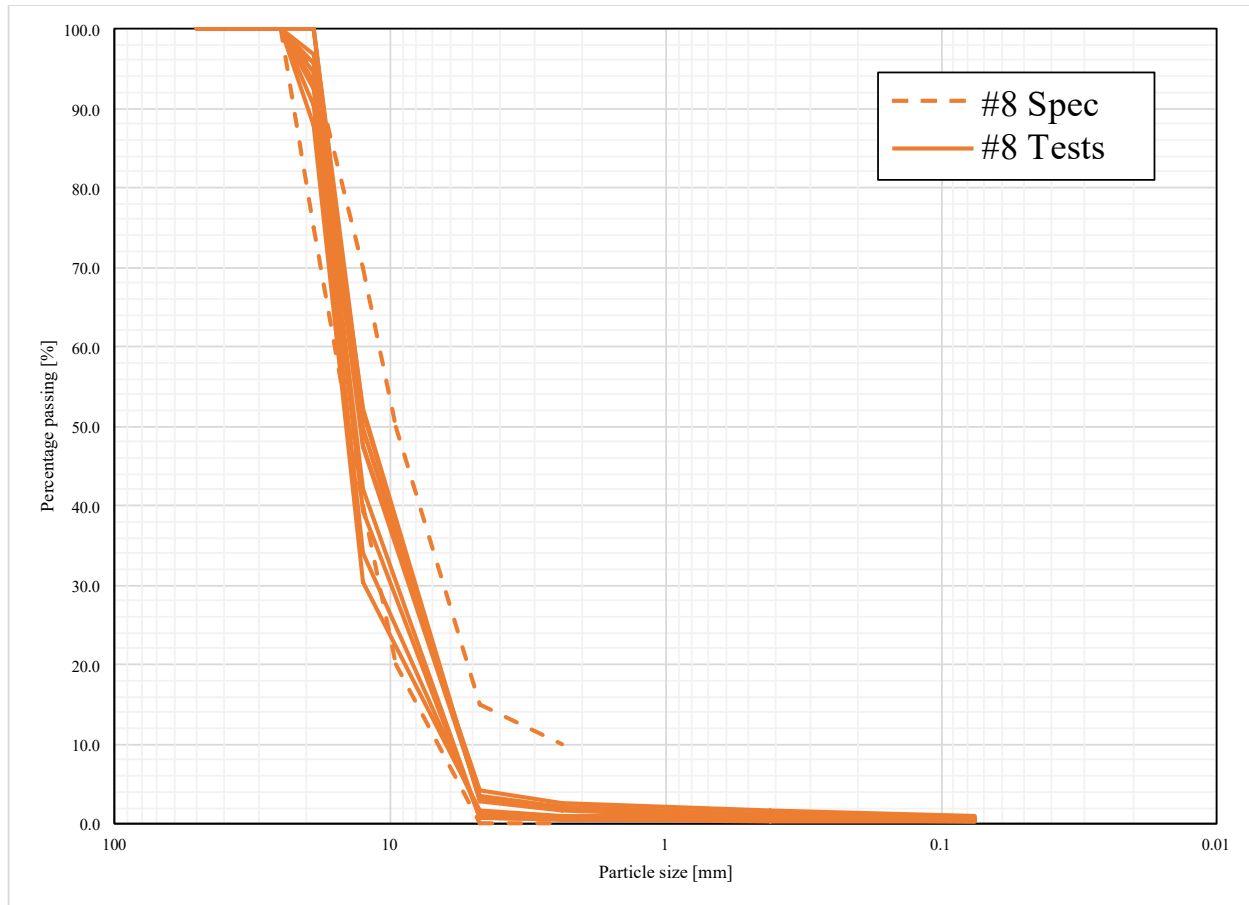


Figure C.1 Comparison of particle size distributions obtained from tests on virgin samples and samples used for vibratory compaction tests of Indiana #8 to required gradation band.

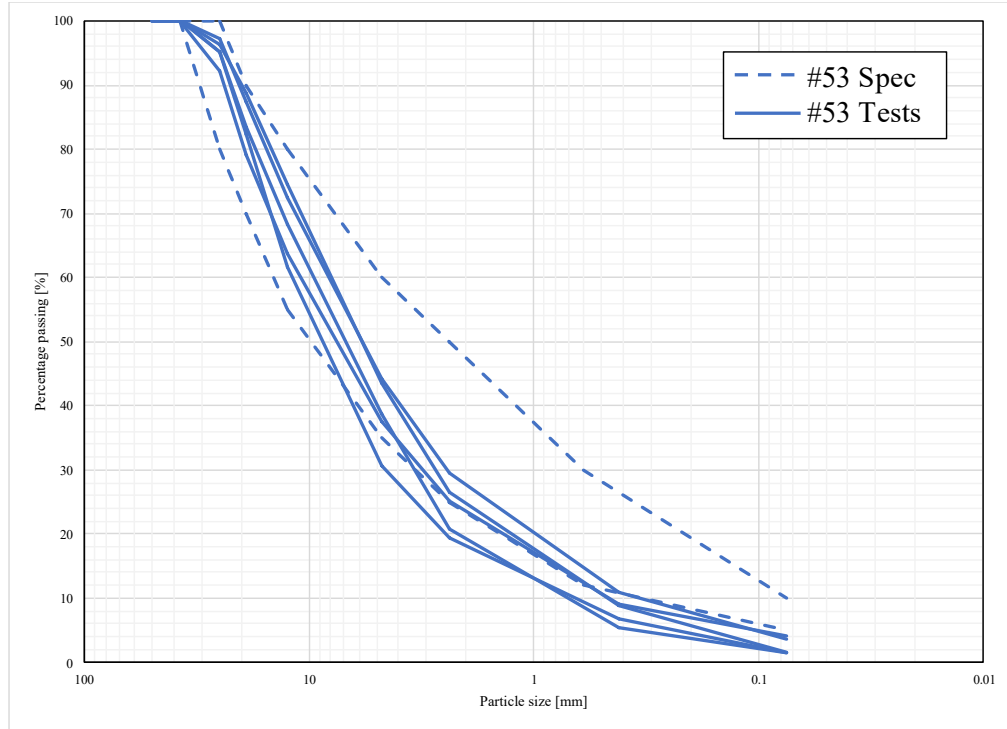


Figure C.2 Comparison of particle size distributions obtained from tests on Indiana #53 to required gradation band.

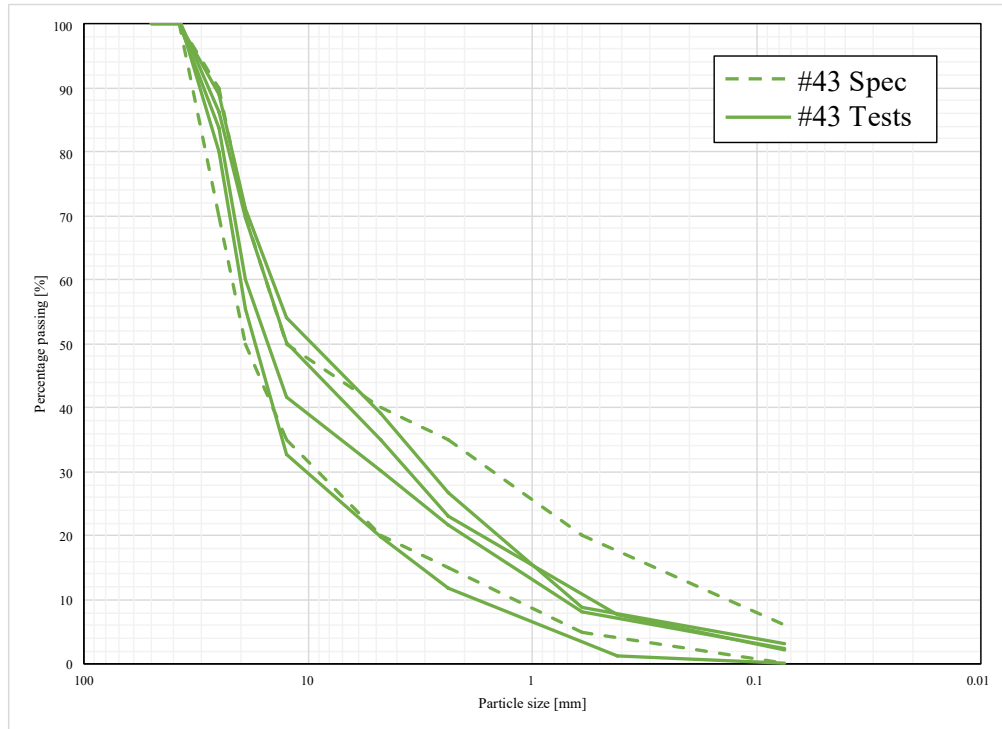


Figure C.3 Comparison of particle size distributions obtained from tests on Indiana #43 to required gradation band.

APPENDIX D. DETAILS ON EMPIRICAL CORRELATIONS USED TO ESTIMATE K

D.1 Moulton (1980)

$$k = \frac{6.214 \times 10^5 (D_{10})^{1.478} n^{6.654}}{(P_{200})^{0.597}} \left(\frac{ft}{day} \right) \quad \text{Equation D.1}$$

where:

- D_{10} : particle size in correspondence to 10% passing expressed in mm
- n = porosity
- P_{200} : percentage passing the sieve #200

This is the correlation employed in the DRIP (Drainage Requirements in Pavement) software (Applied Research Associates, 2002) to estimate the hydraulic conductivity of unbound layers. This expression predicts infinite hydraulic conductivity for a material with no fines and should be used with caution with materials with very low percentages of fines. While from a practical point of view there is no difference between 0.1% and 0.001% fines, this variation is reflected in over one order of magnitude difference in the predicted value of k using the above expression.

D.2 Hazen (1892)

$$k = C_H D_{10}^2 \left(\frac{cm}{s} \right) \quad \text{Equation D.2}$$

where:

- D_{10} : particle size in correspondence to 10% passing (in cm)
- C_H : experimental coefficient, which varies between 1 to 1000. A value of 100 is recommended (Carrier, 2003)

The formula was originally developed for the design of sand filters ($C_u = D_{60}/D_{10} < 2$) but has since been widely used for a broad range of soils.

As indicated by Carrier (2003), the applicability of the formula is generally limited to $0.01 \text{ cm} < D_{10} < 0.3 \text{ cm}$. It should therefore not be applied to materials such as the #8 aggregate examined in this work.

D.3 Kenney (1984)

$$k = \left(\frac{\gamma}{\mu} \right) \beta_\alpha D_\alpha^2 \left(\frac{cm}{s} \right) \quad \text{Equation D.3}$$

where:

- D_α = particle size in correspondence to $\alpha\%$ (in mm).
- β_α = experimental constant that depends on α .

- Kenney recommends using $\alpha = 5$. For this value of α , β_5 shows the least variation, ranging between 4×10^{-4} and 10^{-3} .
- γ = fluid unit weight
- μ = fluid viscosity (Note: for water at 21°C (γ/μ) = $1 \times 10^3 \text{ cm s}^{-1}\text{mm}^{-2}$)

D.4 Kozeny-Carman (1927)

$$k = \left(\frac{\gamma}{\mu}\right) \left(\frac{1}{C_{K-C}}\right) \left(\frac{1}{S_0^2}\right) \left[\frac{e^3}{1+e}\right] \quad \text{Equation D.4}$$

where:

- γ = fluid unit weight
- μ = fluid viscosity (Note: for water at 21°C (γ/μ) = $1 \times 10^3 \text{ cm s}^{-1}\text{mm}^{-2}$)
- C_{K-C} = Kozeny-Carman empirical coefficient, usually taken to be equal to 5.
- e = void ratio
- S_0 = specific surface area per unit volume of particles (1/cm). The procedure for estimating S_0 based on the particle size distribution is discussed in detail by Carrier (2003).

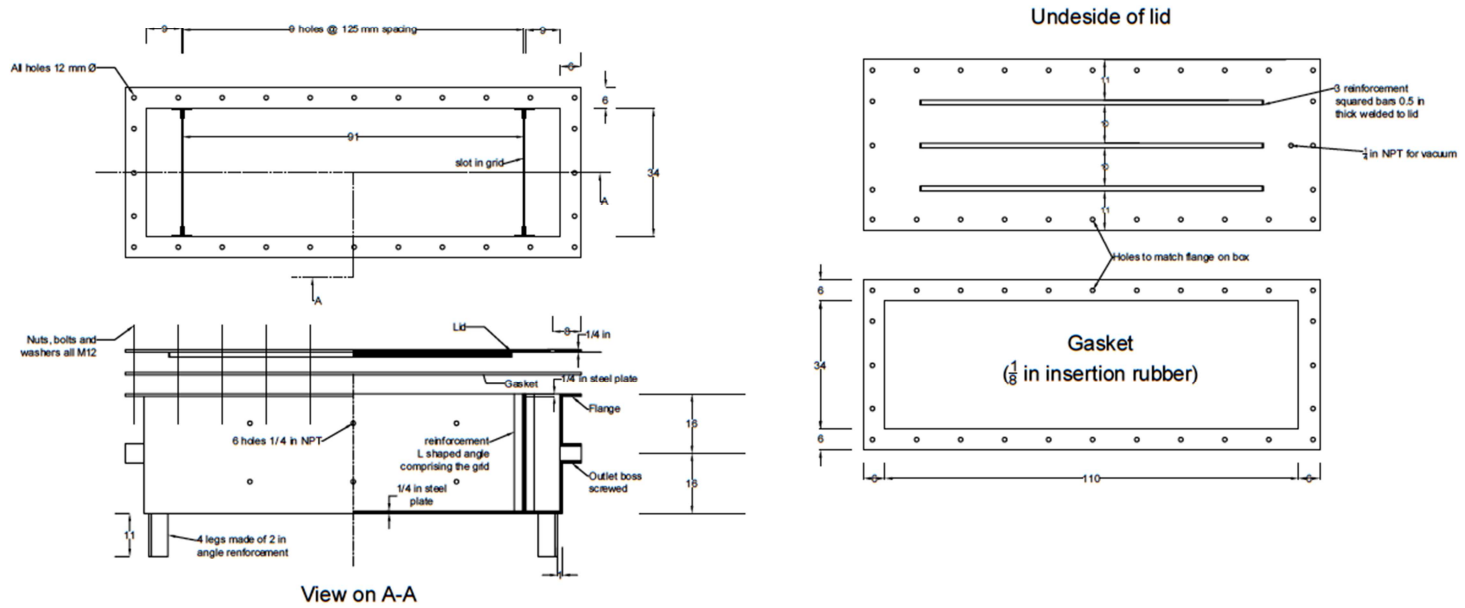
Table D.1 Input parameters used in empirical models

Moulton (1980)			
Case	D_{10} [mm]	n	P_{200} [%]
#8 Loose Lower end	6.70	0.49	0.01
#8 Loose Upper end	2.30	0.49	0.01
#8 Dense Lower end	6.70	0.35	0.01
#8 Dense Upper end	2.30	0.35	0.01
#43 Loose Lower end	1.10	0.38	0.01
#43 Loose Upper end	0.15	0.38	6.00
#43 Dense Lower end	1.10	0.18	0.01
#43 Dense Upper end	0.15	0.18	6.00
#53 Loose Lower end	0.30	0.40	5.00
#53 Loose Upper end	0.08	0.40	10.00
#53 Dense Lower end	0.30	0.19	5.00
#53 Dense Upper end	0.08	0.19	10.00
Hazen (1892)			
Case	D_{10} [mm]	CH	
#8 Lower end	6.70	1	
#8 Lower end (2)	6.70	1000	
#8 Upper end	2.30	1	
#8 Upper end (2)	2.30	1000	
#43 Lower end	1.10	1	
#43 Lower end (2)	1.10	1000	
#43 Upper end	0.15	1	

#43 Upper end (2)	0.15	1000
#53 Lower end	0.30	1
#53 Lower end (2)	0.30	1000
#53 Upper end	0.08	1
#53 Upper end (2)	0.08	1000
Kenney (1984)		
Case	D ₁₀ [mm]	$\beta_{\alpha} \alpha = 5$
#8 Lower end	5.50	8
#8 Lower end (2)	5.50	10
#8 Upper end	1.50	8
#8 Upper end (2)	1.50	10
#43 Lower end	0.50	6
#43 Lower end (2)	0.50	6
#43 Upper end	0.07	6
#43 Upper end (2)	0.07	6
#53 Lower end	0.06	6
#53 Lower end (2)	0.06	6
#53 Upper end	0.04	6
#53 Upper end (2)	0.04	6
Kozeny-Carman (1927)		
Case	e	S ₀
#8 Loose Lower end angular	0.96	6.33
#8 Loose Lower end rounded	0.96	4.93
#8 Dense Lower end angular	0.54	6.33
#8 Dense Lower end rounded	0.54	4.93
#8 Loose Upper end angular	0.96	7.82
#8 Loose Upper end rounded	0.96	6.09
#8 Dense Upper end angular	0.54	7.82
#8 Dense Upper end rounded	0.54	6.09
#43 Loose Lower end angular	0.61	29.47
#43 Loose Lower end rounded	0.61	22.97
#43 Dense Lower end angular	0.22	29.47
#43 Dense Lower end rounded	0.22	22.97
#43 Loose Upper end angular	0.61	64.37
#43 Loose Upper end rounded	0.61	50.16
#43 Dense Upper end angular	0.22	64.37
#43 Dense Upper end rounded	0.22	50.16
#53 Loose Lower end angular	0.67	39.22
#53 Loose Lower end rounded	0.67	30.56
#53 Dense Lower end angular	0.24	39.22
#53 Dense Lower end rounded	0.24	30.56
#53 Loose Upper end angular	0.67	90.33
#53 Loose Upper end rounded	0.67	70.39
#53 Dense Upper end angular	0.24	90.33
#53 Dense Upper end rounded	0.24	70.39

APPENDIX E. TECHNICAL DRAWINGS OF PERMEAMETER

Scale 1:15



Measurements in cm if not written otherwise

Figure E.1 Technical drawings of permeameter.

APPENDIX F. SHEAR STRENGTH DATABASE

Table F.1 Overview of database

ID Used in This Report	Source	Gradation Designation Used in Source	Mineralogy
N1	Nicks et al., 2015	5	Diabase
N2		56	
N3		57	
N4		6	
N5		67	
N6		68	
N7		7	
N8		8	
C1	Chow et al., 2014	Arrowood	Granite, Basalt, Limestone
C2		Belgrade	
C3		Fountain	
C4		Franklin	
C5		Goldhill	
C6		Hendersonville	
C7		Jamestown	
C8		Lemon Spring	
C9		Moncure	
C10		Nash County	
C11		N. Wilkesboro	
C12		Princeton	
C13		Raleigh	
C14		Rockingham	
C15		Rocky Point	
C16		Rougemont	
A1/L/B	Aghaei Araei et al., 2010	Roodbar dam- Blasting	Limestone
A2/S/B		Vanyar dam- Blasting	Sandstone
A3/AB/B		Sabalan dam- Blasting	Andesi-Basalt
A4/Das/B		Zonoz dam- Blasting	Dasite
A5/A/B_1		Aydoghmosh dam (G1) - Blasting	Andesite
A5/A/B_1R		Aydoghmosh dam (G1-R) - Blasting	Andesite

A5/A/B_2		Aydoghmosh dam (P)-Blasting	Andesite
A6/L/B_1		CFRD Siah Bisheh (21) - Blasting	Limestone
A6/L/B_1R		CFRD Siah Bisheh (21.5) - Blasting	Limestone
A7/ADas/A_1		Yamchi dam (G2) -Alluvium	Andesite and Dasite
A7/ADas/A_2R		Yamchi dam (G2-R) - Alluvium	Andesite and Dasite
A7/ADas/A_2		Yamchi dam (G1) -Alluvium	Andesite and Dasite
A8/AB/A		Ghale Chi dam- Alluvium	Andesite and Basalte
A9/DeuB/A_1		Sahand dam (G2) -Alluvium	Deurite and Basite
A9/DeuB/A_2		Sahand dam (G1) -Alluvium	Deurite and Basite
A10/A/A		Aydoghmosh dam (G2) - Alluvium	Andesite

APPENDIX G. DETAILS OF STATISTICAL ANALYSES

As shown earlier in this report, the peak value of the angle of internal friction decreases significantly with increasing confining stress, which is consistent with known behavior of granular material (e.g., Lambe & Whitman, 1969). Logically, this relationship should translate statistically into a significant correlation with a negative coefficient, which will be verified in the following sections. However, because the relationship between peak shear strength and confining stress could interfere in relationships with other properties, the correlation analysis was performed on separate data sets corresponding to small ranges of confining stress.

The parameters examined in the analysis can be grouped in two main categories: *shape parameters* and *mineral and resistance parameters*. Each is briefly described below. The analysis for each of the three referenced data sources is the presented.

Shape parameters:

- Angularity Index (AI): quantifies the average sharpness of the edges of the particles in the material. The index increases as the edges of the aggregate are sharper (i.e., materials with lower AI would be formed mainly by rounded particles).
- While both Chow et al. (2014) and Nicks et al. (2015) provide values of this index for their materials, their scales do not match, and the values cannot be converted from one scale to the other.
- Texture Index: it characterizes the average roughness of the particles' surfaces: the rougher the particles, the higher the value of this index. Again, while both Chow et al. (2014) and Nicks et al. (2015) consider this parameter, the scales used by the authors are significantly different.
- Sphericity: It is obtained by dividing the longest dimension of the particle by its shortest dimension. This parameter is used by the Nicks et al. (2015) to characterize the aggregates investigated in their study.
- Flat and elongated ratio: it is calculated by dividing the shortest dimension of the particle by its longest dimension. This parameter is used by Chow et al. (2014).

Note that the last two parameters are the inverse of each other. To maintain consistency, values of the flat to elongated ratio were converted into sphericity, and this parameter was used as input for the statistical analysis.

Mineral and resistance parameters:

- Los Angeles: Obtained preforming the Los Angeles abrasion test, this informs about the hardness of the material by presenting the percentage of its mass that has been grinded upon a standardized mixing procedure inside of a cylinder.
- Point load–Strength Index: Records the stress required to take a normalized specimen of intact rock to breakage by applying load through two aligned indenters. This index can be used to extrapolate tentative values of the unconfined shear strength of intact rock.

G.1 Analysis of Nicks et al. (2015) Data

These are data from a material, close to INDOT#8 in terms of particle size distribution. Table G.1 provides a summary of the data used in the analysis including, for each confining stress subset, the ranges of values of all the parameters examined. Computed coefficients of correlation of the normalized peak stress deviator (q/σ_3) and the peak friction angle (ϕ'_p) with each granular property, are shown in Figure G.1. In both plots included in this figure, vertical bars represent the coefficient of correlation, in magnitude and sign, with colors relating to confining stress ranges. Correlation coefficients with the confining stress, σ_3 , are also included for reference (high negative values are obtained, as expected). The highest coefficient of correlation is with the average particle size (+0.6) for low confining stress, while correlations with other parameters are weak to moderate. These trends are confirmed and somewhat amplified when correlations are computed with logarithmic transforms of the parameters, as seen in Figure G.2.

Table G.1 Characteristics of Nicks et al. (2015) statistical analysis

σ_3 [kPa]	Sample Size	q/σ_3	ϕ'_p	C_u	C_c	D_{50} [mm]	Angularity	Roughness	Sphericity
Full Set	48	3.11–7.13	51.29–37.49	1.48–6.67	0.38–2.08	0.7–20	2577.2–3295.5	149.8–447.4	1.34–1.72
34–40	12	3.79–7.13	40.92–51.29	1.48–6.66	0.38–2.08	0.7–20	2577.2–3295.5	149.8–447.4	1.34–1.72
68–71	12	3.74–5.96	40.66–47.68	1.48–6.67	0.38–2.08	0.7–20	2577.2–3295.5	149.8–447.4	1.34–1.72
137–140	12	3.49–5.08	39.51–45.56	1.48–6.00	0.38–2.08	0.7–20	2577.2–3295.5	149.8–447.4	1.34–1.72
206–209	12	3.11–4.14	37.49–42.27	1.48–6.67	0.38–2.08	0.7–20	2577.2–3295.5	149.8–447.4	1.34–1.72

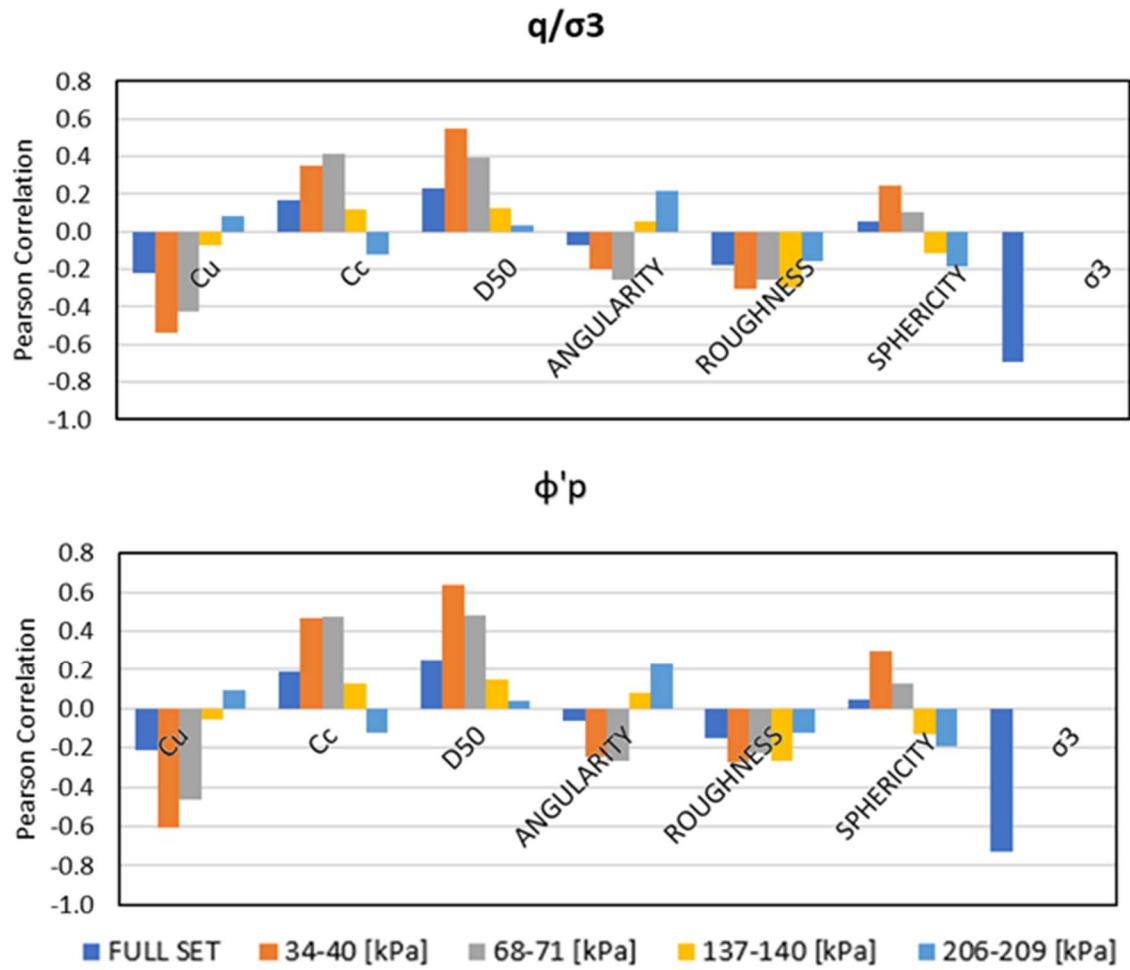


Figure G.1 Correlation coefficients for Nicks et al. (2015) data.

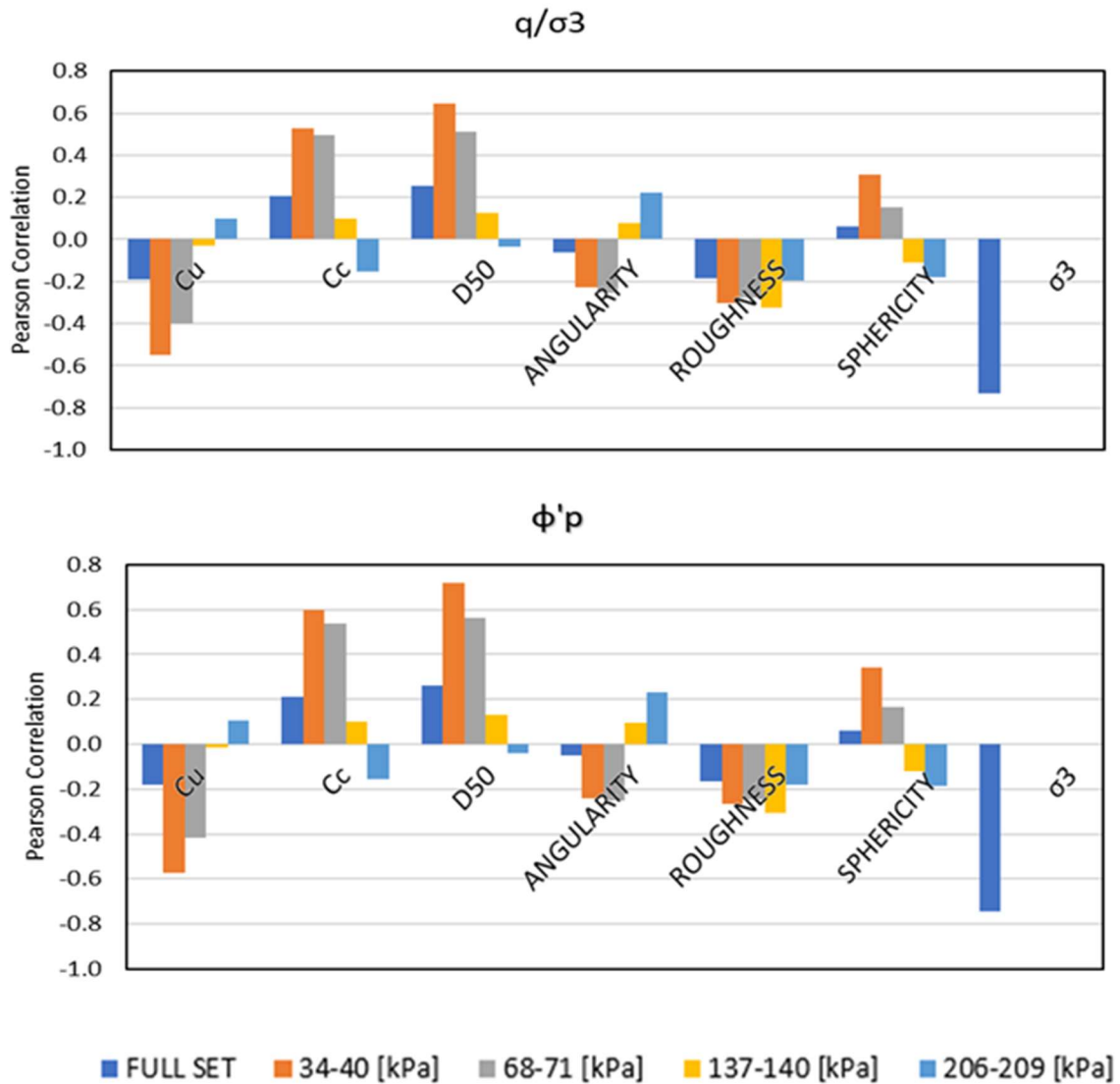


Figure G.2 Correlation coefficients computed with logarithmic transforms for Nicks et al. (2015) data.

Once the hypothesis testing has been performed and the correlation coefficients for which the P value is higher than 0.05 have been discarded, a clearer picture is obtained (Figure G.3 and Figure G.4). A fairly strong, consistent correlation exists between the peak angle of internal friction and the average particle size, D_{50} , but only within the range of small confining stresses. This suggests the peak shear strength tends to be higher when the material is coarser. The relationship is better captured when the analysis is performed in terms of peak friction angle. A negative correlation with the coefficient of uniformity, C_u is evidenced only for a non-linear relationship, while a possible relationship, with positive correlation, to the coefficient of curvature, C_c would rather be linear. There is no trusted correlation between peak shear strength and particle shape or surface properties; this could be related to the narrow range in which these properties vary in this data set.

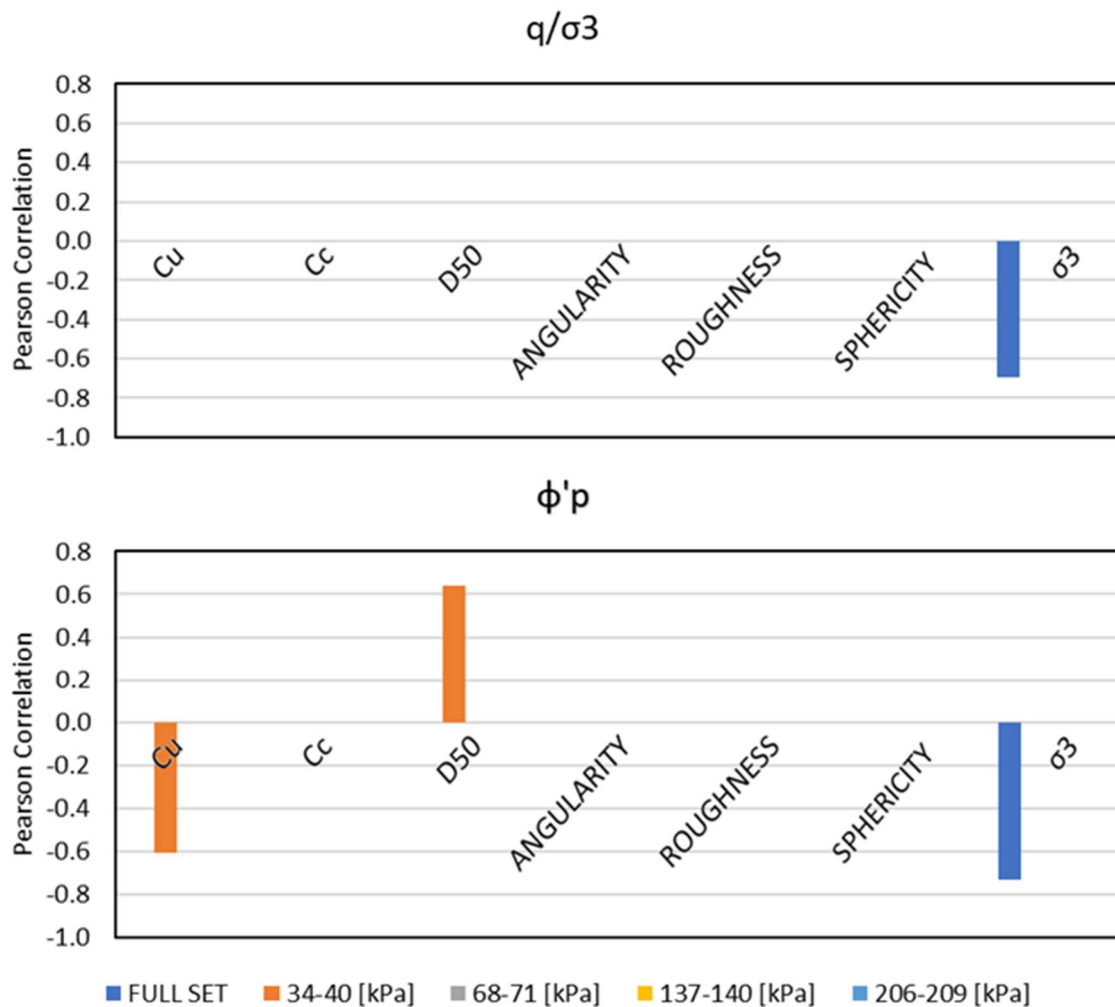


Figure G.3 Correlation coefficients for Nicks et al. (2015) data with P-Value < 0.05.

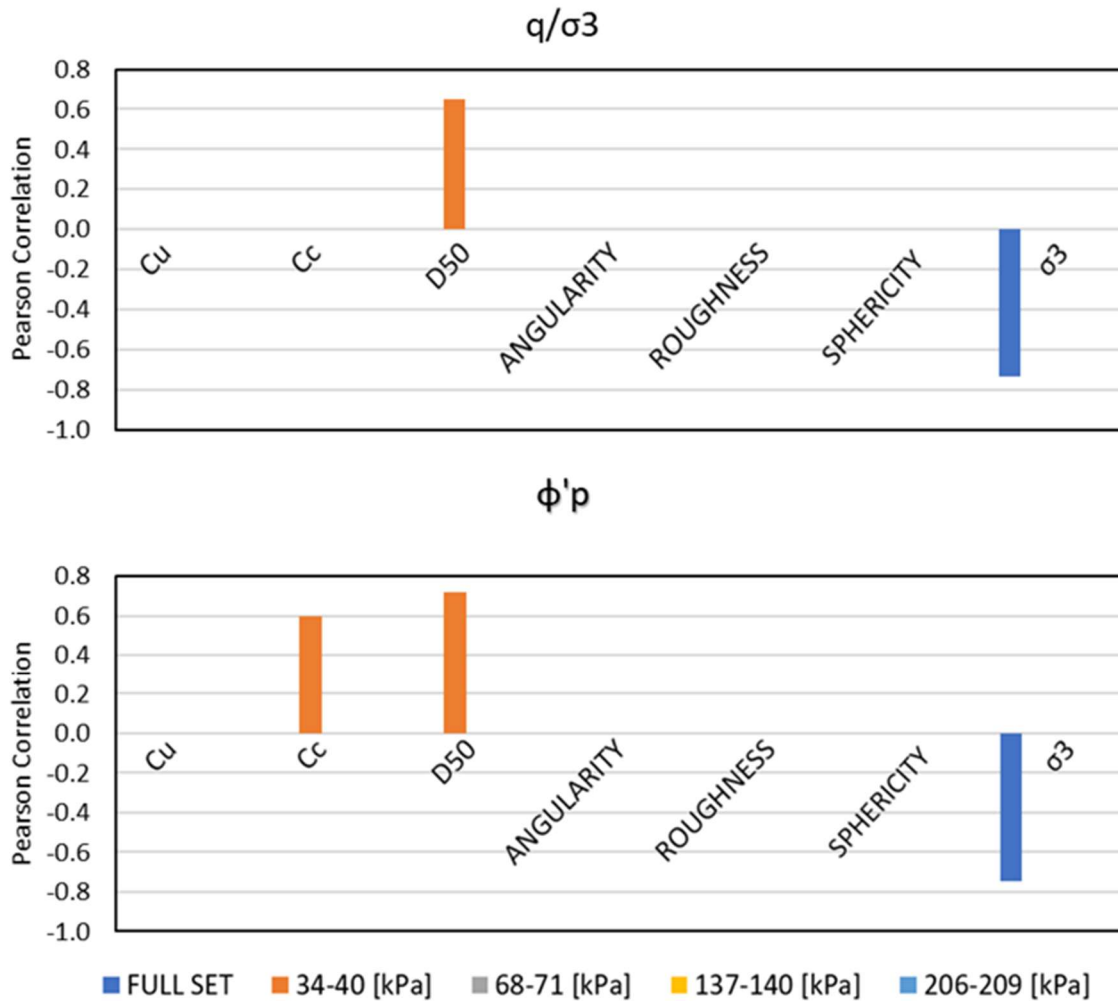


Figure G.4 Correlation coefficients computed with logarithmic transforms for Nicks et al. (2015) data with P-Value < 0.05.

G.2 Analysis of Chow et al. (2014) Data

These data, summarized in Table G.2, represent material, close to INDOT#43 and #53 in terms of particle size distribution. Computed coefficients of correlation are presented in Figure G.5 and Figure G.6, respectively for raw data and after logarithmic transformation. These correlations are generally low, except for D_{50} in the high stress range, roughness in the high stress range as well, and sphericity. It is noted that the expected negative correlation coefficient between peak shear strength and confining stress is weak; this is hardly surprising, considering the scattering of data in Figure G.5 and the fact that only three values of confining stress were available with each triaxial test.

Table G.2 Characteristics of Chow et al. (2014) statistical analysis

σ_3 [kPa]	Sample size	q/σ_3	ϕ'_p	C_u	C_c	D_{50} [mm]	Angularity	Roughness	Sphericity
Full Set	46 ^a	2.31– 21.20	32.42– 66.03	18.51– 140.00	0.64– 4.00	3–9	394–558	1.68–2.74	1.85–2.83
34– 42	17	4.00– 21.20	41.81– 66.03	18.51– 140.00	0.64– 4.00	3–9	394–558	1.68–2.74	1.85–2.83
68– 76	12	4.30– 14.10	43.04– 61.14	18.51– 140.00	0.64– 4.00	3–9	394–558	1.68–2.74	1.85–2.83
103– 114	13	2.31– 10.93	32.42– 57.71	18.51– 127.27	0.64– 4.00	3–9	394–511	1.68–2.67	1.97–2.73
127– 138	4	2.43– 8.20	33.28– 53.50	58.33– 140	1.26– 3.15	5–9	424–558	1.77–2.74	1.85–2.86

^a Three results were eliminated from the original data setoff 49 as the confining stresses (55.2, 79.3, and 96.5 kPa) fell outside of the ranges of the selected subsets.

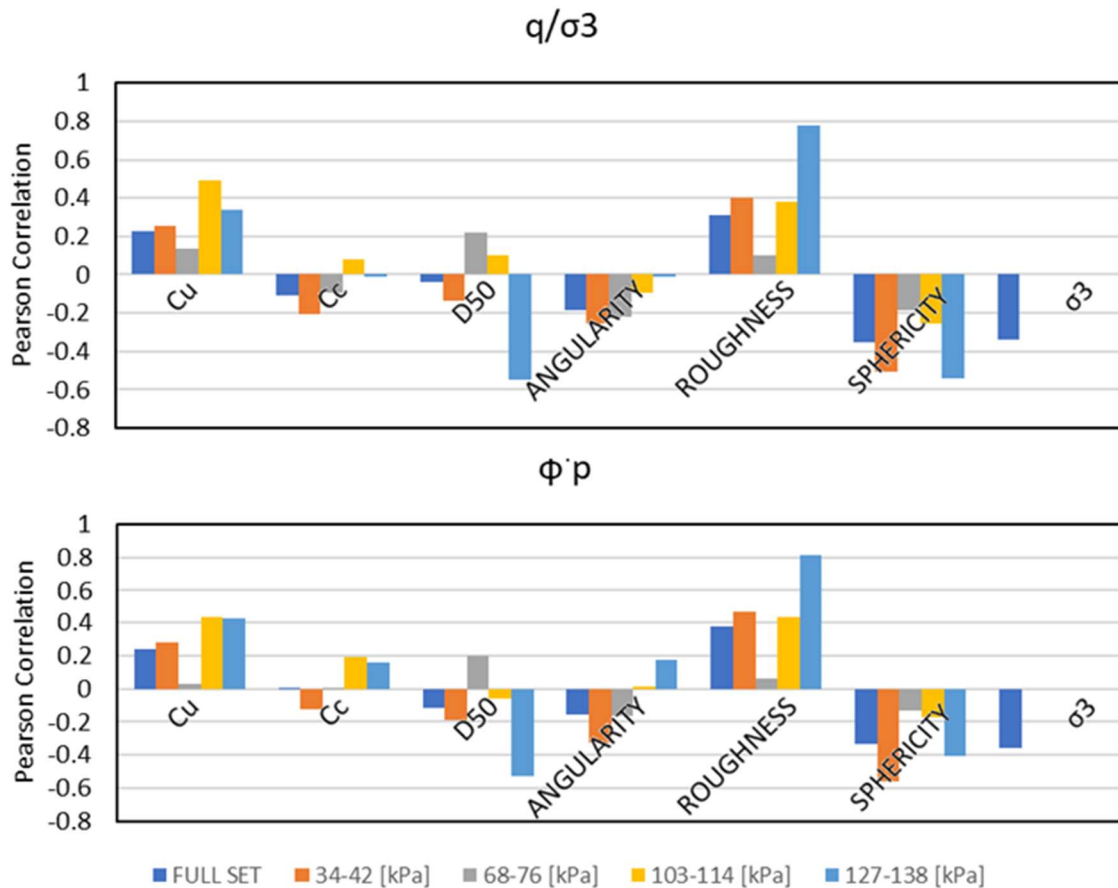


Figure G.5 Correlation coefficients for Chow et al. (2014) data.

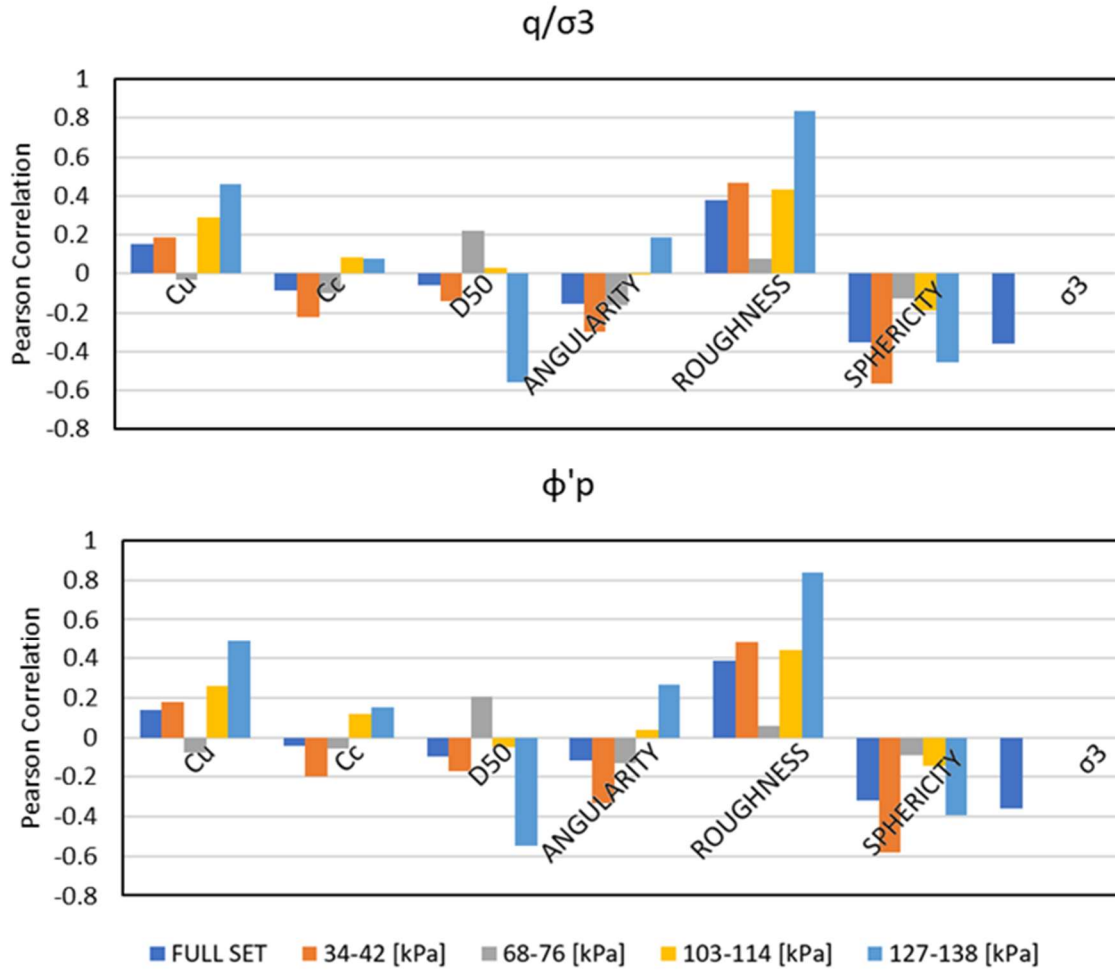


Figure G.6 Correlation coefficients computed with logarithmic transforms for Chow et al. (2014) data.

Figure G.7 and Figure G.8 show only those results which are still trusted after hypothesis testing: only weak or medium-range correlations remain between peak shear strength and roughness (positive coefficient) and sphericity (negative coefficient), both in low to medium ranges of confining stresses. Although the numerical evidence is weak, these results are physically logical, as they indicate the shear strength would, for instance, increase with increasing particle roughness and decrease with increasingly spherically-shaped particles.

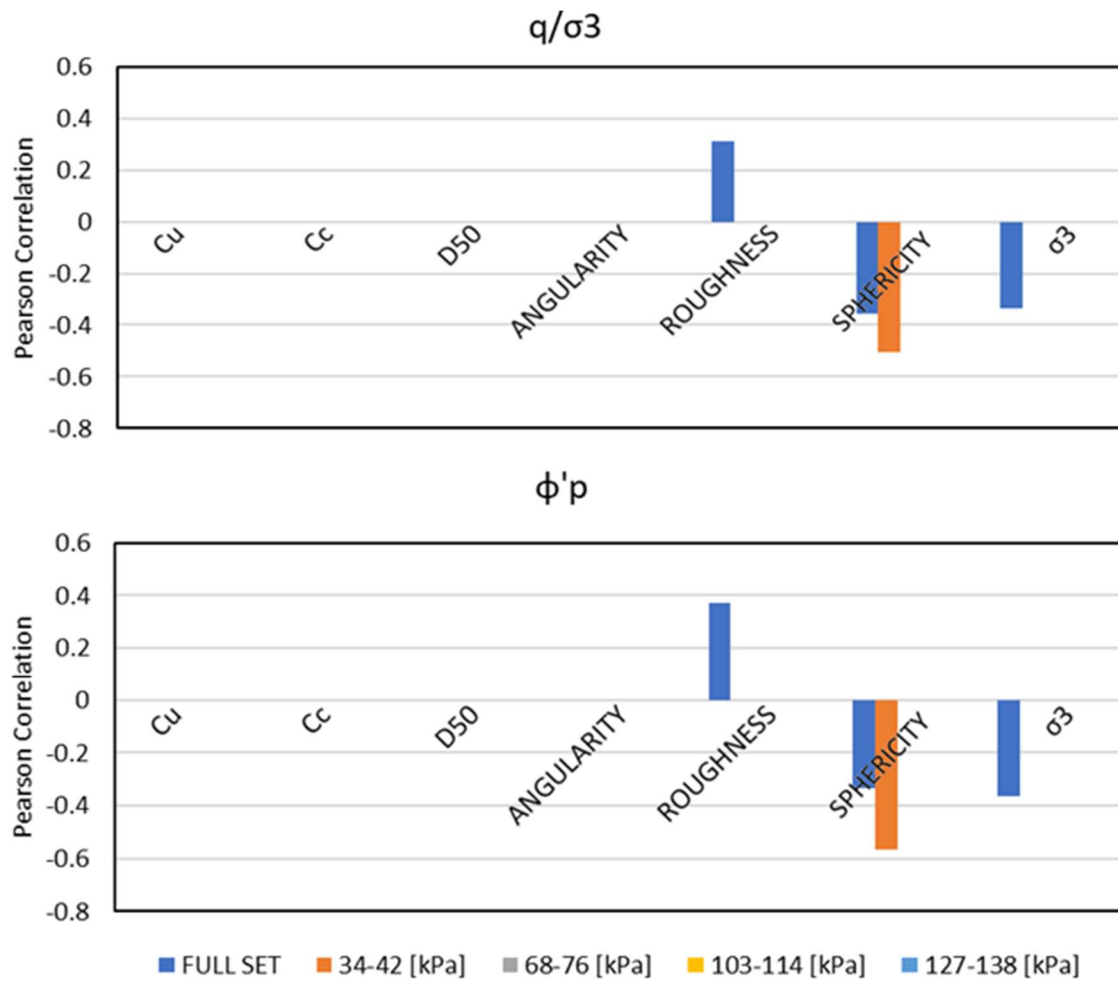


Figure G.7 Correlation coefficients for Chow et al. (2014) data with P-Value < 0.05.

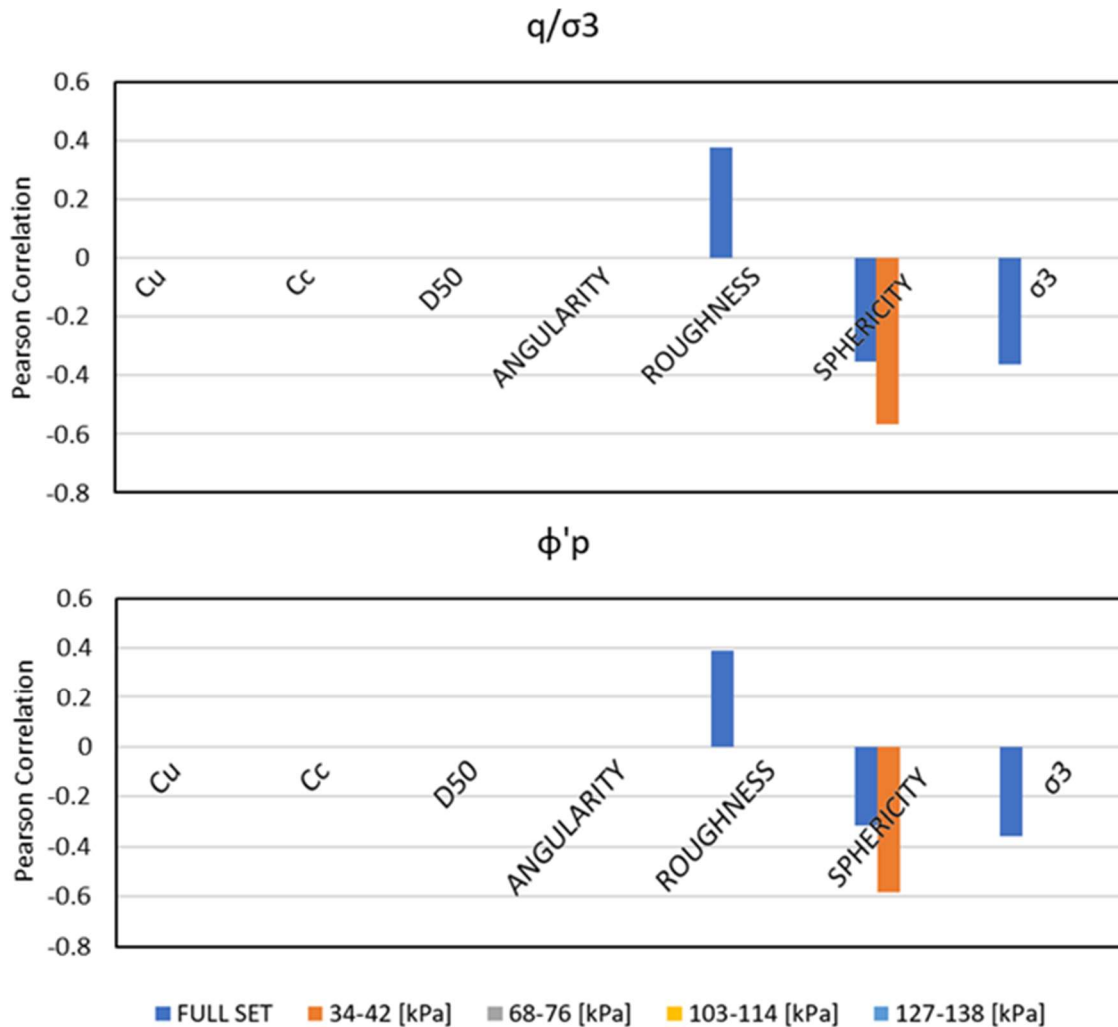


Figure G.8 Correlation coefficients computed with logarithmic transforms for Chow et al. (2014) data with P-Value < 0.05.

G.3 Analysis of Data from Aghaei Araei et al. (2010)

These data are also representative of INDOT #43 and #53 materials. In this set, aggregates were categorized as either from a quarry (blasted material) or from a pit (alluvial material), the former being of angular shape and the latter rounded, as a result of their origin. This distinction was based on visual inspection, with no standardized protocol being reported. Two classes we added to the specimen subsets for the purpose of analyzing separately these two categories.

Two additional parameters are included in this data set; they address hardness and abrasion resistance of the aggregate using the *Point Load* and the *Los Angeles* tests, respectively. A summary of the ranges of the parameters evaluated is presented in Table G.3. As above, the data were grouped according to the confining stress at which the tests were performed in order to isolate the analysis from the influence of σ_3 over the shear strength. In addition, the data were also analyzed after being separated in in two groups: aggregates that had predominantly angular shapes (blasted origin) and the ones that were mostly rounded (alluvial). The data contained in

these two categories is the same used in the full set, just regrouped. Note that results from different stress levels fall within each group.

Table G.3 Characteristics of Aghaei Araei et al. (2010) statistical analysis

σ_3 [kPa]	Sample Size	q/σ_3	ϕ'_p	C_u	C_c	D_{50} [mm]	Los Angeles	Point Load
Full Set	60 ^a	3.0– 12.5	36.86– 59.54	12.5– 75.0	0.16– 3.16	2.1– 12.0	19–46	2.11– 5.45
100	6	4.3–8	43.04– 53.13	12.5– 75.0	0.63– 1.65	2.5– 9.0	19–32	2.11– 5.42
200	9	3.1– 12.5	37.43– 59.54	20.5– 75.0	0.16– 1.65	2.1– 10.0	19–46	2.75– 5.42
300	7	3.33– 5.00	38.66– 45.58	12.5– 42.8	0.63– 3.16	2.5– 12.0	19–32	2.11– 5.45
400	7	3.25– 9.75	38.24– 56.07	20.5– 75.0	0.16– 1.65	2.1– 10.0	20–46	-5.45
700	13	3.00– 8.14	36.86– 53.39	12.5– 75.0	0.16– 3.16	2.1– 12.0	19–46	2.11– 5.42
Blasted	39	3.0– 12.5	36.86– 59.54	12.5– 75.0	0.63– 1.65	2.5– 9.0	19–40	2.11– 5.45
Alluvial	21	3.00– 5.85	36.86– 48.17	20.5– 53.3	0.16– 3.16	2.1– 12.0	16–49	—

^a Of the 60 total tests 18 are not included in the subsets for different σ_3 . They are for tests at 50, 500, 600, 800, 900, 1,000, 100, and 1,500 kPa. At these stress levels the number of tests available were not sufficient to perform a statistical analysis.

Correlation coefficients presented in Figure G.9 and Figure G.10 would suggest relationships between peak shear strength and both coefficients of uniformity and curvature (positive, medium-range correlation coefficients) while the correlation coefficients with the abrasion and the hardness test results are respectively negative and positive. Correlations with D_{50} exhibit weak, negative coefficients under low confining stress but positive values for higher stresses. There is a strong anomaly in the results for C_u , C_c , D_{50} , and the Los Angeles test at a confining stress of 100 kPa, for which we have no explanation. However, most of these results are invalidated by the hypothesis test, as seen in Figure G.11 and Figure G.12.

The only remaining trusted correlations are of weak to medium magnitude, and are not systematic at all confining stresses. These are between peak shear strength and C_u (positive coefficient), C_c (positive coefficient), abrasion (negative coefficient) and hardness (positive coefficient). There is no clear indication of differences between blasted and alluvial aggregates, as the corresponding coefficients of correlation are weak and inconsistent.

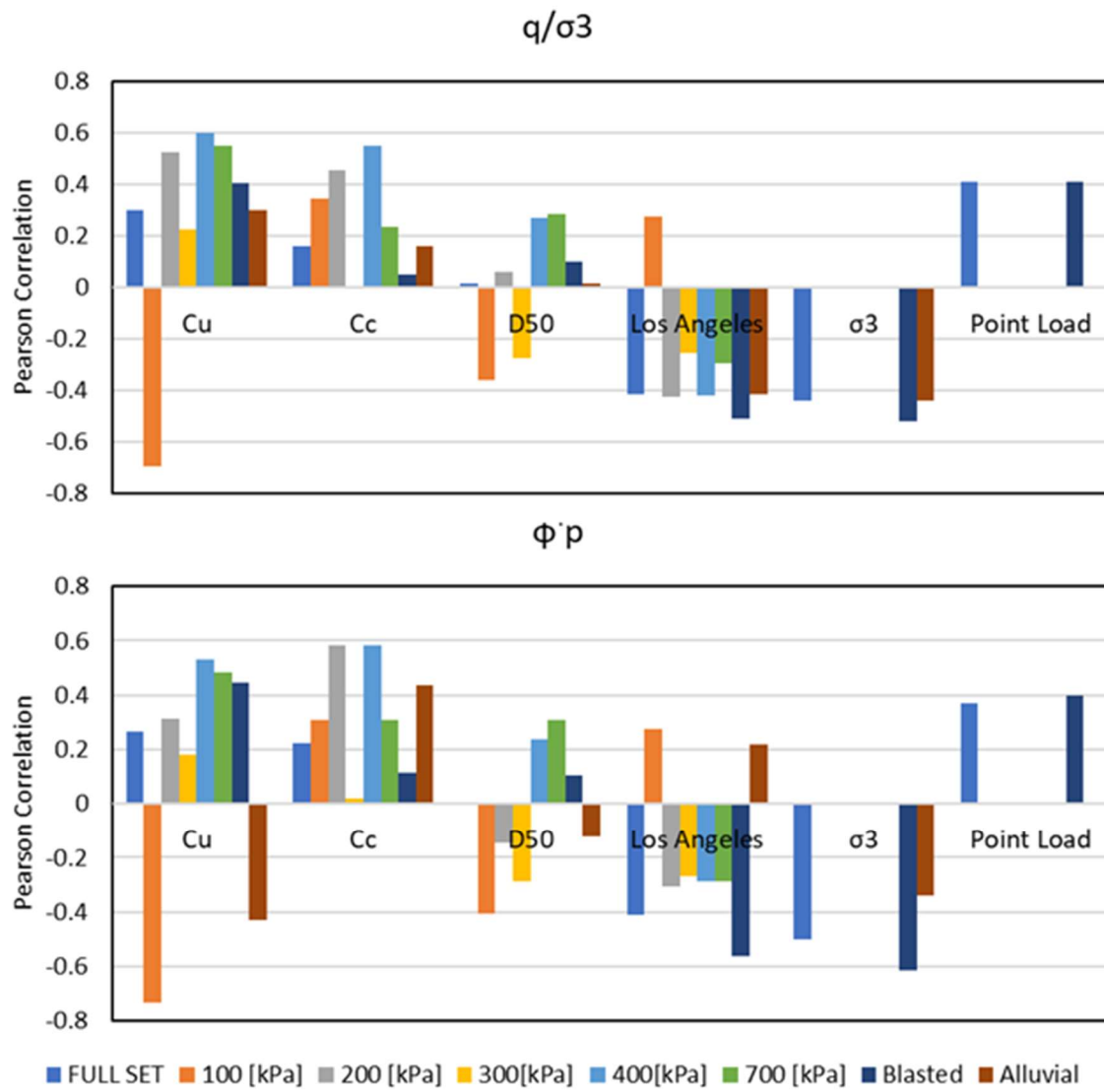


Figure G.9 Correlation coefficients for Aghaei Araei et al. (2010) data.

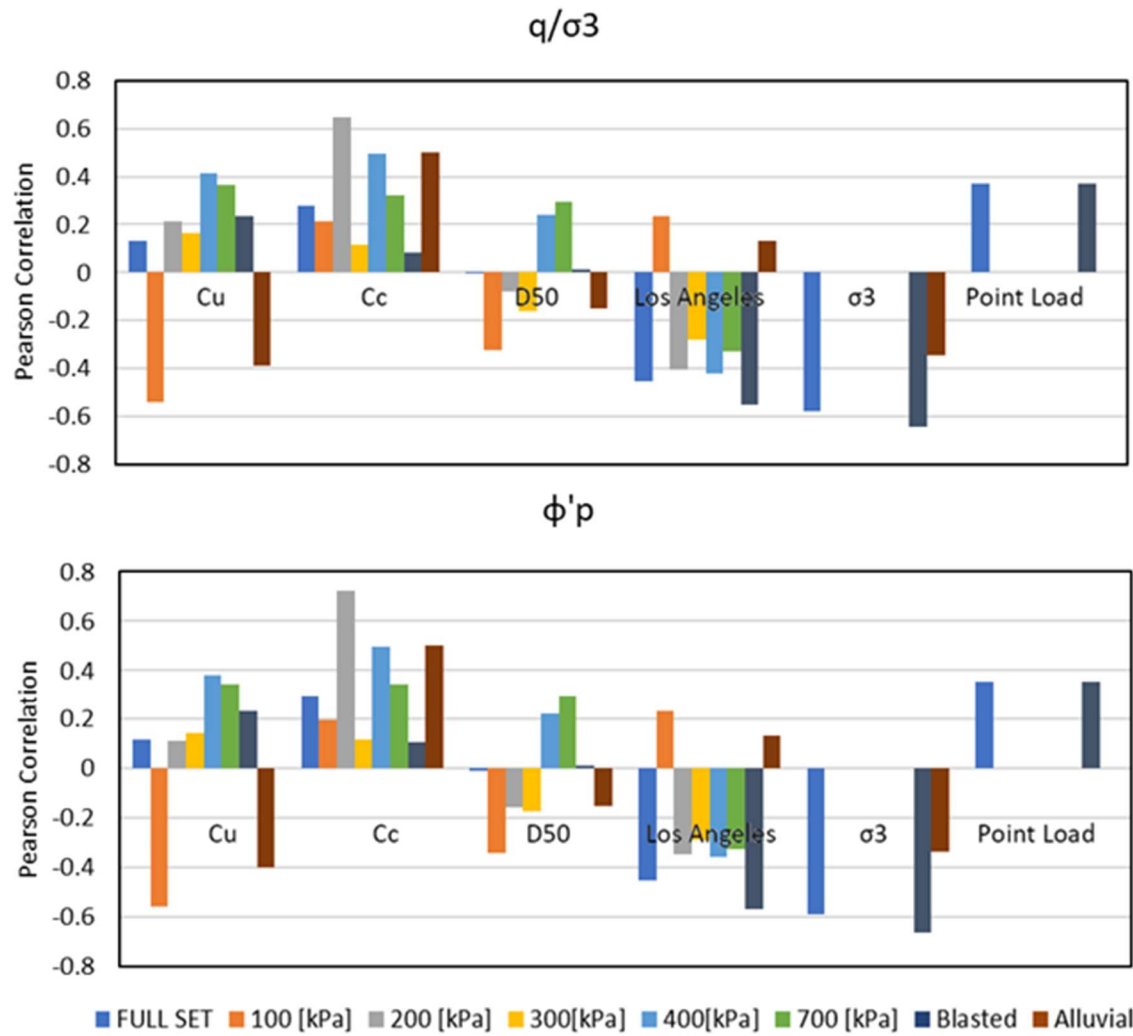


Figure G.10 Correlation coefficients computed with logarithmic transform for Aghaei Araei et al. (2010) data.

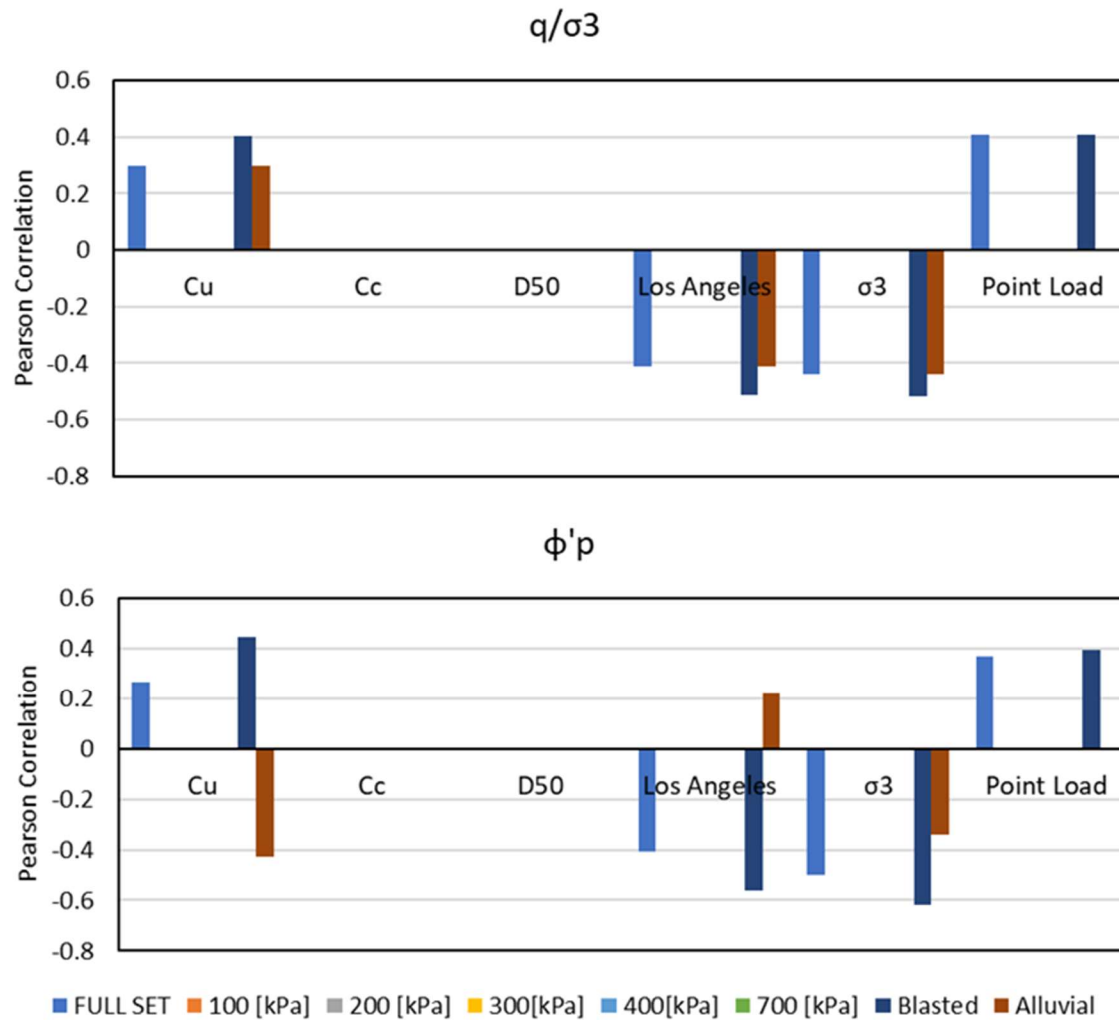


Figure G.11 Correlation coefficients for Aghaei Araei et al. (2010) data with P-Value < 0.05.

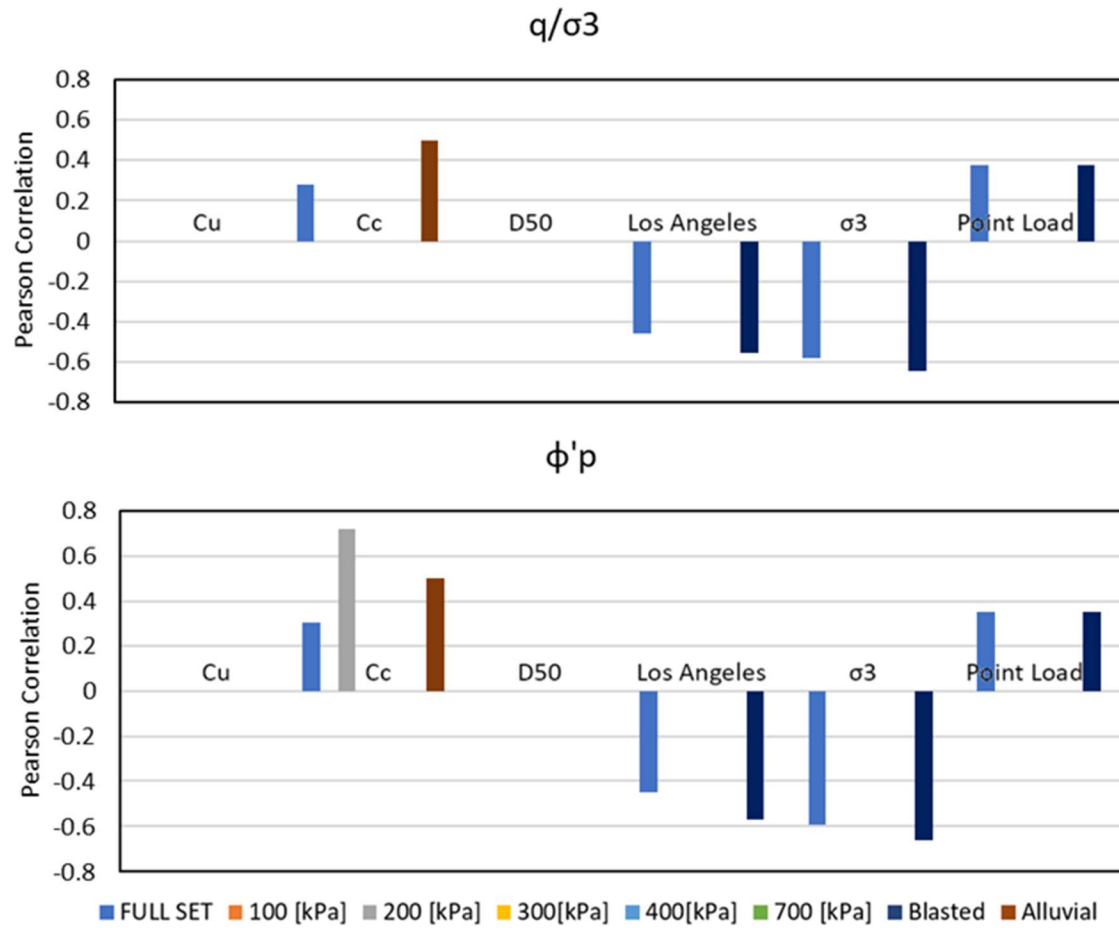


Figure G.12 Correlation coefficients computed with logarithmic transform for Aghaei Araei et al. (2010) data with P-Value < 0.05.

APPENDIX H. OVERVIEW OF BEARING CAPACITY ANALYSIS

The general bearing capacity equation for a shallow foundation on horizontal, homogeneous ground is (Meyerhof, 1963):

$$q_{ult} = cN_cF_{cs}F_{cd}F_{ci} + qN_qF_{qs}F_{qd}F_{qi} + \frac{1}{2}\gamma BF_{\gamma s}F_{\gamma d}F_{\gamma i} = \frac{1}{2}\gamma BN_{\gamma}F_{\gamma s}F_{\gamma d}F_{\gamma i} \quad \text{Equation H.1}$$

And

$$Q_{ult} = q_{ult} BL \quad \text{Equation H.2}$$

Where

q_{ult} is the ultimate bearing pressure of the foundation soil

c is the cohesion of the foundation soil

q is the overburden pressure, equal to $\gamma_{(ov)} D_f$

$\gamma_{(ov)}$ is the unit weight of the overburden soil

D_f is the depth of embedment of the footing

$\gamma = \gamma_f$ is the foundation soil unit weight

B is the width of the footing

L is the length of the footing

N_c , N_q , and N_{γ} are bearing capacity factors, functions of the angle of internal friction, computed according to Vesic (1973).

$F_{\gamma s}$, $F_{\gamma d}$, $F_{\gamma i}$ are correction coefficients for shape of the loaded area, depth of embedment and load inclination, respectively.

Q_{ult} is the ultimate bearing load of the foundation soil.

In our case, $c = 0$ and $D_f = 0$, thus the equation reduces to

$$q_{ult} = \frac{1}{2}\gamma BN_{\gamma}F_{\gamma s}F_{\gamma i} \quad \text{Equation H.3}$$

And, since the load is vertical,

$$q_{ult} = \frac{1}{2}\gamma BN_{\gamma}F_{\gamma s} \quad \text{Equation H.4}$$

The general form of the equation, including the Vesic's bearing capacity factor, was programmed as a spreadsheet application (Wolff, 1995; Bourdeau, 2016). Notations are defined in Figure H.1 and an example of the BEARING1 spreadsheet, in EXCEL format, is shown in Figure H.2.

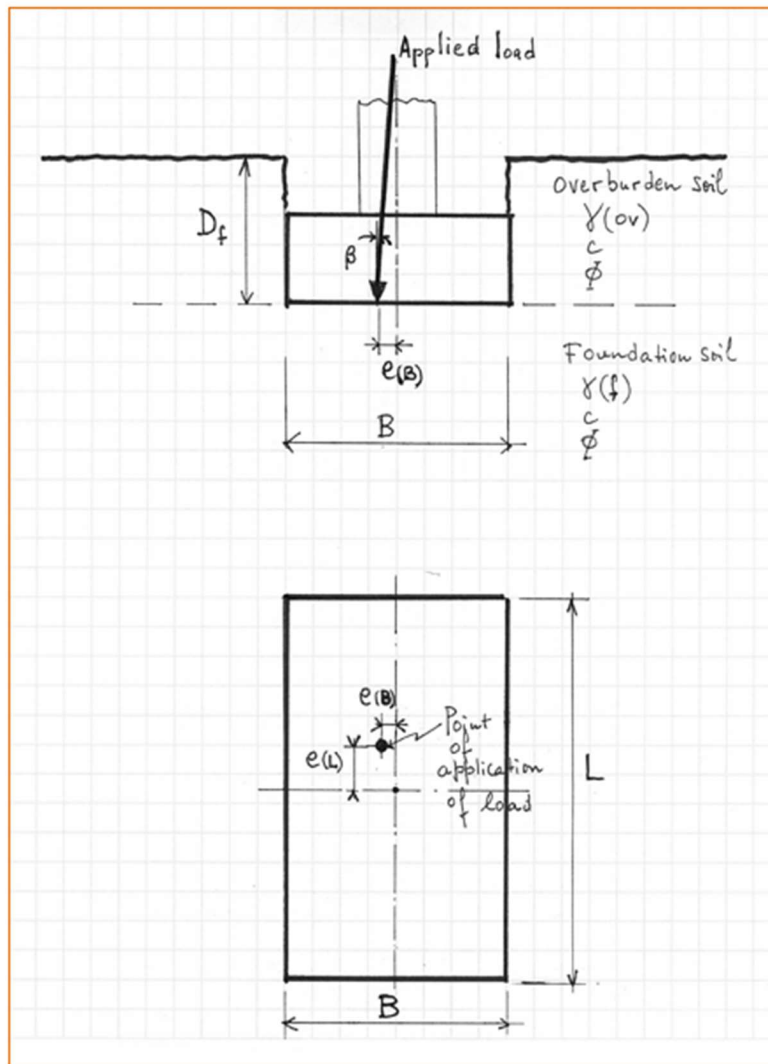


Figure H.1 Bearing capacity parameters for shallow foundations (Bourdeau, 2016).

BEARING CAPACITY OF RECTANGULAR FOOTINGS USING GENERAL BEARING CAPACITY EQUATION AND BEARING CAPACITY FACTORS ACCORDING TO VESIC

Spreadsheet Name: BEARING1

1993 by Thomas Wolff

Modified 10/20, 2008, 3/9, 2010, 3/19, 2012, 3/23 2014, 3/8 2016 by P.L. Bourdeau

Enter data in " **bold** " cells using consistent units

Phi(deg)=	57.00	Nc =	933.17	B =	0.91	e(B)=	0.00	B' =	0.91
Phi(rad)=	0.99	Nq =	1437.96	L =	2.44	e(L)=	0.00	L' =	2.44
beta(deg)=	0.00	Ngamma =	4431.60	Area =	2.22	Df/B=	0.00	Eff Area =	2.22

(B' <= L')

c	Nc	Fcs	Fcd	Fci	Pressure q	Load Q
0.00	933.17	1.57	1.00	1.00	0	0
gamma(ov)	Df	Nq	Fqs	Fqd	Fqi	
17.56	0.00	1437.96	1.57	1.00	1.00	0
B or B'	gamma(f)	Ngamma	Fgs	Fgd	Fgi	
0.50	0.91	17.56	4431.60	0.85	1.00	1.00
1.79	g/cm ³					
1790.00	kg/m ³					
17.56	kN/m ²					
					ultimate =	30125
					required FS =	1.00
					allowable =	30125

INPUT NOTATIONS: Phi: Angle of internal friction of foundation soil and overburden
B: Footing width
L: Footing length
e(B): load excentricity in B direction
e(L): load excentricity in L direction
beta: inclination of load with respect to vertical
c: cohesion of foundation soil and overburden
gamma(ov): unit weight of overburden soil
gamma(f): unit weight of foundation soil
Df: foundation depth or embedment
required FS: required safety factor (optional)

OUTPUT NOTATIONS: ultimate: values of ultimate pressure (q) or ultimate load (Q)
allowable: values of allowable pressure (q) or allowable load (Q)
Nc, Nq, Ngamma: bearing capacity factors according to Vesic (see handout)
F*: correction coefficients for shape, depth, load inclination (see handout)
B': reduced width to account for load excentricity in B direction (see handout)
L': reduced length to account for load excentricity in L direction
Area: surface area of footing
Eff Area: surface area reduced to account for excentricity of load

Figure H.2 Example of BEARING1 spreadsheet for bearing capacity computation.

APPENDIX I. SUPPORTING DATA FOR COMPATIBILITY ANALYSES

**Table I.1 Particle size distribution for example subgrades (based on Jung and Bobet, 2008)—
values interpolated using DRIP**

Sieve		DRIP Values for Treated Subgrade				
		A-4 (Site 2)	A-7-6 (Site 3)	A-4 (Site 4)	A-6 (Site 5)	A-6 (Site 6)
No.	(mm)	Percent Passing (%)				
No. 4	4.75	87	83	77	90	87
No. 10	2	75	65	67	80	67
No. 40	0.42	55	42	47	70	43
No. 100	0.149	20	30	29	67	37
No. 200	0.075	16	25	22	65	35
D ₁₂ (in.)		0.0016	0.000578	0.000768	0.0000691	0.000274
D ₁₅ (in.)		0.0026	0.000949	0.0013	0.000114	0.000449
D ₅₀ (in.)		0.0148	0.0317	0.0225	0.0016	0.0289
D ₈₅ (in.)		0.1643	0.3619	0.8946	0.1236	0.1732
P ₂₀₀ (%)		16	25	22	65	35
C _u		25.93	150.2	95.67	53.61	289.4

Table I.2 Particle size distribution for INDOT #8, #43, #53, and for NJDOT (specified ranges and interpolations using DRIP)

Sieve			INDOT Specs.				Interpolated DRIP Values						
			#8	#43	#53	NJDOT	#8	#43 AG	#53 Modified	#53 Mod 6	#53 Mod 7	NJDOT - Unstabilized	AASHTO A-7-6
No.	(in.)	(mm)	Percentage Passing (%)										
1.5	1.5	37.5	—	100	100	100	—	100	100	—	100	100	100
1	1	25	100	70-90	80–100	—	100	80	90	—	90	97.5	98.8
0.75	0.75	19	75–95	50–70	70–90	55-90	85	60	80	100	80	—	98.3
0.5	0.5	12.5	40–70	35–50	55–80	—	55	42.5	67.5	98	67.5	70	97.5
0.375	0.375	9.5	20–50	—	—	—	35	—	—	—	—	—	96.9
No. 4	0.187	4.75	0–15	20-40	35-60	25-60	7.5	30	47.5	80	40	47.5	94.9
No. 8	0.093	2.36	0–10	15-35	25-50	—	5	22.5	37.5	75	—	15	—
No. 10	0.079	2	—	—	—	—	—	—	—	—	—	—	93
No. 16	0.047	1.19	—	—	—	—	—	—	—	65	12.5	4	—
No. 30	0.024	0.6	—	5-20	12-30	—	—	12.50	21	50	—	—	—
No. 40	0.017	0.42	—	—	—	—	—	—	—	—	—	—	88.8
No. 50	0.012	0.3	—	—	—	5-25	—	—	—	20	5	2.5	—
No. 200	0.003	0.08	—	0-6	5-10	3-12	—	3	7.5	7.5	2.5	—	79.1
D ₁₅ (in)							0.2310	0.0363	0.0075	0.0075	0.0550	0.0929	0.000073
D ₈₅ (in)							0.7480	1.0971	0.2559	0.2559	0.8617	0.7375	0.0098
P ₂₀₀ (%)							0	3	7.5	7.5	2.5	0	79.1

APPENDIX J. LIST OF GEOTEXTILES APPROVED BY INDOT

May 31, 2016

GEOTEXTILES USED WITH RIPRAP AND UNDERDRAINS

Specification Reference: 918.02 & 918.03 SM Material Code: 913M00090 to 913M00095

Items listed below are approved for field installations which join adjacent pieces by overlapping and pinning. If joining is by sewing, seams shall be sown in accordance with the manufacturer's instructions and shall have a seam strength in accordance with specification requirements. Geotextiles shall be used for riprap or underdrains as indicated.

Source Code	Manufacturer Product Name	Type	Approval Number	Comments
<u>RIPRAP OR UNDERDRAIN</u>				
SM Material Code 913M00090				
8412	AMOCO FABRICS AND FIBERS CO----- PROPEX 4553	PLASTIC FILTER CLOTH	W028400	RIPRAP OR UNDERDRAINS
8411	BRADLEY MATERIALS CO----- 8NW	PLASTIC FILTER CLOTH	W028401	RIPRAP OR UNDERDRAINS
8413	CARTHAGE MILLS----- FX-70CF	PLASTIC FILTER CLOTH	W028402	RIPRAP OR UNDERDRAINS
8413	CARTHAGE MILLS----- FX-70HS	PLASTIC FILTER CLOTH	W028403	RIPRAP OR UNDERDRAINS
8413	CARTHAGE MILLS----- FX-75NW	PLASTIC FILTER CLOTH	W028404	RIPRAP OR UNDERDRAINS
8413	CARTHAGE MILLS----- FX-80NW	PLASTIC FILTER CLOTH	W028406	RIPRAP OR UNDERDRAINS
8413	CARTHAGE MILLS----- FX-80HS	PLASTIC FILTER CLOTH	W028405	RIPRAP OR UNDERDRAINS
8413	CARTHAGE MILLS----- POLY-FILTER X	PLASTIC FILTER CLOTH	W028407	RIPRAP OR UNDERDRAINS
8418	CHICOPEE----- STYLE NO. 50093X9	PLASTIC FILTER CLOTH	W028448	RIPRAP OR UNDERDRAINS
8400	DALCO NONWOVENS----- DALTEX 1080	PLASTIC FILTER CLOTH	W108401	RIPRAP OR UNDERDRAINS
8419	EXXON CHEMICAL CO----- GTF-225EX	PLASTIC FILTER CLOTH	W028410	RIPRAP OR UNDERDRAINS
8419	EXXON CHEMICAL CO----- GTF-400E	PLASTIC FILTER CLOTH	W028411	RIPRAP OR UNDERDRAINS
8421	HOECHST CELANESE CORP----- TREVIRA SPUNBOND 1125	PLASTIC FILTER CLOTH	W028412	RIPRAP OR UNDERDRAINS
8474	LINQ----- GTF 180EX	PLASTIC FILTER CLOTH	W028413	RIPRAP OR UNDERDRAINS

May 31, 2016

GEOTEXTILES USED WITH RIPRAP AND UNDERDRAINS

Specification Reference: 918.02 & 918.03 SM Material Code: 913M00090 to 913M00095

Source Code	Manufacturer	Product Name	Type	Approval Number	Comments
8421 8420	PHILLIPS FIBERS CORP	SUPAC 8NF	PLASTIC FILTER CLOTH	W028414	RIPRAP OR UNDERDRAINS
8421 8426	PROPEX INC	PROPEX GEOTEX 801	PLASTIC FILTER CLOTH	W078400	RIPRAP OR UNDERDRAINS
8480	SKAPS	GT 180	PLASTIC FILTER CLOTH	W048400	RIPRAP OR UNDERDRAINS
8422	SPARTAN TECHNOLOGIES	ST 70	PLASTIC FILTER CLOTH	W028415	RIPRAP OR UNDERDRAINS
8423	SYNTHETIC INDUSTRIES INC	EROSION I	PLASTIC FILTER CLOTH	W028416	RIPRAP OR UNDERDRAINS
8423	SYNTHETIC INDUSTRIES INC	PO 801	PLASTIC FILTER CLOTH	W028417	RIPRAP OR UNDERDRAINS
8415	TENCATE	FILERWEAVE 700	PLASTIC FILTER CLOTH	W028418	RIPRAP OR UNDERDRAINS
8415	TENCATE	GEO-MIRAFI 180N	PLASTIC FILTER CLOTH	W028420	RIPRAP OR UNDERDRAINS
8414	TENEX	TENSAR TG-650	PLASTIC FILTER CLOTH	W028409	RIPRAP OR UNDERDRAINS
8414	TENEX	TENSAR TG-700	PLASTIC FILTER CLOTH	W028408	RIPRAP OR UNDERDRAINS
8424	CROWN RESOURCES	STYLE R080	PLASTIC FILTER CLOTH	W028421	RIPRAP OR UNDERDRAINS
8478	US FABRICS INC	US 205NW	PLASTIC FILTER CLOTH	W028422	RIPRAP OR UNDERDRAINS
8478	US FABRICS INC	US 205NW-C	PLASTIC FILTER CLOTH	W028423	RIPRAP OR UNDERDRAINS
8416	HANES GEO COMPONENTS	TERRATEX EP	PLASTIC FILTER CLOTH	W028424	RIPRAP OR UNDERDRAINS
8416	HANES GEO COMPONENTS	TERRATEX N08	PLASTIC FILTER CLOTH	W028426	RIPRAP OR UNDERDRAINS

May 31, 2016

GEOTEXTILES USED WITH RIPRAP AND UNDERDRAINS

Specification Reference: 918.02 & 918.03 SM Material Code: 913M00090 to 913M00095

Source Code	Manufacturer	Product Name	Type	Approval Number	Comments
<u>UNDERDRAIN ONLY</u>					
SM Material Code 913M00095					
8412	AMOCO FABRICS AND FIBERS CO	4535	PLASTIC FILTER CLOTH	W028430	UNDERDRAINS ONLY
8412	AMOCO FABRICS AND FIBERS CO	4545	PLASTIC FILTER CLOTH	W028431	UNDERDRAINS ONLY
8413	CARTHAGE MILLS	FX 30HS	PLASTIC FILTER CLOTH	W028432	UNDERDRAINS ONLY
8413	CARTHAGE MILLS	FX-35HS	PLASTIC FILTER CLOTH	W028433	UNDERDRAINS ONLY
8413	CARTHAGE MILLS	FX-35ML	PLASTIC FILTER CLOTH	W028434	UNDERDRAINS ONLY
8413	CARTHAGE MILLS	FX-40CF	PLASTIC FILTER CLOTH	W028435	UNDERDRAINS ONLY
8400	DALCO NONWOVENS	DALTEX 1031	PLASTIC FILTER CLOTH	W108430	UNDERDRAINS ONLY
8421	HOECHST CELANESE CORP	TREVIRA SPUNBOND 1112	PLASTIC FILTER CLOTH	W028437	UNDERDRAINS ONLY
8421	HOECHST CELANESE CORP	TREVIRA SPUNBOND 1114	PLASTIC FILTER CLOTH	W028438	UNDERDRAINS ONLY
8426	PROPEX INC	PROPEX GEOTEX 311	PLASTIC FILTER CLOTH	W078401	UNDERDRAINS ONLY
8480	SKAPS	GT 131	PLASTIC FILTER CLOTH	W048401	UNDERDRAINS ONLY
8480	SKAPS	GT 135	PLASTIC FILTER CLOTH	W048402	UNDERDRAINS ONLY
8422	SPARTAN TECHNOLOGIES	ST 31	PLASTIC FILTER CLOTH	W028439	UNDERDRAINS ONLY
8423	SYNTHETIC INDUSTRIES INC	PO 311	PLASTIC FILTER CLOTH	W028440	UNDERDRAINS ONLY
8423	SYNTHETIC INDUSTRIES INC	PO 351	PLASTIC FILTER CLOTH	W028441	UNDERDRAINS ONLY
8415	TENCATE	135N	PLASTIC FILTER CLOTH	W028428	UNDERDRAINS ONLY

May 31, 2016

GEOTEXTILES USED WITH RIPRAP AND UNDERDRAINS

Specification Reference: 918.02 & 918.03 SM Material Code: 913M00090 to 913M00095

Source Code	Manufacturer	Product Name	Type	Approval Number	Comments
8415	TENCATE	140 NL	PLASTIC FILTER CLOTH	W028429	UNDERDRAINS ONLY
8414	TENEX	TENSAR TG-500	PLASTIC FILTER CLOTH	W028436	UNDERDRAINS ONLY
8474	THRACE - LINQ	120EX	PLASTIC FILTER CLOTH	W108440	UNDERDRAINS ONLY
8474	THRACE - LINQ	GTF 125EX	PLASTIC FILTER CLOTH	W028427	UNDERDRAINS ONLY
8474	THRACE - LINQ	150EX	PLASTIC FILTER CLOTH	W108441	UNDERDRAINS ONLY
8424	TNS ADVANCED TECHNOLOGIES	TNS R031	PLASTIC FILTER CLOTH	W028442	UNDERDRAINS ONLY
8424	TNS ADVANCED TECHNOLOGIES	TNS R035	PLASTIC FILTER CLOTH	W028443	UNDERDRAINS ONLY
8478	US FABRICS INC	US 80NW	PLASTIC FILTER CLOTH	W028444	UNDERDRAINS ONLY
8478	US FABRICS INC	US 90NW	PLASTIC FILTER CLOTH	W028445	UNDERDRAINS ONLY
8478	US FABRICS INC	US 120NW-C	PLASTIC FILTER CLOTH	W028446	UNDERDRAINS ONLY
8416	HANES GEO COMPONENTS	TERRATEX NO3	PLASTIC FILTER CLOTH	W028447	UNDERDRAINS ONLY

About the Joint Transportation Research Program (JTRP)

On March 11, 1937, the Indiana Legislature passed an act which authorized the Indiana State Highway Commission to cooperate with and assist Purdue University in developing the best methods of improving and maintaining the highways of the state and the respective counties thereof. That collaborative effort was called the Joint Highway Research Project (JHRP). In 1997 the collaborative venture was renamed as the Joint Transportation Research Program (JTRP) to reflect the state and national efforts to integrate the management and operation of various transportation modes.

The first studies of JHRP were concerned with Test Road No. 1 — evaluation of the weathering characteristics of stabilized materials. After World War II, the JHRP program grew substantially and was regularly producing technical reports. Over 1,600 technical reports are now available, published as part of the JHRP and subsequently JTRP collaborative venture between Purdue University and what is now the Indiana Department of Transportation.

Free online access to all reports is provided through a unique collaboration between JTRP and Purdue Libraries. These are available at <http://docs.lib.purdue.edu/jtrp>.

Further information about JTRP and its current research program is available at <http://www.purdue.edu/jtrp>.

About This Report

An open access version of this publication is available online. See the URL in the citation below.

Recommended Citation

Getchell, A., Garzon Sabogal, L., Bourdeau, P. L., & Santagata, M. (2020). *Investigation of design alternatives for the subbase of concrete pavements* (Joint Transportation Research Program Publication No. FHWA/IN/JTRP-2020/03). West Lafayette, IN: Purdue University. <https://doi.org/10.5703/1288284317114>